60047

THE POLARIZATION OF DOWNCOMING IONOSPHERIC RADIO WAVES

By

Kenneth A. Norton

FEDERAL COMMUNICATIONS COMMISSION

Report Prepared in Connection with

NATIONAL BUREAU OF STANDARDS PROJECT

Sponsored by the

NATIONAL DEFENSE RESEARCH COMMITTEE

For Restricted Circulation Only

THE POLARIZATION OF DOWNCOMING IONOSPHERIC RADIO WAVES 60047

Prepared by Kenneth A. Norton for the National Defense Research Committee.

I. Introduction.

In the development of radio direction finders and the study of the bearing errors encountered in their use, it is valuable to have information regarding the polarization of the downcoming radio waves. This information is of value since it is generally recognized that the largest source of bearing error in the average direction finder now in use is the "polarization error" due to the presence in the downcoming wave at the direction finder of wave components polarized both parallel and perpendicular to the plane of incidence and with random relative phases. The theoretical calculation of the expected intensities of these two components at the direction finder may be divided into two parts: First, the calculation of the intensities of these two components in the downcoming ionospheric wave and second, the calculation of the resultant intensities of these two components at the direction finder due to the summation of the direct and ground-reflected waves. The first step in these calculations has been covered previously by W. G. Baker and A. L. Green[1]; however, the analysis in Part II of this report leads to somewhat simpler results and also includes the effects of fading. The second step was carried out in a discussion by the author on "Ground Wave Propagation" presented at the Fourth Annual Broadcast Engineering Conference held at Ohio State University in 1941; this study is considerably amplified in Part III of this report. Part IV deals with methods of testing direction finders and a new method of measuring the electrical constants of the ground. The conclusions reached as a result of this theoretical study are presented in Part V.

II. The Calculation of the Intensities of the Components Parallel and Perpendicular to the Plane of Incidence in the Downcoming Ordinary and Extraordinary Ionospheric Waves.

It is well known that the presence of the magnetic field of the earth causes a wave incident on the ionosphere to split into ordinary and extraordinary waves, each of which thereafter travel independently in the ionosphere and are reflected at different heights. At frequencies near the magneto-ionic frequency (i.e. near 1500 kc in the United States) the extraordinary wave is subject to much greater absorption than the ordinary wave in traveling through the ionosphere and is thus a negligible component of the downcoming wave. In the following a derivation is given showing the effect of this splitting on the magnitudes of the components of the downcoming ordinary and extraordinary waves. Expressions are derived for the intensities of the components polarized parallel and perpendicular to the plane of incidence in the two cases when the incident wave is polarized either parallel or perpendicular to the plane of incidence. In this derivation the assumption will be made that only the

[1] W. G. Baker and A. L. Green, "The Limiting Polarization of Downcoming Radio Waves Traveling Obliquely to the Earth's Magnetic Field", Proc. IRE, August 1933, pp. 1103-1131.

(over)

free electrons in the ionized air directly affect the propagation of the radio waves through the ionosphere; this must certainly be true at least as a good first approximation since, if heavier ions were primarily responsible for the reflection, the magnetic field of the earth would not have the effects on the propagation of the waves which are observed in practice. In this derivation, Heaviside-Lorentz units and the following notation will be used.

e = charge on an electron; e is negative for negative electrons.
m = mass of an electron.
N = electron density (number of free electrons per cubic centimeter).
$\underline{H}^o$ = earth's magnetic field.
ν = mean frequency of collisions between a free electron and neutral air molecules.
$k = 2\pi/\lambda$.
λ = vacuum wavelength of the radio wave.
c = velocity of light.
$\omega = kc = 2\pi f$.
f = radio wave frequency.
$f_h = e\underline{H}^o/2\pi m c$ = magneto-ionic frequency.
$x = Ne^2/m\omega^2$.
$\underline{y} = (e/mc\omega)\,\underline{H}^o = y_1\,\underline{i} + y_2\,\underline{j} + y_3\,\underline{k}$.
$y = f_h/f$.
$z = \nu/\omega$.
$u = 1 + iz$.
ϕ = angle of incidence at the ionosphere.
I = dip or angle of inclination of the earth's magnetic field; I is positive north of the magnetic equator and negative south of the magnetic equator, being zero at the magnetic equator.
Θ = angle between the plane of incidence of the radio wave and the magnetic meridian; thus Θ is zero for propagation from South to North along a line parallel to the direction of the earth's magnetic field, $\Theta = 90^\circ$ for propagation from West to East perpendicular to the earth's field, $\Theta = 180^\circ$ for propagation from North to South along the earth's field and $\Theta = 270^\circ$ for propagation from East to West perpendicular to the earth's field.
$\underline{V}$ = velocity of electron motion in the ionosphere.
$\underline{E}$ = electric field of the radio wave.
$\underline{H}$ = magnetic field of the radio wave.
$\underline{S}$ = Poynting vector.
$\underline{i}$, $\underline{j}$, $\underline{k}$ = righthanded set of mutually perpendicular unit vectors.

Following Darwin[2], Lorentz's polarization term will not be used; this term could be added simply by adding $1/3x$ to the definition of u.[3,4]

---

[2] C. G. Darwin, "The Refractive Index of an Ionized Medium", Proc. Roy. Soc., Series A, Vol. 146, pp. 17-46, August 1934.
[3] H. G. Booker and L. V. Berkner, "An Ionospheric Investigation Concerning the Lorentz Polarization Correction", Terr. Mag. and Atmospheric Elec., Vol. 43, No. 4, December 1938, pp. 427-450.
[4] Newbern Smith, "Oblique-Incidence Radio Transmission and the Lorentz Polarization Term", Jr. of Res. of the Nat'l. Bur. of Stds., Vol. 26, Feb. 1941, pp. 105-116.

When a radio wave passes through an ionized medium, such as the ionosphere, it causes the ionized particles, which are here considered to be free electrons only, to oscillate with the period of the radio wave. The actual paths followed by the electrons in these oscillations are determined by the electric force in the radio wave $e\,\underline{E}$ which is opposed by the inertial force $-m\,\dot{\underline{V}}$ (the dot over the $\underline{V}$ denotes differentiation with respect to time so that $\dot{\underline{V}}$ denotes the acceleration) and a dissipative force due to the electron collisions equal to $-v\,m\,\underline{V}$.[5] This motion is further modified by a force $\frac{e}{c}\,\underline{V} \times \underline{H}^o$ due to the magnetic field of the earth; the corresponding force on the electron due to the magnetic field of the radio wave is negligibly small compared to that of the magnetic field of the earth and will be neglected. Even for an electric field intensity of one volt per meter the corresponding magnetic field intensity of the radio wave would be only $\frac{1}{30,000}$ gauss whereas the magnetic field of the earth is of the order of 0.5 gauss. Thus the equation of force for the electron may be written:

$$e\,\underline{E} - m\,\dot{\underline{V}} - v\,m\,\underline{V} + \frac{e}{c}\,\underline{V} \times \underline{H}^o = 0 \qquad (1)$$

Since the electric force in the radio wave contains the time factor $e^{-i\omega t}$, that part of the velocity $\underline{V}$ affecting the radio wave propagation will also be proportional to this time factor so that (1) may be written

$$\dot{\underline{E}} + \frac{\omega^2 m}{e}\,\underline{V} + \frac{i\omega v\,m}{e}\,\underline{V} - \frac{i\omega}{c}\,\underline{V} \times \underline{H}^o = 0 \qquad (2)$$

Solving (2) for $\dot{\underline{E}}$ we obtain

$$\dot{\underline{E}} = -\frac{\omega^2 m}{e}\left[\left(1 + i\,\frac{v}{\omega}\right)\underline{V} - i\,\frac{e}{mc\,\omega}\,\underline{V} \times \underline{H}^o\right]$$

$$\text{or } \dot{\underline{E}} = -\frac{\omega^2 m}{e}\left[u\,\underline{I} + i\,\underline{y} \times \underline{I}\right] \cdot \underline{V} \equiv -\frac{\omega^2 m}{e}\,\underline{\Phi}^{-1} \cdot \underline{V} \qquad (3)$$

where $\underline{I} = \underline{ii} + \underline{jj} + \underline{kk}$ is the unit dyadic and $\underline{\Phi}$ is the dyadic whose reciprocal is expressed

$$\underline{\Phi}^{-1} = u\,\underline{I} + i\,\underline{y} \times \underline{I} \qquad (4)$$

The theory and use of dyadics are described in detail in the book "Vector Analysis" in which J. Willard Gibbs' theory is presented by E. B. Wilson; the theory is also presented in the recent book "Electrodynamics" by Leigh Page and N. I. Adams. By means of this theory we may determine the reciprocal dyadic $\underline{\Phi}$ from (4):

---

[5] This form for this term in the force equation was first obtained by H. W. Nichols and J. C. Schelleng in their paper "Propagation of Electric Waves Over the Earth", Bell Sys. Tech. Jr., Vol. 4, April 1925. For another discussion leading to this same form for this term in the force equation see reference [2]. For a solution leading to somewhat different results see D. Burnett, "The Propagation of Radio Waves in an Ionized Atmosphere", Proc. Cambridge Phil. Soc., Vol. 27, Part IV, 1931, pp. 578-587.

$$(u^2 - y_1^2)\ \underline{i}\,\underline{i} + (i\,u\,y_3 - y_1 y_2)\ \underline{i}\,\underline{j} - (i\,u\,y_2 + y_1\,y_3)\ \underline{i}\,\underline{k}$$

$$u\,(u^2 - y^2)\ \underline{\underline{\Phi}} = -(i\,u\,y_3 + y_1\,y_2)\ \underline{j}\,\underline{i} + (u^2 - y_2^2)\ \underline{j}\,\underline{j} + (i\,u\,y_1 - y_2\,y_3)\ \underline{j}\,\underline{k} \qquad (5)$$

$$+ (i\,u\,y_2 - y_1\,y_3)\ \underline{k}\,\underline{i} - (i\,u\,y_1 + y_2\,y_3)\ \underline{k}\,\underline{j} + (u^2 - y_3^2)\ \underline{k}\,\underline{k}$$

Now (3) may be written in terms of $\underline{\underline{\Phi}}$:

$$\underline{V} = -\frac{e}{\omega^2 m}\ \underline{\underline{\Phi}} \cdot \dot{\underline{E}} \qquad (6)$$

If we assume that there are N free electrons per cubic centimeter in the ionosphere, then we may write for the total current $\underline{J}$ (displacement plus conduction current) due to the radio wave:

$$\underline{J} = \dot{\underline{E}} + N\,e\,\underline{V} = \dot{\underline{E}} - \frac{N e^2}{\omega^2 m}\ \underline{\underline{\Phi}} \cdot \dot{\underline{E}} \equiv \underline{\underline{\Psi}} \cdot \dot{\underline{E}} \qquad (7)$$

$$\underline{\underline{\Psi}} = \underline{\underline{I}} - x\ \underline{\underline{\Phi}} \qquad (8)$$

Maxwell's equations may be written for a medium defined as above:

$$\nabla \times \underline{E} = -\frac{1}{c}\dot{\underline{H}} \qquad (9)$$

$$\nabla \times \underline{H} = \frac{1}{c}\underline{\underline{\Psi}} \cdot \dot{\underline{E}} \qquad (10)$$

We will obtain the plane wave solution of (9) and (10) by considering $\underline{E}$ and $\underline{H}$ to be proportional to the plane wave function:

$$\exp\left[i\left\{k\mu\,\underline{n}\cdot\underline{r} - \omega t\right\}\right] \qquad (11)$$

where μ denotes the (in general complex) index of refraction of the radio waves, $\underline{n}$ denotes a unit vector normal to the wave front and $\underline{r}$ is a vector denoting the position of the field point from a fixed origin, for example, the transmitting antenna. Using (11) in (9) and (10) gives:

$$\underline{n} \times \underline{E} = \frac{1}{\mu}\underline{H} \qquad (12)$$

$$\underline{n} \times \underline{H} = -\frac{1}{\mu}\underline{\underline{\Psi}} \cdot \underline{E} \qquad (13)$$

If we multiply (12) and (13) by $\underline{n}$, we find that

$$\underline{n} \cdot \underline{H} = 0 \qquad (14)$$

$$\underline{n} \cdot \underline{\underline{\Psi}} \cdot \underline{E} = 0 \qquad (15)$$

Thus we see that, although $\underline{H}$ lies in the plane of the wave front everywhere, the vector $\underline{\Psi} \cdot \underline{E}$ and not $\underline{E}$ lies in the plane of the wave front in the ionosphere; thus for finite values of x (see equation (8), the magnetic field of the earth is responsible for a component of electric force in the direction of propagation.

Next multiply (12) by $\underline{n}$ x and combine with (13) to obtain:

$$(\underline{n}\,\underline{n} - \underline{I} + \frac{1}{\mu^2}\,\underline{\Psi}) \cdot \underline{E} = 0 \tag{16}$$

We wish to determine the relative magnitudes of the components of $\underline{E}$ normal to the plane of the wave front, E_n, parallel to the plane of incidence at the layer or at the ground, $E_{\parallel}$, and normal to the plane of incidence, $E_{\perp}$. Thus we may set $\underline{n} = \underline{i}$ and let the $\underline{i} - \underline{k}$ plane be the plane of incidence so that $\underline{y} = y_n\,\underline{i} + y_{\perp}\,\underline{j} + y_{\parallel}\,\underline{k}$ and

$$\underline{E} = E_n\,\underline{i} + E_{\perp}\,\underline{j} + E_{\parallel}\,\underline{k} \tag{17}$$

Substituting the above in (16) yields the following three equations:

$$E_n\left(1 - \frac{x(u^2 - y_n^2)}{u(u^2 - y^2)}\right) - E_{\perp}\frac{x}{u(u^2 - y^2)}(iuy_{\parallel} - y_n y_{\perp}) + E_{\parallel}\frac{x}{u(u^2 - y^2)}(iuy_{\perp} + y_n y_{\parallel}) = 0 \tag{18}$$

$$E_n\frac{x}{u(u^2 - y^2)}(iuy_{\parallel} + y_n y_{\parallel}) + E_{\perp}\left[1 - \mu^2 - \frac{x}{u(u^2 - y^2)}(u^2 - y_{\perp}^2)\right] - E_{\parallel}\frac{x}{u(u^2 - y^2)}(iuy_n - y_{\perp}y_{\parallel}) = 0 \tag{19}$$

$$-E_n\frac{x}{u(u^2 - y^2)}(iuy_{\perp} - y_n y_{\parallel}) + E_{\perp}\frac{x}{u(u^2 - y^2)}(iuy_n + y_{\perp}y_{\parallel}) + E_{\parallel}\left[1 - \mu^2 - \frac{x}{u(u^2 - y^2)}(u^2 - y_{\parallel}^2)\right] = 0 \tag{20}$$

The above three equations may be solved simultaneously to determine μ^2, $(E_n/E_{\parallel})$ and $(E_{\perp}/E_{\parallel})$:

$$\mu^2 = 1 - x\,\frac{u(u - x) - y_{\parallel}^2 - \{y_{\perp}y_{\parallel} + i\,y_n(u - x)\}\,(E_{\perp}/E_{\parallel})}{u(u^2 - y^2) - x(u^2 - y_n^2)} \tag{21}$$

$$\left(\frac{E_n}{E_{\parallel}}\right) = x\,\frac{(i\,u\,y_{\parallel} - y_n\,y_{\perp})(E_{\perp}/E_{\parallel}) - (i\,u\,y_{\perp} + y_n\,y_{\parallel})}{u(u^2 - y^2) - x(u^2 - y_n^2)} \tag{22}$$

$$\left(\frac{E_{\perp}}{E_{\parallel}}\right) = \frac{y_{\perp}^2 - y_{\parallel}^2 \pm \sqrt{(y_{\parallel}^2 + y_{\perp}^2)^2 + 4\,y_n^2(u - x)^2}}{2\{y_{\perp}\,y_{\parallel} + i\,y_n(u - x)\}} \tag{23}$$

If we write $y_{\parallel}\,y_{\perp} + i\,y_n(u - x) \equiv A\,e^{iB}$ (24)

then (23) may be written

$$\left(\frac{E_\perp}{E_\parallel}\right) = \left\{ \frac{y_\perp^2 - y_\parallel^2}{2A} \pm \sqrt{\left(\frac{y_\perp^2 - y_\parallel^2}{2A}\right)^2 + 1} \right\} e^{-iB} \qquad (25)$$

The two signs in (23) and (25) correspond to the polarizations of the two magnetoionic components of the wave, the upper (positive sign) corresponding to the ordinary wave while the lower sign corresponds to the extraordinary wave. If we write:

$$\left(\frac{E_\perp}{E_\parallel}\right)_o \equiv R_o\, e^{-iB} = \left\{ \frac{y_\perp^2 - y_\parallel^2}{2A} + \sqrt{\left(\frac{y_\perp^2 - y_\parallel^2}{2A}\right)^2 + 1} \right\} e^{-iB} \qquad (26)$$

$$\left(\frac{E_\perp}{E_\parallel}\right)_x \equiv R_x\, e^{-iB} = \left\{ \frac{y_\perp^2 - y_\parallel^2}{2A} - \sqrt{\left(\frac{y_\perp^2 - y_\parallel^2}{2A}\right)^2 + 1} \right\} e^{-iB} \qquad (27)$$

it is evident from (26) that R_o is always positive; $R_o < 1$ when $y_\perp^2 < y_\parallel^2$ and $R_o > 1$ when $y_\perp^2 > y_\parallel^2$. Also we see by obtaining the product of (26) and (27) that:

$$R_x = -\frac{1}{R_o} \qquad (28)$$

Upon using the above relation and substituting (24), (26) and (27) in (21) we obtain:

$$\mu_o^2 = 1 - x\, \frac{u(u - x) - y_\parallel^2 - A R_o}{u(u^2 - y^2) - x(u^2 - y_n^2)} \qquad (29)$$

$$\mu_x^2 = 1 - x\, \frac{u(u - x) - y_\parallel^2 + (A/R_o)}{u(u^2 - y^2) - x(u^2 - y_n^2)} \qquad (30)$$

(29) and (30) are respectively the indices of refraction for the ordinary and extraordinary waves. We see by (24) and (25) that the polarization of the waves depends upon the values of x and of $u = (1 + iz)$ and these in turn depend upon the height in the ionosphere, x increasing with the height while z decreases with height; thus it is necessary to have some way of determining the height at which the radio wave splits into its two components.

It has been shown by H. G. Booker [6] that this splitting takes place at the height where the difference between the indices of refraction for the ordinary and extraordinary waves $|\mu_o - \mu_x|$ is equal to the change $|\Delta \mu_o|$ or $|\Delta \mu_x|$ which takes place for a change of height equal to one vacuum wavelength divided by 2π. Unfortunately, there is not sufficient data available at present to determine this height quantitatively; for our present purposes, it will be sufficient to know that this splitting does take place at a definite height in the ionosphere, this height being at a level such that the electron density and consequently x is quite small.

We are now in a position to determine the division of energy between the extraordinary and ordinary waves. Consider first a plane wave, incident on the ionosphere at an angle ϕ and polarized so that its electric vector is in the plane of incidence. If we use the subscript i to denote the incident wave just below the point at which the wave is split into ordinary and extraordinary components, then:

$$\underline{E}_i = E_{\parallel i}\, \underline{k} \tag{31}$$

Just above the point at which the wave is split we may write the following expressions for the ordinary and extraordinary wave components, making use of (26), (27) and (28):

$$\underline{E}_o = a \left[\underline{k} + R_1\, e^{-iB}\, \underline{j}\right] \tag{32}$$

$$\underline{E}_x = b \left[\underline{k} - \frac{1}{R_1}\, e^{-iB}\, \underline{j}\right] \tag{33}$$

In the above equations R_1 denotes the value of R_o corresponding to the point in the layer at which the incident wave is split into its two components. Since x is small at this point we see by (22) that E_n may be neglected. Now since the electric vector of the incident wave must equal the sum of the electric vectors of the resulting ordinary and extraordinary waves we obtain by equating (31) to the sum of (32) and (33):

$$E_{\parallel i}\, \underline{k} = (a+b)\, \underline{k} + \left(a R_1 - \frac{b}{R_1}\, e^{-iB}\, \underline{j}\right) \tag{34}$$

and we see that:

$$a + b = E_{\parallel i} \tag{35}$$

$$a R_1 - \frac{b}{R_1} = 0 \tag{36}$$

---

[6] H. G. Booker, "Oblique Propagation of Electromagnetic Waves in a Slowly-Varying Non-Isotropic Medium", Proc. Roy. Soc. London, Vol. 155, pp. 235-257, June 1936.

Solving (35) and (36) for a and b gives $a = E_{\parallel i}/(1+R_i^2)$ and $b = R_i^2 E_{\parallel i}/(1+R_i^2)$; thus we may write:

$$\underline{E}_o = \frac{E_{\parallel i}}{1+R_i^2}\left[\underline{k} + R_i e^{-iB}\underline{j}\right] \tag{37}$$

$$\underline{E}_x = \frac{E_{\parallel i}}{1+R_i^2}\left[R_i^2\underline{k} - R_i e^{-iB}\underline{j}\right] \tag{38}$$

In order to determine the division of energy between the ordinary and extraordinary waves it will be necessary to calculate the average flow of energy by averaging the Poynting vector throughout a period of the radio wave. We may use (12) to determine $\underline{H}$ and, since x is very small at the point where the splitting takes place, μ may be set equal to unity; thus:

$$\underline{H}_i = \underline{i} \times \underline{E}_i = -E_{\parallel i}\underline{j} \tag{39}$$

$$\underline{H}_o = \underline{i} \times \underline{E}_o = -\frac{E_{\parallel i}}{1+R_i^2}\left[\underline{j} - R_i e^{-iB}\underline{k}\right] \tag{40}$$

$$\underline{H}_x = \underline{i} \times \underline{E}_x = -\frac{E_{\parallel i}}{1+R_i^2}\left[R_i^2\underline{j} + R_i e^{-iB}\underline{k}\right] \tag{41}$$

If we write $\underline{S}$ for the Poynting vector and $\overline{\underline{S}}$ for its average throughout a period of the radio wave then, introducing the time factor $e^{-i\omega t}$ and taking the real parts of the expressions for $\underline{E}$ and $\underline{H}$, we obtain:

$$\underline{S}_i = c\,\underline{E}_i \times \underline{H}_i = c\,E_{\parallel i}^2 \cos^2\omega t\,\underline{i} \tag{42}$$

$$\underline{S}_o = c\frac{E_{\parallel i}^2}{(1+R_i^2)^2}\left[\cos^2\omega t + R_i^2\cos^2(\omega t + B)\right]\underline{i} \tag{43}$$

$$\underline{S}_x = c\frac{E_{\parallel i}^2}{(1+R_i^2)^2}\left[R_i^4\cos^2\omega t + R_i^2\cos^2(\omega t + B)\right]\underline{i} \tag{44}$$

$$\overline{\underline{S}}_i = \frac{c}{2}E_{\parallel i}^2\,\underline{i} \tag{45}$$

$$\overline{\underline{S}}_o = \frac{c}{2}E_{\parallel i}^2\frac{1}{1+R_i^2}\underline{i} \tag{46}$$

$$\overline{\underline{S}}_x = \frac{c}{2}E_{\parallel i}^2\frac{R_i^2}{1+R_i^2}\underline{i} \tag{47}$$

We see from the above equations that the average energy in the incident wave is equal to the sum of the average energies in the ordinary and extraordinary waves, as would be expected, and that the ordinary wave carries the fractional part $1/(1 + R_i^2)$ of the energy in the incident wave. Thus the field intensity of the ordinary wave will be reduced by the factor $1/\sqrt{1 + R_i^2}$ due to this splitting of the incident wave.

If we now introduce the attenuation factors A_o and A_x to denote the absorption of energy in the wave while traveling through the ionosphere, then we obtain the following expressions for the average energy of the ordinary and extraordinary downcoming waves as they emerge from the ionosphere:

$$\bar{S}_o = \frac{c}{2} E_{\parallel i}^2 \frac{A_o^2}{1 + R_i^2} \, i \tag{48}$$

$$\bar{S}_x = \frac{c}{2} E_{\parallel i}^2 \frac{R_i^2 A_x^2}{1 + R_i^2} \, i \tag{49}$$

Now if we write R_d for the value of R_o at the point where the ordinary wave assumes its limiting polarization as it emerges from the ionosphere, then we obtain the following expressions for the electric and magnetic field intensities and the average energy of the ordinary downcoming wave:

$$E_{od} = a \left[\cos \omega t \, k + R_d \cos (\omega t + B) \, j \right] \tag{50}$$

$$H_{od} = - a \left[\cos \omega t \, j - R_d \cos (\omega t + B) \, k \right] \tag{51}$$

$$\bar{S}_{od} = \frac{c}{2} a^2 (1 + R_d^2) \, i \tag{52}$$

Since (48) and (52) are equal we obtain the following expression for a:

$$a = \frac{A_o E_{\parallel i}}{\sqrt{1 + R_i^2} \sqrt{1 + R_d^2}} \tag{53}$$

and, upon substituting this in (50), we obtain finally the following expression for the downcoming ordinary wave:

$$E_{od} = \frac{A_o E_{\parallel i}}{\sqrt{1 + R_i^2} \sqrt{1 + R_d^2}} \left[\cos \omega t \, k + R_d \cos(\omega t + B) \, j \right] \tag{54}$$

In a similar manner we may obtain an expression for the downcoming extraordinary wave:

$$\underline{E}_{xd} = \frac{R_i A_x E_{\parallel i}}{\sqrt{1 + R_i^2}\ \sqrt{1 + R_d^2}} \left[R_d \cos\omega t\ \underline{k} - \cos(\omega t + B)\ \underline{j} \right] \qquad (55)$$

The above expressions are for the case when the electric field of the incident wave lies in the plane of incidence; we shall next consider the case where the electric field of the incident wave is normal to the plane of incidence:

$$\underline{E}_i = E_{\perp i}\ \underline{j} \qquad (56)$$

By carrying through a procedure similar to that used above we obtain the following expressions for the downcoming ordinary and extraordinary waves when the incident wave is polarized normal to the plane of incidence:

$$\underline{E}_{od} = \frac{R_i A_o E_{\perp i}}{\sqrt{1 + R_i^2}\ \sqrt{1 + R_d^2}} \left[\cos\omega t\ \underline{k} + R_d \cos(\omega t + B)\ \underline{j} \right] \qquad (57)$$

$$\underline{E}_{xd} = \frac{A_x E_{\perp i}}{\sqrt{1 + R_i^2}\ \sqrt{1 + R_d^2}} \left[R_d \cos\omega t\ \underline{k} - \cos(\omega t + B)\ \underline{j} \right] \qquad (58)$$

The above equations (54), (55), (57) and (58) are applicable at any radio frequency and for transmission paths between any two points on the surface of the earth;[7] they indicate that, for an incident wave on the ionosphere with its electric vector either parallel or perpendicular to the plane of incidence, both ordinary and extraordinary waves will, in general, be transmitted through the ionosphere. An observer, of course, sees only the resultant vector sum of the ordinary and extraordinary downcoming waves; before discussing this resultant downcoming wave in more detail, however, it will be desirable to determine separately the polarization characteristics of the ordinary and extraordinary waves. In order to evaluate the above equations it will be necessary to obtain expressions for x and for y_n, $y_\perp$ and $y_\parallel$. If we take $(e/m) = 1.7592 \times 10^7$ e.m.u., $e = 4.8025 \times 10^{-10}$ e.s.u. and $c = 2.99776 \times 10^{10}$ cm./sec., then

$$x = 8.0618 \times 10^{-5}\ N/f_{mc}^2 \qquad (59)$$

where f_{mc} = radio frequency expressed in megacycles per second

$$f_{hmc} = 2.800\ H^o(\text{gauss}) \qquad (60)$$

---

[7] In certain rare cases, the ordinary and extraordinary waves reverse their modes of propagation before returning to the earth; equations (54) to (58) would not be applicable in those cases. However, such situations are seldom encountered in practice; these phenomena are described in the paper by Booker cited in footnote[6].

where f_{hmc} = magneto-ionic frequency expressed in megacycles per second H^o is the intensity of the magnetic field of the earth at the point in the ionosphere under consideration. The relation between the intensity of the earth's field at the height h (expressed in kilometers) and its value, H_o^o, at the earth's surface may be approximately written as follows:

$$H^o = H_o^o (1 - 0.0005\ h) \tag{61}$$

Since the radio waves, irrespective of frequency, are probably split into their separate components in the E layer of the ionosphere at a height of approximately 100 km., equation (60) may be expressed in terms of the magnetic field intensity at the surface of the earth as follows:

$$f_{hmc}\ (\text{at } 100 \text{ km}) = 2.660\ \ H_o^o\ (\text{gauss}) \tag{62}$$

Since H_o^o varies from about 0.25 at the magnetic equator up to about 0.7 at the magnetic poles, f_{hmc} varies from about 0.65 mc at the magnetic equator up to about 1.9 mc at the magnetic poles.

The expressions for y_n, $y_\perp$ and $y_\parallel$ involve the direction of propagation Θ, the angle of incidence at the ionosphere, ϕ, and the angle of inclination of the earth's magnetic field, I; thus:

$$y_n = (f_h/f)\ (\pm \sin I \cos \phi - \cos I \sin \phi \cos \Theta) \tag{63}$$

$$y_\perp = -(f_h/f) \sin \Theta \cos I \tag{64}$$

$$y_\parallel = (f_h/f)\ (\sin I \sin \phi \pm \cos I \cos \phi \cos \Theta) \tag{65}$$

In the above equations the upper (positive sign) corresponds to the incident wave while the lower sign corresponds to the downcoming wave.

To determine the values of R_i and R_d we may set $x = 0$ in equation (24) and obtain

$$A\ e^{iB} = (y_\parallel y_\perp - z\ y_n) + i\ y_n \tag{66}$$

The value of z to use in evaluating (66) is rather uncertain due to the lack of knowledge of the exact height at which the downcoming waves assume their limiting polarizations. There is some evidence that this absorption has an influence on the limiting polarizations at broadcast frequencies, so we will arbitrarily take $z = 0.306$ at 1 mc; at higher frequencies $z = \nu/f$ and will consequently decrease very rapidly with increasing frequency. Since a greater number of electrons are required for a given effect on the radio waves at the higher frequencies (see (59)), the downcoming waves will assume their limiting polarizations at higher heights on the high frequencies and, at these heights, ν will be smaller. Consequently, in the calculations which follow, it will be assumed that $z = 0.306/f_{mc}^2$. It is to be hoped that measure-

ments of the limiting polarization of radio waves, or other types of measurements, can be made to determine more accurately the appropriate values of z to be used in equation (66); in the meantime the above assumption will probably yield results which will properly illustrate the phenomena involved.

From the above equations we see that the polarization of the downcoming waves depends upon the frequency, f, the magneto-ionic frequency, f_h, the direction of propagation, θ, the angle of incidence at the ionosphere, ϕ,[8] and the angle of inclination of the earth's magnetic field, I. In order to illustrate the phenomena we will consider the nature of the propagation between points in the United States. The value of f_h varies throughout the United States from about 1.37 up to 1.65 mc, averaging about 1.53 mc while the value of I varies from about 60° to 76° averaging about 68° 30'; we will use these average values of f_h and of I in the following calculations.

Figure 1 shows the polarization ellipses for the downcoming ordinary and extraordinary waves for propagation in the United States at a frequency of 1 mc from West to East ($\theta = 90°$) and for an angle of incidence at the ionosphere, ϕ, equal to 45°. Notice that the major axis of the ordinary wave ellipse (solid curve) is at right angles to the major axis of the extraordinary wave ellipse (dotted curve) and that the ratios of the major to the minor axes of the ellipses are the same for the two waves; this will always be the case when the ordinary and extraordinary waves leave the ionosphere at the same or nearly the same place. The shape of the extraordinary wave ellipse can always be determined by rotating the ordinary wave ellipse in a clockwise direction in the $\underline{j} - \underline{k}$ plane. The rotation with time of the electric vector of the ordinary wave as viewed by an observer looking back along the wave normal in the negative $\underline{i}$ direction is clockwise while it is counterclockwise for the extraordinary wave in this particular case. In general, the rotation of the electric vector of the ordinary wave is clockwise when the direction of propagation of the wave makes an acute angle with the direction of the earth's magnetic field and is counterclockwise when the direction of propagation makes an obtuse angle with the direction of the earth's magnetic field. The electric vector always rotates in opposite directions for the ordinary and extraordinary waves. It should be noted that the major axis of the ordinary wave ellipse lies very nearly along the line formed by the projection of the earth's magnetic field on the $\underline{j} - \underline{k}$ plane; the slight difference in these directions (3° 20' in this case) is due to the finite value of collision frequency at the point where the downcoming ordinary wave assumes its limiting polarization. At this frequency the downcoming extraordinary wave is much weaker than the downcoming ordinary wave ($A_x << A_o$) so that, for most practical purposes, the resultant downcoming wave is represented by the ordinary wave alone.

---

[8] The relation between the angle of incidence, ϕ, at the ionosphere, the angle of elevation of the downcoming radio waves, the virtual height of the ionosphere and the distance are discussed in the paper by K. A. Norton, S. S. Kirby, and G. H. Lester, "An Analysis of Continuous Records of Field Intensity at Broadcast Frequencies", Proc. IRE, Vol. 23, pp. 1183-1200, October 1935.

Figure 2 is the same as figure 1 except that the propagation is from East to West instead of from West to East; we see that the downcoming waves are substantially different in this case, illustrating the fact that reciprocity relations do not apply for ionospheric wave propagation.

Figure 3 is the same as Figures 1 and 2 but now for the case of North to South propagation. In this case the ordinary wave ellipse has a rather small component and, at this frequency, since the extraordinary wave is comparatively weak, the resultant downcoming wave may be expected to have a fairly small horizontal component of electric force. The slight tilt of the major axis of the ellipse in this case is due entirely to the slight amount of absorption (finite value of z) assumed at the point where the downcoming wave assumes its limiting polarization. When the angle of incidence at the ionosphere in this case of North-South propagation is increased to a value such that $\phi = I$ ($68^\circ\ 30'$ in this particular case), the ordinary wave ellipse degenerates into a line along the $\underline{k}$ axis while the extraordinary wave ellipse degenerates into a line along the $\underline{j}$ axis. This occurs at all frequencies; at frequencies near the magneto-ionic frequency, f_h, it should result in downcoming ionospheric waves with practically no horizontal component of electric force since the extraordinary component will be negligibly small ($A_x << A_o$). When reflection is assumed at a 100 km layer, as is probably the case for frequencies near f_h, the distance of propagation corresponding to $\phi = 68^\circ\ 30'$ is equal to 335 miles. Thus, at this distance South of a broadcasting station operating on a frequency near 1.5 mc, the electric vector of the downcoming ionospheric wave should lie almost entirely in the plane of incidence. This condition might be found useful in testing a direction finder for errors other than polarization error, or possibly for determining the magnitude of the changes from the great circle transmission path in such a case. When ϕ is greater than I in this case of North-South propagation, the direction of propagation makes an obtuse angle with the earth's magnetic field and the rotation of the electric vector of the ordinary wave is then counterclockwise.

Figure 4 shows the downcoming extraordinary and ordinary wave ellipses for the case of South-North transmission in the United States on a frequency of 1 mc and now for three different values of $\phi = 21^\circ\ 30' = (90^\circ - I)$, 45° and 75°. It will be noted that R_d decreases with increasing ϕ (and thus also with increasing distance) having a value of 1 for $\phi = 21^\circ\ 30'$, a value of 0.8812 for $\phi = 45^\circ$ and a value of 0.4826 for $\phi = 75^\circ$; because of the curvature of the earth ϕ never has a value much greater than 75° -- see reference in footnote 8. The case of $\phi = (90^\circ - I)$ is of particular interest because it affords a method of measuring the value of z to be used in making calculations of the polarization of downcoming ionospheric waves. If measurements are made near the magneto-ionic frequency, f_h, only the ordinary wave will be received and it will be possible to study its polarization ellipse alone. When $\phi = (90^\circ - I)$ and $\Theta = 0$, R_d will be equal to 1, irrespective of the value of z, and cot $B = -z$. Thus, when $z = 0$, $B = 270^\circ$ and the ordinary wave ellipse is a circle but, for finite values of z, B will lie between 270° and 360° and z may be determined by measuring the ratio of the minor to the major axes of the ordinary wave ellipse. In fact, if we write K for this ratio then:

$$z = (1 - K^2)/2K \qquad \text{(where } \phi = 90^\circ - I \text{ and } \Theta = 0\text{)} \qquad (67)$$

Measurements might also be made at frequencies far removed from f_h by separating the ordinary and extraordinary waves by means of a pulse technique.

Figures 1 to 4 illustrate the general nature of the polarization of downcoming radio waves in regions, such as the United States, where the earth's magnetic field has a larger vertical than horizontal component. The propagation in equatorial regions, on the other hand, where the earth's field is nearly horizontal, will be markedly different. Consider, for example, the case of propagation at the magnetic equator where I = 0. When I = 0 we obtain by (63), (64) and (65):

$$y_n = \mp (f_h/f) \sin \phi \cos \theta \qquad (I = 0) \qquad (68)$$

$$y_\perp = - (f_h/f) \sin \theta \qquad (I = 0) \qquad (69)$$

$$y_\parallel = \pm (f_h/f) \cos \phi \cos \theta \qquad (I = 0) \qquad (70)$$

The upper sign in (68) and (70) corresponds to the incident wave while the lower sign corresponds to the downcoming wave. Now in the case of East-West or West-East propagation $y_n = y_\parallel = 0$, $A = 0$, $R_i = R_d = 0$ and we see by equations (54) and (58) that the resultant downcoming wave may be expressed:

$$\underline{E}_{od} = A_o E_{\parallel i} \cos \omega t \, \underline{k} \qquad (71)$$

where $I = 0$, $\theta = 90^\circ$ or 270°, $\underline{E}_i = E_{\parallel i} \underline{k}$

in case the electric vector of the incident wave lies in the plane of incidence or by:

$$\underline{E}_{xd} = - A_x E_{\perp i} \cos \omega t \, \underline{j} \qquad (72)$$

where $I = 0$, $\theta = 90^\circ$ or 270°, $\underline{E}_i = E_{\perp i} \underline{j}$

when the electric vector of the incident wave is normal to the plane of incidence. Thus we see that the downcoming wave will be linearly polarized in the same plane as the incident wave. At frequencies near the magneto-ionic frequency, f_h, there will be no downcoming wave when the incident wave is horizontally polarized.

On the other hand, for North-South or South-North propagation at the magnetic equator (I = 0), the propagation will be similar to that in the United States, differing principally in the magnitudes of the parameters and in the absence of the particular case $\phi = 90^\circ - I$.

We will now turn to a consideration of the effect of frequency on the propagation. Figures 1 to 4 are all for a frequency of 1 mc; as we go to the higher frequencies R_i and R_d become larger and B approaches nearer to 90° or 270° -- both of these effects causing the downcoming wave ellipses to become more nearly circular. Figure 5 shows the polarization ellipses for propagation from West to East in the United States for $\phi = 70^\circ$ and for the frequencies f = 1, 2, 5 and 20 mc. At the higher frequencies, the

attenuation of the extraordinary wave is approximately the same as that of the ordinary wave so that both the extraordinary and ordinary waves are important components of the resultant downcoming wave.

Before considering in more detail the nature of the resultant downcoming wave (the vector sum of the ordinary and extraordinary downcoming waves) it will be desirable to discuss the nature and cause of the fading of radio waves. There are two causes for the fading of ionospheric waves: Phase interference between waves traveling along slightly different paths in the ionosphere and changes in the absorption of the radio waves due to variations in the ionization distribution in the ionosphere. The phase interference is responsible for the rapid changes in intensity which occur from minute to minute while the changes of absorption are responsible for the slower changes in the average level of the received fields which occur from hour to hour and from day to day.

The fading due to phase interference will be discussed first. The under surface of the ionosphere is irregular, probably consisting of clouds of ions, etc., distributed in such a manner that a single downcoming ionospheric wave actually consists of a large number of component waves, each of which has been reflected at a slightly different place in the ionosphere. These separate wave components, since they have traveled along slightly different paths through the ionosphere, will arrive at the ground with random relative phases. As these relative phases of the separate wave components change with time, the resultant downcoming ionospheric wave (the vector sum of the component waves) will vary in amplitude over a wide range. This is the cause of the rapid changes in intensity which occur from minute to minute in a downcoming ionospheric wave. The distribution of the intensity of such an ionospheric wave with time is given by the Rayleigh distribution.[9] If we write P for the percentage of time that the field intensity, E, of the resultant downcoming wave is exceeded, we obtain by the use of Lord Rayleigh's theory:

$$P = 100\, e^{-(E/E_o)^2} \tag{73}$$

$$E\, e^{-i(\omega t + \alpha)} = E_1\, e^{-i(\omega t + \alpha_1)} + \ldots + E_1\, e^{-i(\omega t + \alpha_i)} + \ldots + E_n\, e^{-i(\omega t + \alpha_n)} \tag{74}$$

$$E_o^2 = E_1^2 + E_2^2 + \ldots + E_i^2 + \ldots + E_n^2 \tag{75}$$

In the above E_i represents the field intensity of one of the n component downcoming waves; α_i represents the phase of the i^{th} component wave and is assumed to be random; E_o^2 is proportional to the average energy of the

---

[9] Lord Rayleigh, "On the Resultant of a Large Number of Vibrations of the Same Pitch and of Arbitrary Phase", Phil. Mag., Vol. 10, pp. 73-78, 1880; see also the book "Theory of Sound", 2nd edition, paragraph 42a, 1894.

downcoming wave over a period of several fading cycles; E_o would be the intensity of the downcoming wave if the under surface of the ionosphere had been smooth and there were no fading; α is the phase of the resultant wave. Equation (73) may be used to determine the distribution of the intensity with time of the vector sum of several waves with random relative phases whenever n is large (greater than 4 or 5) and each wave is much smaller than the root-sum-square value of all of the waves, i.e., $E_i^2 << E_o^2$. It has been found experimentally[10] that equation (73) is applicable to downcoming ionospheric waves at broadcast frequencies both in the standard band and in the international bands; it seems likely that it will be applicable to ionospheric waves at any frequency except possibly at very low frequencies (below 100 kc) where the path length differences between the component waves may not be comparable to the wavelength. It may be observed that the above theory as to the cause of fading is consistent with the observed fact that the fading rate increases with increasing frequency since a given change in the ionosphere would be responsible for larger phase changes at the higher frequencies.

If we let $F \equiv E/E_o$ denote the ratio of the instantaneous amplitude E to the amplitude E_o of the electric field which would be present if the energy of the downcoming wave had not been separated into n wave components with random relative phases, then

$$P = 100\, e^{-F^2} \qquad (76)$$

The above equation (which is the equivalent of (73)) is shown graphically in Figure 6 and we see that, as a result of the separation of the downcoming wave into a large number of component waves, the instantaneous intensity will exceed 2 E_o for 1.83% of the time, will exceed E_o for only 36.8% of the time, will be less than 0.5 E_o for 22.1% of the time and will be less than 0.1 E_o for 1% of the time.

It should be noted that the instantaneous energy of the resultant wave (the vector sum of the scattered components) will reach values much greater than the average energy of the corresponding unscattered wave; for example, for 1.83% of the time the instantaneous energy of the vector sum of the scattered waves will be four or more times the average energy of the corresponding unscattered wave. Nevertheless, the average energy of the resultant wave (averaged over a period of time including several fading cycles) will be equal to the average energy of the corresponding

---

[10] The experimental proof that equation (73) is applicable to the fading of ionospheric waves was given in a paper by Kenneth A. Norton, "The Nature of Sky Wave Propagation" presented at a meeting of the Baltimore section of the Institute of Radio Engineers in January 1941 and later at the Fourth Annual Broadcast Engineering Conference at Ohio State University in February 1941. It is expected that this paper will be published in the Proceedings of the Institute of Radio Engineers.

unscattered wave. This may be proven as follows: The instantaneous energy of the resultant wave will be proportional to E^2 and E will lie between E and E d E for the percentage of time

$$d P = 200 \frac{E}{E_o^2} e^{-(E/E_o)^2} d E \qquad (77)$$

Thus we may determine the average value of E^2 over a large number of fading cycles as follows:

$$\overline{E^2} = \frac{\int_o^\infty E^2 \, d P}{\int_o^\infty d P} = E_o^2 \qquad (78)$$

and we see that the average energy of the vector sum of the scattered waves is equal to the average energy of the equivalent unscattered wave.

From the above discussion we see that, in order to take account of the fading due to phase interference, equations (54), (55), (57) and (58) may simply be multiplied by the factor F; F may have any value between o and ∞, the percentage of time that F exceeds a particular value being given by equation (76). Since the instantaneous value of F for the ordinary wave will be different in general from the instantaneous value of F for the extraordinary wave (since the bundle of waves making up the ordinary wave will have traveled separate paths from those followed by the bundle of waves constituting the extraordinary wave) we will write F_o for the ordinary wave phase interference factor and F_x for the extraordinary wave phase interference factor.

We are now in a position to write down our final expressions for the instantaneous intensity of the resultant downcoming ionospheric waves. If we write δ where $\delta \equiv (\alpha_x - \alpha_o)$ for the instantaneous phase difference between the ordinary and extraordinary waves due to the difference in the paths followed by the ordinary and extraordinary wave bundles in traveling through the ionosphere, we obtain the following expressions for the instantaneous intensity of the resultant downcoming ionospheric waves for the two cases when the incident wave is polarized either $\parallel$ or $\perp$ to the plane of incidence:

$$\underline{E}_d = \frac{E_{\parallel i} A_o e^{-i(\omega t + \alpha_o)}}{\sqrt{1 + R_i^2} \sqrt{1 + R_d^2}} \left[\left\{ F_o + \frac{R_i R_d A_x F_x}{A_o} e^{-i\delta} \right\} \underline{k} + \left\{ R_d F_o - \frac{R_i A_x F_x}{A_o} e^{-i\delta} \right\} e^{-iB} \underline{j} \right] \qquad (79)$$

where $\underline{E}_i = E_{\parallel i} \underline{k}$

$$\underline{E}_d = \frac{E_{\perp i} A_o e^{-i(\omega t + \alpha_o)}}{\sqrt{1 + R_i^2}\sqrt{1 + R_d^2}} \left[\left\{ R_i F_o + \frac{R_d A_x F_x}{A_o} e^{-i\delta} \right\} \underline{k} + \left\{ R_i R_d F_o - \frac{A_x F_x}{A_o} e^{-i\delta} \right\} e^{-iB} \underline{j} \right] \qquad (80)$$

where $\underline{E}_i = E_{\perp i} \underline{j}$

So far we have discussed only the rapid fading, occurring from minute to minute, and due to phase interference. The changes in absorption in the ionosphere are also responsible for very large changes in the received field, but these take place at a much less rapid rate; these changes exhibit themselves in equations (79) and (80) by changes in the attenuation factors A_o and A_x. We know from experiment that A_o and A_x may change from hour to hour and from day to day over ranges of more than 100 to 1; in general, however, these changes will occur more or less simultaneously for the ordinary and extraordinary waves so that the ratio of A_x to A_o will be comparatively constant; this is particularly true at the higher frequencies where, in addition, the actual changes in A_o and A_x are less than at the lower frequencies. In any case, since this fading, due to changes in ionosphere absorption, occurs at a comparatively slow rate, we can assume that the ratio A_x/A_o will be comparatively constant for periods of an hour or more.

We are now in a position to interpret (79) and (80). F_o and F_x vary independently of each other from minute to minute from 0 up to very large values while simultaneously δ will vary at random in such a manner that all values of δ between 0 and π are equally likely. For given values of F_o and F_x, the $\parallel$ component of the resultant downcoming wave will be a maximum when $\delta = 0$ and the $\perp$ component will simultaneously be a minimum; conversely, when $\delta = \pi$ the $\parallel$ component will be a minimum while the $\perp$ component will simultaneously be a maximum. As these changes in the relative intensities of the $\parallel$ and $\perp$ components of the downcoming wave take place the resultant wave will change from an ellipse with its major axis vertical to an ellipse with its major axis horizontal, these changes taking place within a few seconds. It should be noted that the phase between the $\perp$ and $\parallel$ components will also be varying rapidly with time and this will also cause the polarization ellipse of the resulting wave to change its shape and the angle of its major axis to the vertical.

In the study of radio direction finding the variables of particular interest are the ratio of the amplitude and the relative phase between the $\parallel$ and $\perp$ components in the downcoming wave. We see by (79) and (80) that they may be expressed as follows:

$$\left(E_{\perp d}/E_{\parallel d}\right) = \frac{\left[R_d - R_i\, q(A_x/A_o) \cos\delta + i\, R_i\, q(A_x/A_o) \sin\delta\right] e^{-iB}}{\left[1 + R_i R_d\, q(A_x/A_o) \cos\delta - i\, R_i R_d\, q(A_x/A_o) \sin\delta\right]} \qquad (81)$$

where $\underline{E}_i = E_{\parallel i}\,\underline{k}$

$$(E_{\perp d}/E_{\parallel d}) = \frac{\left[R_i R_d - q(A_x/A_o)\cos\delta + i\,q(A_x/A_o)\sin\delta\right] e^{-iB}}{\left[R_i + R_d\,q(A_x/A_o)\cos\delta - i\,R_d\,q(A_x/A_o)\sin\delta\right]} \qquad (82)$$

where $\underline{E}_i = E_{\perp i}\,\underline{j}$

To obtain the above equations, we have introduced the ratio $q \equiv F_x/F_o$ so that the only quantities varying rapidly with time in (81) and (82) are q and δ, q being variable from zero up to a very large value and δ between 0 and π. In order to determine the distribution of q with time we may make use of the following theorem.[11]

Suppose a variable x is distributed in accordance with a probability law $\int_o^\infty f(x)\,dx = 1$; and a variable y in accordance with a probability law $\int_o^\infty g(y)\,dy = 1$, x and y being independently distributed. Then the quotient, $z = x/y$, will be distributed according to the law $\int_o^\infty Q(z)\,dz = 1$, where

$$Q(z) = \int_o^\infty f(zy)\,g(y)\,y\,dy \qquad (83)$$

In order to apply the above theorem to the determination of the distribution of q with time we may identify F_o with x, F_x with y and q with z. Then:

$$f(F_o) = 2F_o e^{-F_o^2} \qquad (84)$$

$$g(F_x) = 2F_x e^{-F_x^2} \qquad (85)$$

$$Q(q) = 4\int_o^\infty q\,F_x^3\,e^{-(1+q^2)F_x^2}\,dF_x = \frac{2q}{(1+q^2)^2} \qquad (86)$$

Thus, we see that the percentage of time, P, that the instantaneous ratio (F_x/F_o) will be greater than q is given by:

$$P = 100\left[1 - \int_o^q \frac{2q}{(1+q^2)^2}\,dq\right] = \frac{100}{1+q^2} \qquad (87)$$

This distribution of q with time is shown graphically in Figure 7; we see that for 1% of the time q will be greater than 10, for 10% of the time q will be greater than 3, for 50% of the time q will be greater than 1 and for 90% of the time q will be greater than 1/3. In order finally to calculate the distribution with time of the amplitudes and phases of $(E_{\perp d}/E_{\parallel d})$ we must introduce the variations of q and of δ with time in (81) and (82).

---

[11] E. V. Huntington, "Frequency Distribution of Product and Quotient", "The Annals of Mathematical Statistics", pp. 195-198, Vol. X, No. 2, June, 1939.

There is no simple means of accomplishing this analytically so we will resort to graphical methods, keeping q fixed at 10 predetermined values and calculating the distribution of $(E_{\perp d}/E_{\parallel d})$ as a function of δ, all values of δ between 0 and π being considered equally likely. The 10 values of q used are the averages of the values of q in the intervals from 0 to 10%, 10% to 20%, etc., as shown on Figure 7. These 10 values of q are 6.218, 2.419, 1.743, 1.366, 1.108, 0.9058, 0.7334, 0.5783, 0.4190, and 0.2175.

For purposes of calculation, equations (81) and (82) may be still further simplified by introducing the following angles:

$$\tan C_1 = \frac{\sin \delta}{(R_d A_o/R_i\, q\, A_x) - \cos \delta} \tag{88}$$

$$\tan C_2 = \frac{\sin \delta}{(A_o/R_i\, R_d\, q\, A_x) + \cos \delta} \tag{89}$$

$$\tan C_3 = \frac{\sin \delta}{(R_i\, R_d\, A_o/q\, A_x) - \cos \delta} \tag{90}$$

$$\tan C_4 = \frac{\sin \delta}{(R_i\, A_o/R_d\, q\, A_x) + \cos \delta} \tag{91}$$

$$(E_{\perp d}/E_{\parallel d}) = \frac{\sin C_2}{R_d \sin C_1}\, e^{i(C_1 + C_2 - B)} \equiv \left| E_{\perp d}/E_{\parallel d} \right| \cdot e^{-i(B - \gamma)} \tag{92}$$

where $\underline{E}_i = E_{\parallel i}\, \underline{k}$

$$(E_{\perp d}/E_{\parallel d}) = \frac{\sin C_4}{R_d \sin C_3}\, e^{i(C_3 + C_4 - B)} \equiv \left| E_{\perp d}/E_{\parallel d} \right| \cdot e^{-i(B - \gamma)} \tag{93}$$

where $\underline{E}_i = E_{\perp i}\, \underline{j}$

When a determination is to be made of the distribution of the relative phase alone the following equations will be found useful:

$$\tan \gamma = \frac{(1 + R_d^2) \sin \delta}{(R_d A_o/R_i A_x\, q) - R_i R_d\, q\, (A_x/A_o) - \cos \delta\, (1 - R_d^2)} \tag{94}$$

where $\underline{E}_i = E_{\parallel i}\, \underline{k}$

$$\tan \gamma = \frac{(1 + R_d^2) \sin \delta}{(R_i R_d A_o/A_x\, q) - (R_d\, q\, A_x/A_o\, R_i) - \cos \delta\, (1 - R_d^2)} \tag{95}$$

where $\underline{E}_i = E_{\perp i}\,\underline{j}$

Figure 8 shows $|E_{\perp d}/E_{\parallel d}|$ while Figure 9 shows $(B = \gamma)$ as a function of δ for the above 10 values of q and for the particular case of an ionospheric wave on 5 mc for West to East transmission and for an angle of incidence at the ionosphere, $\phi = 70^\circ$; the curves in this figure correspond to a wave from the transmitting station polarized perpendicular to the plane of incidence at the ionosphere, e.g. horizontally polarized. (Parenthetically it may be mentioned that the waves from a horizontal dipole transmitting antenna are actually polarized parallel to the plane of incidence when the direction of transmission is off the end of the dipole).* In determining these curves the assumption was made that $(A_x/A_o) = 1$; this will be approximately true under most circumstances at the higher frequencies. Figures 8 and 9 are drawn only for the positive values of δ between 0° and 180°; we may obtain the corresponding values for a complete cycle of δ from -180° to $+180^\circ$ by noting that a change in the sign of δ does not change the value of $|E_{\perp d}/E_{\parallel d}|$ but does change the sign of γ. Since all values of δ are equally likely we see that Figure 8 also shows (for a given value of q) the percentage of time that $|E_{\perp d}/E_{\parallel d}|$ is less than the value shown on the curve. Finally, since these 10 values of q will each be present (on the average) for 1/10 of the time, we may determine the percentage of time that $|E_{\perp d}/E_{\parallel d}|$ is less than some particular value by averaging the ten percentages shown on Figure 8 for the 10 values of q; for example, the percentage of time that $|E_{\perp d}/E_{\parallel d}| < 4$ is given by $(84 + 84.5 + 86 + 88.5 + 98 + 100 + 100 + 100 + 100 + 100)/10 = 94.1\%$. These overall percentages are shown on Figure 10 but now the percentage scale at the bottom of the figure shows the percentage of the time that $|E_{\perp d}/E_{\parallel d}|$ exceeds the ordinate values, e.g. $|E_{\perp d}/E_{\parallel d}| > 4$ for $(100 - 94.1) = 5.9\%$ of the time. The distribution of $|E_{\perp d}/E_{\parallel d}|$ is also shown on Figure 10 for the case where the wave from the transmitter is polarized parallel to the plane of incidence at the ionosphere, e.g. vertically polarized. Figure 10 also gives the distributions for a 1 mc wave for the two cases where the wave from the transmitter is polarized either perpendicular or parallel to the plane of incidence; since 1 mc is near the magneto-ionic frequency, f_h, (A_x/A_o) has been assumed to be 0.1 in this case.

It will be noted on Figure 10 that, for both frequencies, $|E_{\perp d}/E_{\parallel d}|$ is larger when the transmitted wave is polarized perpendicular to the plane of incidence. In the limit, as (A_x/A_o) approaches zero, $|E_{\perp d}/E_{\parallel d}|$ becomes constant and equal to R_d regardless of the polarization of the transmitted wave; this is the case, for example, at the magneto-ionic frequency, f_h, where the extraordinary wave is completely absorbed. Under certain circumstances, near the maximum usable frequency[12] for a given layer in the ionosphere, the ordinary wave will penetrate the layer and will not be returned

---

* See Appendix I.

[12] The maximum usable frequency was formerly given in the National Bureau of Standards reports on "High Frequency Radio Transmission Conditions" as published each month in the Proceedings of the Institute of Radio Engineers. These data may now be obtained by responsible organizations by writing directly to the National Bureau of Standards.

to the earth while, simultaneously, the extaordinary wave will be received with its normal intensity; in this case (A_x/A_o) will become very large and $|E_{\perp d}/E_{\parallel d}|$ will again be constant regardless of the polarization of the transmitted wave but, in this case, will be equal to $1/R_d$ since the extraordinary wave alone is received. As the frequency is increased well above the magneto-ionic frequency R_i and R_d approach 1 and, except near the maximum usable frequency, (A_x/A_o) approaches 1 and the distribution of $|E_{\perp d}/E_{\parallel d}|$ becomes equal to the distribution of q as shown by the dashed curve on Figure 10. On the other hand, as the frequency is decreased well below the magneto-ionic frequency, (A_x/A_o) approaches 1, as before, but R_i and R_d become smaller rather than larger; thus, the median (50%) values of $|E_{\perp d}/E_{\parallel d}|$ will be much less than one when the transmitted wave is vertically polarized as is usually the case at these lower frequencies. The median values of $|E_{\perp d}/E_{\parallel d}|$ are given by the following formulas:

$$\left|E_{\perp d}/E_{\parallel d}\right|_m = \sqrt{\frac{R_d^2 + R_i^2 (A_x/A_o)^2}{1 + R_i^2 R_d^2 (A_x/A_o)^2}} \qquad (96)$$

where $\underline{E}_i = E_{\parallel i}\, \underline{k}$

$$\left|E_{\perp d}/E_{\parallel d}\right|_m = \sqrt{\frac{R_i^2 R_d^2 + (A_x/A_o)^2}{R_i^2 + R_d^2 (A_x/A_o)^2}} \qquad (97)$$

where $\underline{E}_i = E_{\perp i}\, \underline{j}$

The values calculated from the above formulas in the examples shown on Figure 10 are (a) 0.4312, (b) 0.4691, (c) 0.9254, and (d) 1.0806 and when these are compared with the values shown on Figure 10 it is evident that the graphical method gives values which are slightly too large. The reason for this is that too few values of q were used in the graphical method. Another possible means of improving the accuracy of the graphical method would be the use of values of q determined by averaging the logarithms of q through the intervals from 0 to 10%, etc; the ten values of q obtained in this way are 5.081, 2.403, 1.737, 1.364, 1.106, 0.9042, 0.7329, 0.5756, 0.4162, and 0.1968 and, since the values less than 1 are the reciprocals of the values greater than 1, their use would probably yield slightly more accurate results in the graphical method of determining the distribution curves than the arithmetic average values of q actually used.

We turn now to a discussion of the relative phase between $E_{\perp d}$ and $E_{\parallel d}$. We see by equations (92) and (93) that it is given by $(B - \Upsilon)$ and, since $\Upsilon_{-\delta} = -\Upsilon + \delta$, the relative phase is determined for a complete cycle of δ from -180° to $+180^\circ$ when calculations of Υ are made for δ between 0 and $+180^\circ$. Figure 11 shows the percentage of time that the relative phase between $E_{\perp d}$ and $E_{\parallel d}$ exceeds the ordinate values. For example, 50% of curve

(d) was obtained by averaging the percentages on Figure 9 for the 10 values of q and the remaining 50% obtained by using the average percentages corresponding to negative values of γ. Figure 12 gives the results of Figure 11 in a more useful way, showing the relative probability that the relative phase between $E_{\perp d}$ and $E_{\parallel d}$ will be within $\pm$ 10° of the abscissae; it shows that the most probable value of the relative phase is B in cases (a), (b) and (c) while the most probable value of the relative phase in case (d) is (B - 180°). In general, the most probable value of the relative phase between $E_{\perp d}$ and $E_{\parallel d}$ in the downcoming wave is the relative phase between $E_{\perp}$ and $E_{\parallel}$ in the stronger of the two ordinary and extraordinary wave components in the downcoming wave. The distribution of relative phase is of importance in direction finding since a direction finder will be subject to large errors only when the relative phase between $E_{\perp d}$ and $E_{\parallel d}$ lies between certain fairly narrow ranges of values; if, in the design of the direction finder, these undesired relative phases could be made to have values much different from B or (B - 180°), an improvement in the bearings obtained by the direction finder would result. However, as is evident on the curves of Figure 12, this possibility of improvement would be less at the higher frequencies and would not exist at all in the limit as $R_i = R_d = (A_x/A_o) = 1$, in which case the relative phase between $E_{\perp d}$ and $E_{\parallel d}$ becomes truly random. As we approach the magneto-ionic frequency, f_h, (A_x/A_o) approaches zero and the values of the relative phase near B become more and more probable. Also, as we approach the maximum usable frequency for a given ionospheric layer, (A_x/A_o) will, more or less discontinuously, become very large and the relative phase between $E_{\perp d}$ and $E_{\parallel d}$ will again become constant and equal to (B - 180°). At low frequencies, where the transmitted waves are usually vertically polarized, the ordinary wave will be the stronger component in the downcoming wave so that the most probable value of the relative phase will be B.

The examples given and some of the conclusions reached in the above discussion are typical only of the case where $y_{\parallel}^2 > y_{\perp}^2$ so that R_i and R_d are less than 1; we see by (64) and (65) that this is always the case for North-South or South-North propagation regardless of the value of I and is also the case for East-West or West-East propagation when $\sin \phi > \cot I$. As we go from the extreme northern to the extreme southern parts of the United States, cot I varies from about 0.25 up to 0.58 and we see that R_i and R_d will be less than 1 for any direction of propagation in the United States when the angle of incidence, ϕ, at the ionosphere is greater than 15° in the northern and greater than 35° 30' in the southern parts of the United States. Since, for E layer transmission, ϕ will be greater than 15° for transmission at distances greater than 35 miles and will be greater than 35° 30' for transmission at distances greater than 90 miles, we see that R_i and R_d will be less than 1 for all conditions of propagation in the United States except very short distance transmission in directions other than North-South or South-North.

This completes the discussion of the polarization of the downcoming ionospheric waves. In general, we see that the relative amplitude and the relative phase of the components in the downcoming wave polarized parallel and perpendicular to the plane of incidence become more nearly random the higher the frequency. The two exceptions to this rule are the cases where the propagation is on a frequency near (1) the magneto-ionic frequency, f_h, at which the polarization of the downcoming wave assumes the polarization characteristic of the ordinary wave as shown by the solid curves in Figures 1

to 5 or (2) the maximum usable frequency of a given ionospheric layer near which the polarization of the downcoming wave assumes the polarization characteristic of the extraordinary wave as shown by the dotted curves in Figures 1 to 5. Thus, near the magneto-ionic frequency, $E_{\perp d} < E_{\parallel d}$ in the most commonly encountered case where $y_{\parallel}^2 > y_{\perp}^2$ but $E_{\perp d} > E_{\parallel d}$ when $y_{\parallel}^2 < y_{\perp}^2$; on the other hand, near the maximum usable frequency $E_{\perp d} > E_{\parallel d}$ when $y_{\parallel}^2 > y_{\perp}^2$ and $E_{\perp d} < E_{\parallel d}$ when $y_{\parallel}^2 < y_{\perp}^2$. In these two cases, since the relative phase between $E_{\perp d}$ and $E_{\parallel d}$ is constant, the average bearing indicated by a direction finder subject to polarization error will not be the correct bearing as would be the case when the relative phase is truly random.

III. The Effect of the Ground on the Intensity and Polarization of a Downcoming Wave Received Above or Below Its Surface.

We will now consider the effect of the ground on the intensity and phase of the downcoming ionospheric wave. It will be convenient to use a slightly different coordinate system in the following. We will take the $\underline{i}$ - $\underline{k}$ plane as the plane of incidence, as before, but now $\underline{k}$ will be chosen perpendicular to the ground so that the normal to the wave front of the downcoming ionospheric wave may be expressed as the unit vector $\underline{n}_d = \cos\psi\,\underline{i} - \sin\psi\,\underline{k}$, where ψ is the angle of elevation of the downcoming wave. After reflection at the ground, the wave normal of the ground-reflected wave will be $\underline{n}_r = \cos\psi\,\underline{i} + \sin\psi\,\underline{k}$. The resultant wave above the surface of the ground will always consist of two parts: the incident wave plus the ground-reflected wave. Figure 13 shows the geometry of the problem for the case in which the electric vector lies in the plane of incidence. The electric vector of the incident downcoming ionospheric wave, $\underline{E}_{\parallel d}$, is shown as a dotted line while the electric vector of the corresponding ground-reflected wave, $\underline{E}_{\parallel r}$, is shown as a solid line. Since the vertical component, $E_{\parallel z}$, of the resultant field is, in general, out of phase with the component parallel to the ground, $E_{\parallel x}$, the resultant electric vector, $\underline{E}_{\parallel}$, will rotate in an ellipse in the $\underline{i}$ - $\underline{k}$ plane. Figure 13 has been drawn for the particular case of a downcoming wave on a frequency $f = 1$ mc arriving at an angle $\psi = 4^\circ$ over land with average conductivity $\sigma = 5 \times 10^{-14}$ e.m.u. and with the dielectric constant $\epsilon = 15$; the ellipse represents the resultant field at a height $z = 10$ feet. In general, if we write for the incident plane wave[13] at the height z above the ground:

---

[13] The downcoming ionospheric wave is effectively plane since it has come from a source at a very great distance. In general, a plane wave in free space may be expressed as being proportional to the real part of $e^{i(k\,\underline{n}\cdot\underline{r} - \omega t)}$ where $\underline{r} = x\,\underline{i} + y\,\underline{j} + z\,\underline{k}$ and $\underline{n}$ is a unit vector normal to the wave front. If we choose our origin of coordinates at the surface of the ground at a distance z immediately below the point at which we wish to specify the wave, then $\underline{r} = z\,\underline{k}$ and the incident wave will be proportional to $e^{-i(k\,z\sin\psi + \omega t)}$ while the ground-reflected wave will be proportional to $e^{+i(k\,z\sin\psi - \omega t)}$. Finally, if the phase of the incident wave at the height z is taken to be zero, we obtain (98) and (99).

$$\underline{E}_{\parallel d} = E_{\parallel d} (\cos\psi\, \underline{k} + \sin\psi\, \underline{i})\, e^{-i\omega t} \tag{98}$$

then the corresponding ground-reflected wave will be:

$$\underline{E}_{\parallel r} = R_{\parallel} E_{\parallel d} (\cos\psi\, \underline{k} - \sin\psi\, \underline{i})\, e^{i(2kz\sin\psi - \omega t)} \tag{99}$$

$$R_{\parallel} = \frac{n^2 \sin\psi - \sqrt{n^2 - \cos^2\psi}}{n^2 \sin\psi + \sqrt{n^2 - \cos^2\psi}} \tag{100}$$

On the other hand, if the electric vector of the incident plane wave is $\perp$ to the plane of incidence we have:

$$\underline{E}_{\perp d} = E_{\perp d}\, \underline{j}\, e^{-i\omega t} \tag{101}$$

$$\underline{E}_{\perp r} = R_{\perp} E_{\perp d}\, \underline{j}\, e^{i(2kz\sin\psi - \omega t)} \tag{102}$$

$$R_{\perp} = \frac{\sin\psi - \sqrt{n^2 - \cos^2\psi}}{\sin\psi + \sqrt{n^2 - \cos^2\psi}} \tag{103}$$

In the above equations $k = 2\pi/\lambda$, n is the index of refraction of the earth and $n^2 = \varepsilon + i\,x$ where $x = 1.79731 \cdot 10^{15}\, \sigma_{e.m.u.}/f_{mc}$; $\sigma_{e.m.u.}$ is the conductivity of the ground expressed in electromagnetic units, f_{mc} is the frequency expressed in megacycles per second and ε is the dielectric constant of the ground referred to air as unity. The numerical magnitude of the quantity x is of fundamental importance in connection with the effect of the ground on the radio waves, the nature of the reflection being radically different in the two cases when x is very much larger than the dielectric constant and when x is very much smaller than the dielectric constant. Table I shows the value of x for various frequencies and for the ground conductivities normally encountered in practice.

Table No. I

x	f_{mc}	$\sigma_{e.m.u.}$	Description
1.95360	46	5×10^{-14}	Land of Average Conductivity
11.2332	1.6	10^{-14}	Land of Low Conductivity
17.9731	5	5×10^{-14}	Land of Average Conductivity
89.8655	1	5×10^{-14}	Land of Average Conductivity
7.18924×10^{2}	0.5	2×10^{-13}	Land of High Conductivity
1.95360×10^{3}	46	5×10^{-11}	Sea Water
1.79731×10^{4}	5	5×10^{-11}	Sea Water
1.79731×10^{5}	0.5	5×10^{-11}	Sea Water
6.362×10^{10}	10	3.54×10^{-4}	Aluminum
1.042×10^{11}	10	5.80×10^{-4}	Copper

The dielectric constant varies over a much more limited range, the minimum value ordinarily encountered being 1 for air while the maximum value is 80 for water, either inland lake or sea water. The dielectric constant of ice is only about 2 while the values of ε encountered over land vary from about 5 up to about 30. The dielectric constant of metals is probably less than 10 and consequently is of little importance at radio frequencies since x is so much larger for metals. A simple method for measuring the ground constants is described in Part IV.

Notice that the magnitude of $R_{\parallel}$ (or of $R_{\perp}$) is equal to the magnitude of the resulting ground-reflected wave for an incident wave of unit intensity and that the phase of $R_{\parallel}$ (or of $R_{\perp}$) denotes the change in phase when the incident wave is reflected at the ground. The phase of the incident wave at the height z is taken as zero. The phase $2 k z \sin \psi$ added to the ground-reflected wave is due to the additional distance traveled by the ground-reflected wave in reaching the height z above the ground; this may be seen most readily by considering the case of normal incidence so that $\psi = 90^{\circ}$ and $\sin \psi = 1$.

Figure 14 illustrates the intensity and phase relationship (as given by $R_{\parallel}$ or $R_{\perp}$) between the incident and the ground-reflected waves (for the case $z = 0$) on a vector diagram with the electric vector either $\parallel$ or $\perp$ to the plane of incidence and for three different frequencies and sets of ground constants. The upper diagram corresponds to an ultra high frequency and ground constants such that $x << \varepsilon$; the middle diagram corresponds to a frequency in the standard broadcast band and a typical set of ground constants; while the bottom diagram corresponds to the reflection of 500 kc over sea water. On these diagrams the intensities of the direct and ground-reflected waves are represented by the length of the arrows while the phase of the ground-reflected wave is represented by the angle at which the solid arrow is drawn; the phase of the incident wave is zero in each case. Each of the solid arrows represents the ground-reflected wave for a different angle of incidence of the incident wave. Thus, for grazing incidence ($\psi = 0$) we see that the ground-reflected wave is equal in intensity and 180° out of phase with the incident wave. Now, considering first the case where the electric vector is $\parallel$ to the plane of incidence, as we increase the angle ψ from zero at grazing incidence to larger and larger values, the intensity and phase of the reflected wave decrease until the angle ψ_m is reached at which the phase of the reflected wave is 90°. At this angle, ψ_m, which is called Brewster's angle, the reflected wave has a minimum intensity; this minimum intensity decreases from zero for $x = 0$ up to 0.41 for x very much greater than ε. The angle ψ_m at which this minimum reflection takes place is very near grazing incidence when x is large, being only 8' 6" for 500 kc over sea water but increases to considerably larger values when x is small. In the ultra high frequency case for propagation over land, we see in Figure 14 that the reflected wave is very nearly 180° out of phase with the incident wave when the angle ψ is less than Brewster's angle whereas the reflected wave is very nearly in phase with the incident wave when the angle ψ is greater than Brewster's angle. This is characteristic of the reflection of the electric vector in the plane of incidence when $x << \varepsilon$. This should be contrasted with the reflection of the electric vector when it is $\perp$ to the plane of incidence; in this case, regardless of the value of x or of the angle of incidence, the reflected wave is always very nearly 180° out of phase with the direct wave.

The formula for Brewster's angle is

$$\sin^2 \psi_m = \frac{\varepsilon - 1 + \sqrt{(x^2 + \varepsilon^2)^2 (\varepsilon - 1)^2 + x^2 \left\{ (x^2 + \varepsilon^2)^2 - 1 \right\}}}{(x^2 + \varepsilon^2)^2 - 1} \qquad (104)$$

and this reduces to the following formulas when x is very much larger than or very much smaller than ε.

$$\sin^2 \psi_m = \frac{1}{x} \qquad (x >> \varepsilon) \qquad (105)$$

$$\sin^2 \psi_m = \frac{1}{\varepsilon + 1} \qquad (x << \varepsilon) \qquad (106)$$

As is shown in Figure 14, the phase of the reflected wave, when the electric vector of the incident wave is in the plane of incidence, is 90° at Brewster's angle while its intensity is a minimum. This minimum value of the reflection coefficient at Brewster's angle may be calculated by means of equation (107).

$$\left| R_{\parallel} \right|_m = \tan \left(\frac{\pi}{8} + \frac{b'}{4} - \frac{b''}{2} \right) \qquad (107)$$

where

$$\tan b' = (\varepsilon - \cos^2 \psi_m)/x \qquad (108)$$

$$\tan b'' = \varepsilon/x \qquad (109)$$

Equation (107) reduces to the following equations when x is very much larger than or very much smaller than ε.

$$\left| R_{\parallel} \right|_m = \tan (\pi/8) \qquad (x >> \varepsilon) \qquad (110)$$

$$\left| R_{\parallel} \right|_m = \frac{x}{4} \frac{\varepsilon - 1}{\varepsilon^2} \qquad (x << \varepsilon) \qquad (111)$$

Figure 15 consists of curves relating the Brewster angle, ψ_m, and the corresponding minimum value of plane wave reflection coefficient, $\left| R_{\parallel} \right|_m$, with ε and x. We see that when x is very small, as is usually the case at the ultra high frequencies, Brewster's angle is independent of the ground conductivity and the frequency, being dependent only upon the dielectric constant of the ground; ψ_m is much larger over dry ground for which ε is small than over fresh water where ε is approximately equal to 80. Thus the ground-reflected wave is out of phase with the incident wave over a much wider range of angles of incidence over dry ground than over fresh water. When x is very large, as in the case of propagation over sea water, Brewster's angle is very small and we see that it is only at angles very near grazing incidence that the reflected wave will be out of phase with the incident wave.

One characteristic of the reflection of plane radio waves should be mentioned since it might otherwise cause some confusion. When the radio waves are reflected at normal incidence ($\psi = 90°$) no distinction can be made between the cases when the electric vector is $\parallel$ or $\perp$ to the plane of incidence. Thus, when $\psi = 90°$, it may be expected that the reflection coefficient will be the

same in both cases. However, on Figure 14, although the magnitude of the reflected wave is the same for the electric vector || or ⊥ to the plane of incidence when $\psi = 90^\circ$, the two vectors are shown 180° out of phase. The reason for this may be seen by reference to Figure 13. Considering first the case when the electric vector is || to the plane of incidence, if we refer the positive directions of the incident and ground-reflected waves to the positive z direction when ψ is zero, then, as we increase ψ to 90°, the positive direction of the electric vector will be in the positive x direction for the incident wave and in the negative x direction for the ground-reflected wave. Since no such reversal of phase in space takes place in the case when the electric vector is normal to the plane of incidence, we see that it is necessary that the reflection coefficient $R_\perp = - R_{||}$ when $\psi = 90^\circ$.

The resultant wave received on an antenna near the surface of the ground will consist of the vector sum of the incident and ground-reflected waves; thus:

$$\underline{E}_{||} = E_{||d} \cos\psi \left(1 + R_{||} e^{i2kz \sin\psi}\right) \underline{k} + E_{||d} \sin\psi \left(1 - R_{||} e^{i2kz \sin\psi}\right) \underline{i} \qquad (112)$$

$$\underline{E}_{\perp} = E_{\perp d} \left(1 + R_{\perp} e^{i2kz \sin\psi}\right) \underline{j} \qquad (113)$$

For convenience, the time factor $e^{-i\omega t}$ has been omitted in the above equations. It should be noted that, in the || case, the vertical component of $\underline{E}_{||}$ is, in general, out of phase with the horizontal component so that the resultant wave near the surface of the earth is elliptically polarized in the $\underline{i} - \underline{k}$ plane. For example, in the particular case shown in Figure 13, $R_{||} = 0.4138\, e^{i\, 122^\circ\, 56'\, 30''}$ and

$$\underline{E}_{||} = 0.84353\, \underline{k}\, e^{i\, 24^\circ\, 6'} + 0.088989\, \underline{i}\, e^{-i\, 15^\circ\, 42'} \qquad (114)$$

$$\text{or } \underline{E}_{||} = 0.84353\, \underline{k} \cos(\omega t - 24^\circ\, 6') + 0.088989\, \underline{i} \cos(\omega t + 15^\circ\, 42') \qquad (115)$$

where $E_{||d} = 1$

Figure 16 shows the resulting ellipses at the surface of the ground for several different values of x in the case when the incident wave arrives at an angle $\psi << \psi_m$. Since the downcoming ionospheric wave is, in general, elliptically polarized in the $\underline{j} - \underline{k}$ plane and since the ground causes the || component of the downcoming wave to be elliptically polarized in the $\underline{i} - \underline{k}$ plane, the electric vector of the resulting wave near the ground may be represented as following a curve on the surface of an ellipsoid of revolution.

For a consideration of the operation of a direction finder, the separate intensities of the $\underline{i}$, $\underline{j}$ and $\underline{k}$ components of the resultant field are of interest. Figure 17 shows these three components when $E_{||d} = E_{\perp d} = 1$ for two different heights above ground and for the following three frequencies and sets of ground constants:

(A) 0.5 mc $\sigma = 5 \times 10^{-11}$ e.m.u. (Sea Water) $\varepsilon = 80$

(B) 1 mc $\sigma = 5 \times 10^{-14}$ e.m.u. (Average Land) $\varepsilon = 15$

(C) 46 mc $\sigma = 5 \times 10^{-14}$ e.m.u. (Average Land) $\varepsilon = 15$

Notice that the vertical component $E_{\parallel z}$ increases with increasing values of x (increasing conductivity or decreasing frequency) for the dipole at the surface of the earth becoming very nearly equal to 2 for 0.5 mc propagation over sea water at certain low elevation angles, while the horizontal components $E_{\parallel x}$ and $E_{\perp}$ decrease with increasing values of x. In fact, for 0.5 mc over sea water, $E_{\parallel x}$ and $E_{\perp}$ are extremely small at the earth's surface, being equal to 0.0047 even for waves arriving at normal incidence. On the other hand, at a height of a quarter wavelength above the ground, $E_{\parallel x}$ and $E_{\perp}$ increase with increasing values of x.

In Part II equations were obtained for the instantaneous ratio of the intensities and the instantaneous relative phase between the $\perp$ and $\parallel$ components of the downcoming ionospheric wave and a determination made of their most probable values. In order to convert these values into the corresponding values for the resultant wave near the surface of the earth we may write:

$$E_{\perp}/E_{\parallel z} = \frac{(1 + R_{\perp} e^{i2kz \sin \psi})}{\cos \psi (1 + R_{\parallel} e^{i2kz \sin \psi})} \cdot (E_{\perp d}/E_{\parallel d}) \qquad (116)$$

where $(E_{\perp}/E_{\parallel z})$ represents the ratio of the horizontal ($\underline{j}$) component to the vertical ($\underline{k}$) component of the resultant wave at a height z above the surface of the earth and $(E_{\perp d}/E_{\parallel d})$ is the appropriate value of this ratio in the downcoming wave as determined by equations (92) or (93). Thus the effect of the ground alone on the polarization of the resulting wave near the ground is given by (116) when we set $(E_{\perp d}/E_{\parallel d}) = 1$.

In the limiting case of grazing incidence ($\psi = 0$) the expression for the field ratio is quite simple; by substituting the values of $R_{\parallel}$ and $R_{\perp}$ in (116) and letting ψ approach zero we obtain:

$$E_{\perp}/E_{\parallel z} = \frac{1}{\varepsilon + i\,x} \cdot (E_{\perp d}/E_{\parallel d}) \qquad (117)$$

where $\psi = 0$

Equation (117) shows that the usually undesired horizontal component of the resultant electric field for an ionospheric wave arriving at grazing incidence is suppressed in comparison to the desired vertical component directly in proportion to the value of $(\varepsilon + i\,x)$; since x is 1000 times as large over sea water as over average land, the advantage of locating a direction finder over sea water becomes obvious. Since ε, in general, increases with the water content of the soil, the advantage of locating a direction finder over swampy soil should also be clear from (117); this advantage would be more than lost, however, when the water freezes.

Another particular case of importance is the case of perfect conductivity; in this case $R_{\parallel} = -R_{\perp} = 1$ and (116) becomes:

$$E_{\perp}/E_{\parallel z} = \frac{\tan (k\, z \sin \psi)}{\cos \psi} (E_{\perp d}/E_{\parallel d})\, e^{-i\pi/2} \qquad (118)$$

where $\sigma = \infty$

Figure 18 shows how the ratio $|E_{\perp}/E_{\parallel z}|$ varies with the height of the receiving point above the ground for a frequency of 2 megacycles per second. The solid curves are for angles of elevation $\psi = 0^{\circ}$, 5° and 60° and correspond to the reception of downcoming ionospheric waves with equal $\parallel$ and $\perp$ components over land of average conductivity. It will be noted that, under most conditions, the effect of the ground is to suppress the horizontal component in the resultant wave in comparison to the vertical component; however, when $\psi = 60^{\circ}$ and z is greater than 34 feet, the vertical component is suppressed in favor of the horizontal component. The dotted curves are for sea water while the dashed curves correspond to a perfect ground ($\sigma = \infty$); it will be noted that sea water is the practical equivalent of a perfect ground. Since the $\perp$ component of E is usually the undesired component for a direction finder, it should be clear from Figure 18 that the wave collectors should be located as near as possible to ground with the highest possible conductivity. Figure 19 shows $E_{\perp}/E_{\parallel z}$ for 20 mc. Notice that, on this frequency and for high downcoming angles, the vertical component rather than the horizontal component is often suppressed; for example, when the wave collectors are at heights between 4 and 24 feet over perfect ground there will be more horizontal than vertical field.

Figure 20 shows the height above perfect ground ($\sigma = \infty$) at which $|E_{\perp}/E_{\parallel z}|$ first becomes equal to $|E_{\perp d}/E_{\parallel d}|$; a direction finder designed to reject the $\perp$ component of E should be kept below this height. Over ground of imperfect conductivity, the height at which $|E_{\perp}/E_{\parallel z}| = |E_{\perp d}/E_{\parallel d}|$ will be considerably less than that over perfect ground as may be seen by reference to Figures 18 and 19.

The equations so far given in this part of the report are for the electric field components; the corresponding magnetic field components may be obtained separately for the incident and ground-reflected waves by means of equation (12) with μ set equal to unity and the resultant magnetic vectors obtained by adding the direct and ground-reflected waves vectorially. The time factor $e^{-i\omega t}$ is omitted in the following equations.

$$\underline{H}_{\perp d} = \underline{n}_d \times \underline{E}_{\parallel d} = -E_{\parallel d}\, \underline{j} \qquad (119)$$

$$\underline{H}_{\perp r} = \underline{n}_r \times \underline{E}_{\parallel r} = -R_{\parallel} E_{\parallel d}\, \underline{j}\, e^{i2kz \sin \psi} \qquad (120)$$

$$\underline{H}_{\perp} = -E_{\parallel d} (1 + R_{\parallel} e^{i2kz \sin \psi})\, \underline{j} \qquad (121)$$

$$\underline{H}_{\parallel d} = \underline{n}_d \times \underline{E}_{\perp d} = E_{\perp d} (\cos \psi\, \underline{k} + \sin \psi\, \underline{i}) \qquad (122)$$

$$\underline{H}_{\parallel r} = \underline{n}_r \times \underline{E}_{\perp r} = R_{\perp} E_{\perp d} (\cos \psi\, \underline{k} - \sin \psi\, \underline{i})\, e^{i2kz \sin \psi} \qquad (123)$$

$$\underline{H}_{\parallel} = E_{\perp d} \left\{ \cos \psi (1 + R_{\perp} e^{i2kz \sin \psi})\, \underline{k} + \sin \psi (1 - R_{\perp} e^{i2kz \sin \psi})\, \underline{i} \right\} \qquad (124)$$

In this case, since the vertical component, $H_{\parallel z}$, of the resultant magnetic field is, in general, out of phase with the component parallel to the ground,

$H_{\parallel x}$, the resultant magnetic vector, $\underline{H}_{\parallel}$ will rotate in an ellipse in the $\underline{i}$ - $\underline{k}$ plane.

In the case of the direction finder consisting of spaced coaxial loops, the undesired component of the field is $\underline{E}_{\perp}$ while the desired component is $\underline{H}_{\perp}$ and we obtain by means of (113) and (121):

$$E_{\perp}/H_{\perp} = - \frac{(1 + R_{\perp} e^{i2kz \sin\psi})}{(1 + R_{\parallel} e^{i2kz \sin\psi})} \cdot (E_{\perp d}/E_{\parallel d}) \qquad (125)$$

A comparison of the above with (116) shows that they are practically identical except for the factor $\cos\psi$ in the denominator of (116); thus Figures 18 and 19 may be used in connection with the spaced coaxial loop direction finder simply by multiplying the values given by the curves by the factor $\cos\psi$.

The equations given for the reflection coefficients $R_{\parallel}$ and $R_{\perp}$ correspond to the case where the ground is flat and electrically homogeneous to very great depths. When the depth to groundwater, bedrock, and orebody or any marked discontinuity in the electrical properties of the ground is known, the following modified values of the reflection coefficients may be used.[14] The coefficients to be used in place of (100) and (103) when there is a single plane of discontinuity at a depth Δ and with index of refraction n above and n_o below this discontinuity are

$$R_{\parallel} = \frac{n^2 \sin\psi - \eta_1 \sqrt{n^2 - \cos^2\psi}}{n^2 \sin\psi + \eta_1 \sqrt{n^2 - \cos^2\psi}} \qquad (126)$$

$$R_{\perp} = \frac{\sin\psi - \eta_2 \sqrt{n^2 - \cos^2\psi}}{\sin\psi + \eta_2 \sqrt{n^2 - \cos^2\psi}} \qquad (127)$$

$$\eta_1 = \frac{1 + \delta_1}{1 - \delta_1} \qquad (128)$$

$$\eta_2 = \frac{1 - \delta_2}{1 + \delta_2} \qquad (129)$$

$$\delta_1 = \frac{n^2 \sqrt{n_o^2 - \cos^2\psi} - n_o^2 \sqrt{n^2 - \cos^2\psi}}{n^2 \sqrt{n_o^2 - \cos^2\psi} + n_o^2 \sqrt{n^2 - \cos^2\psi}} e^{ik2\Delta\sqrt{n^2 - \cos^2\psi}} \qquad (130)$$

---

[14] W. H. Wise, "Asymptotic Dipole Radiation Formulas", Bell System Tech. Jour., Vol. 8, Oct. 1929, pp. 662-671. Typographical errors in his equations are here corrected.

$$\delta_2 = \frac{\sqrt{n^2 - \cos^2\psi} - \sqrt{n_o^2 - \cos^2\psi}}{\sqrt{n^2 - \cos^2\psi} + \sqrt{n_o^2 - \cos^2\psi}} e^{ik2\Delta\sqrt{n^2 - \cos^2\psi}} \qquad (131)$$

If Δ is not large and n_o is considerably different from n then η_1 and η_2 differ considerably from unity.

It may be noted that the attenuation due to absorption of a plane radio wave traveling a distance d in a medium with index of refraction n is given by the factor

$$\left| e^{i\,k\,n\,d} \right|$$

and we see that the exponential factor in (130) and (131) is very nearly equal to the attenuation factor of a plane radio wave in traveling directly downward in the upper medium with index of refraction n to the discontinuity at a depth Δ and back again to the surface.

If we write $B + i\,A \equiv k\,n$, then the attenuation factor of the plane wave is given by e^{-Ad} where

$$A = k\sqrt{\frac{\varepsilon}{\cos\alpha}}\sin(\alpha/2) \qquad (132)$$

$$\tan\alpha = x/\varepsilon \qquad (133)$$

For very low frequencies such that $x >> \varepsilon$, equation (132) may be written

$$A = k\sqrt{\frac{x}{2}} \qquad (x >> \varepsilon) \qquad (134)$$

and we obtain the result that the absorption coefficient, A, is directly proportional to the square root of the frequency and to the square root of the conductivity, being independent of the dielectric constant. On the other hand, at frequencies sufficiently high that $x << \varepsilon$, equation (132) may be written

$$A = \frac{k\,x}{2\sqrt{\varepsilon}} \qquad (x << \varepsilon) \qquad (135)$$

which shows that the absorption coefficient, A, is independent of the frequency, directly proportional to the conductivity and inversely proportional to the square root of the dielectric constant. In order to illustrate the amount of this absorption as a function of the radio frequency, the conductivity and the dielectric constant, Figure 21 has been drawn to show the distance that a radio wave will travel through a medium before its intensity is reduced to one-tenth of its former value. It is interesting to note that the ultra-high frequencies are absorbed only slightly more than frequencies in the standard broadcast band in passing through media of average conductivity. The constant A may be determined for the case where d is expressed in feet simply by dividing the constant 2.30259 by the distance in feet as given in Figure 21. These results may be used for determining the exponential

factor in (130) and (131) by setting $d = 2\Delta$ and using the equivalent dielectric constant $(\varepsilon - \cos^2\psi)$.

So far we have been concerned with calculating the field intensity above the ground. For some types of direction finders the field intensity at a depth Δ below the surface of the ground is also of interest. When the incident wave at the height z above the ground is given by (98), the transmitted wave at a point directly below and at a depth Δ is given by:

$$\underline{E}_{\parallel t} = \frac{E_{\parallel d}}{n^2}(1 + R_{\parallel})(\cos\psi \underline{k} + \sqrt{n^2 - \cos^2\psi}\, \underline{i})\, e^{ik(z \sin\psi + \Delta\sqrt{n^2 - \cos^2\psi})} \quad (136)$$

$$\underline{H}_{\perp t} = - E_{\parallel d}\,(1 + R_{\parallel})\, \underline{j}\, e^{ik(z \sin\psi + \Delta\sqrt{n^2 - \cos^2\psi})} \quad (137)$$

Since the $\underline{k}$ and $\underline{i}$ components of (136) are, in general, out of time phase, $\underline{E}_{\parallel t}$ will oscillate in an ellipse with its major axis very nearly parallel to the ground when n is large. Notice that the amplitude of $\underline{H}_{\perp t}$ is approximately n times that of $\underline{E}_{\parallel t}$. In the case where the electric vector of the downcoming wave is normal to the plane of incidence we obtain:

$$\underline{E}_{\perp t} = E_{\parallel d}\,(1 + R_{\perp})\, \underline{j}\, e^{ik(z \sin\psi + \Delta\sqrt{n^2 - \cos^2\psi})} \quad (138)$$

$$\underline{H}_{\parallel t} = E_{\parallel d}(1 + R_{\perp})(\cos\psi \underline{k} + \sqrt{n^2 - \cos^2\psi}\, \underline{i})\, e^{ik(z \sin\psi + \Delta\sqrt{n^2 - \cos^2\psi})} \quad (139)$$

In this case $\underline{H}_{\parallel t}$ oscillates in an ellipse with its major axis very nearly parallel to the ground; as before, the amplitude of $\underline{H}_{\parallel t}$ is approximately n times that of $\underline{E}_{\perp t}$.[15] The attenuation factors in (136), (137), (138), and (139) may be determined from Figure 21 or by equation (132) by identifying d with Δ and ε with $(\varepsilon - \cos^2\psi)$. The term $kz \sin\psi$ in the above equations relates the phase of the transmitted wave to that of the incident wave at the height z above the ground.

The above completes the discussion of the polarization of received ionospheric radio waves. By means of the equations given in the preceding two sections it is possible to determine the polarization characteristics of the electric or magnetic fields of a downcoming ionospheric wave as received above or below the surface of the earth and to determine the influence on those characteristics of (1) the polarization of the wave as it leaves the transmitting antenna, (2) the magnetic field of the earth, (3) the collision frequency of the electrons in the ionosphere, (4) the angle of incidence at the ionosphere as determined by the virtual height of the ionosphere and the distance between transmitter and receiver, (5) the angle of elevation of the downcoming wave, (6) the electrical constants of the ground at the receiver, (7) the height above or the depth below the ground at which the measurements are made and (8) the radio frequency.

---

[15] In general $\underline{H}_t$ may be determined from $\underline{E}_t$ by means of the relation $\underline{H}_t = n\, \underline{n}_t \times \underline{E}_t$ where $\underline{n}_t = \frac{1}{n}\cos\psi\, \underline{i} - \frac{1}{n}\sqrt{n^2 - \cos^2\psi}\, \underline{k}$ is the (complex) unit vector normal to the wave front of the transmitted wave.

IV. Testing Direction Finders by Means of Fields from Nearby Sources; the Measurement of the Electrical Constants of the Ground.

For the purpose of testing a direction finder for the presence of polarization error, it is customary to transmit waves from a source at a comparatively small distance away; see Figure 22. This introduces many complications since the waves received at the direction finder may no longer be considered to be plane waves as are the downcoming ionospheric waves, and it is the purpose of this section to discuss the resulting differences in the propagation. Waves with their electric vectors ∥ to the plane of incidence should be transmitted from a vertical electric dipole while waves with their electric vectors ⊥ to the plane of incidence should be transmitted from a vertical magnetic dipole, i.e. a small loop antenna with its axis vertical. Sometimes waves are transmitted from horizontal electric dipoles but, in this case, the waves at the receiving point will have components polarized both ∥ and ⊥ to the plane of incidence unless the dipole is exactly horizontal and the receiving point lies in the equatorial plane of the dipole. In testing a direction finder it is impossible for both wave collectors to lie exactly in the equatorial plane of the horizontal electric dipole and, as a consequence, small amounts of electric field polarized parallel to the plane of incidence will be present at each wave collector when the center of the direction finder lies in the equatorial plane of the dipole; furthermore, both the electric and magnetic fields associated with these undesired components are out of phase at the two wave collectors and thus cause still more difficulty.[16] We will take the $\underline{d}$ - $\underline{k}$ plane as the plane of incidence with $\underline{k}$ vertical as in the previous section (see Figure 22). In the case of a perfectly conducting earth ($\sigma = \infty$) the electric and magnetic fields at a distance d and a height z from a vertical electric or a vertical magnetic dipole at a height a are equal to the real parts of the following expressions:

$$\begin{matrix}\underline{E}_{\parallel} \\ \underline{H}_{\parallel}\end{matrix} = \begin{matrix}-iE_{oe} \\ +H_{om}\end{matrix}\left\{\cos\psi_1\left[1+\frac{i}{kr_1}-\frac{1}{(kr_1)^2}\right]\underline{\psi}_1 + 2\sin\psi_1\left[\frac{i}{kr_1}-\frac{1}{(kr_1)^2}\right]\underline{r}_1\right\}\frac{e^{i(kr_1-\omega t)}}{r_1}$$
$$\begin{matrix}+iE_{oe} \\ -H_{om}\end{matrix}\left\{\cos\psi_2\left[1+\frac{i}{kr_2}-\frac{1}{(kr_2)^2}\right]\underline{\psi}_2 - 2\sin\psi_2\left[\frac{i}{kr_2}-\frac{1}{(kr_2)^2}\right]\underline{r}_2\right\}\frac{e^{i(kr_2-\omega t)}}{r_2} \quad (140)$$

$$\begin{matrix}\underline{H}_{\perp} \\ \underline{E}_{\perp}\end{matrix} = \begin{matrix}-iH_{oe} \\ +E_{om}\end{matrix}\underline{\theta}\left\{\cos\psi_1\left[1+\frac{i}{kr_1}\right]\frac{e^{i(kr_1-\omega t)}}{r_1} \pm \cos\psi_2\left[1+\frac{i}{kr_2}\right]\frac{e^{i(kr_2-\omega t)}}{r_2}\right\} \quad (141)$$

In the above equations the upper values and signs correspond to the vertical electric dipole while the lower values and signs correspond to the vertical

---

[16] These undesired electric field components from a horizontal electric dipole have very appropriately been designated as "bad-natured vertical" by Mr. W. H. Wirkler of the Collins Radio Company who first pointed out their significance in direction finder testing. Equations for the fields from horizontal electric and magnetic dipoles are given in Appendix I.

magnetic dipole; $\underline{E}_\perp = \underline{H}_\parallel = 0$ for a vertical electric dipole and $\underline{E}_\parallel = \underline{H}_\perp = 0$ for a vertical magnetic dipole. E_{oe} and H_{oe} are the values of the electric and magnetic radiation fields at a unit distance in free space in the equatorial plane of the electric dipole while E_{om} and H_{om} are the corresponding values for a magnetic dipole.[17] The distance r_1 in the above equations must always be much larger than the largest dimension of the electric or magnetic dipole; the dimensions of the dipole must also be small in comparison to the wavelength. The phase of the field from the electric dipole is referred to the phase of the current in the dipole while the phase of the field from the magnetic dipole is referred to the phase of the magnetic field at the center of the dipole which, in turn, is in phase with the current in the dipole. r_1, r_2, ψ_1 and ψ_2 are adequately defined in Figure 22. Note that $\tan \psi_1 = (a - z)/d$ so that ψ_1 is negative when $z > a$; $\tan \psi_2 = (a + z)/d$. The unit vectors $\underline{\psi}_1 = \cos \psi_1 \underline{k} + \sin \psi_1 \underline{d}$, $\underline{\psi}_2 = \cos \psi_2 \underline{k} - \sin \psi_2 \underline{d}$, $\underline{r}_1 = \cos \psi_1 \underline{d} - \sin \psi_1 \underline{k}$, and $\underline{r}_2 = \cos \psi_2 \underline{d} + \sin \psi_2 \underline{k}$ are also shown on Figure 22. The unit vector $\underline{\theta}$ is perpendicular to both $\underline{k}$ and $\underline{d}$ (see Figure 28) and is defined by the relation $\underline{\theta} = \underline{k} \times \underline{d}$. For distances $d > \lambda$ the terms in (140) and (141) proportional to r^{-2} and r^{-3} may be neglected for most practical purposes unless ψ_1 and ψ_2 are large and this leads to a very substantial simplification in (140) and (141). The terms associated with the subscript 1 in (140) and (141) represent the fields which would be present in free space as may be seen by keeping r_1 fixed and allowing r_2 to increase without limit; these terms in the presence of the ground are called the direct wave. The terms associated with the subscript 2 in (140) and (141) are called the ground-reflected wave; if we let $(a + z)$ approach zero the direct and ground-reflected waves from the magnetic dipole exactly cancel each other while those from the electric dipole add to produce a resulting field which is just twice the free space field. As the height of the dipole above the earth is changed its radiation resistance changes and thus the power for a given current also varies; this variation is not shown explicitly in (140) and (141) since these equations are for a fixed current rather than for a fixed power.

It should be noted that, at distances less than one wavelength or, due to the presence of the ground, even at distances greater than one wavelength, the amplitude of $\underline{E}_\perp$ is not equal to the amplitude of $\underline{E}_\parallel$ (when $H_{oe} = E_{oe}$ so that both are expressed in the same units) as it would be at large distances in free space and, as a consequence, measurements of $\underline{E}_\parallel$ cannot be made with a loop antenna without appropriate correction for this difference. Similarly, in the case of the vertical magnetic dipole, the amplitude of $\underline{H}_\parallel$ is not equal to the amplitude of $\underline{E}_\perp$. In order to investigate this point further we will consider the case where $r >> z$; then ψ_1 and ψ_2 may be set equal to ψ and r_1 and r_2 may be set equal to r, where the amplitude alone is involved, but must be set equal to $r - z \sin \psi$ and $r + z \sin \psi$, respectively, where they occur in the phase.

---

[17] When r_1 is expressed in meters, E_o is expressed in volts per meter, I denotes the antenna current measured in amperes and λ is measured in meters, then $E_{oe} = 30\ k\ I\ h$ and $E_{om} = 30\ k^2\ I\ A$ where h is the effective length of the electric dipole measured in meters and A is the turns area of the magnetic dipole measured in square meters times the number of turns. When field intensity measurements are made using a loop antenna, actually H rather than E is measured; when such field intensities are designated as volts per meter they refer to the related value of E which would be present if the field measured were that of a plane wave in free space; thus our equations for H may be expressed in terms of the volts per meter measured with a loop antenna by setting $H_{oe} = E_{oe}$ and $H_{om} = E_{om}$.

Noting that $\left[e^{-ikz \sin\psi} + e^{ikz \sin\psi}\right] = 2\cos(k z \sin\psi)$ and $\left[e^{-ikz \sin\psi} - e^{ikz \sin\psi}\right] = -2i \sin(k z \sin\psi)$ we obtain from the above equations:

$$E_{\parallel z} = i2E_{oe} \cos(kz \sin\psi) \left\{\cos^2\psi + (1 - 3\sin^2\psi)\left[\frac{i}{kr} - \frac{1}{(kr)^2}\right]\right\}\frac{e^{ikr}}{r} \qquad (142)$$

$$E_{\parallel d} = 2E_{oe}\left[\sin(kz \sin\psi) - i\frac{z}{a}\cos(kz \sin\psi)\right]\sin\psi\cos\psi\left\{1 + 3\left[\frac{i}{kr} - \frac{1}{(kr)^2}\right]\right\}\frac{e^{ikr}}{r} \qquad (143)$$

$$H_{\perp} = -i2H_{oe} \cos(kz \sin\psi) \cos\psi\left[1 + \frac{i}{kr}\right]\frac{e^{ikr}}{r} \qquad (144)$$

$$H_{\parallel z} = -i2H_{om} \sin(kz \sin\psi)\left\{\cos^2\psi + (1 - 3\sin^2\psi)\left[\frac{i}{kr} - \frac{1}{(kr)^2}\right]\right\}\frac{e^{ikr}}{r} \qquad (145)$$

$$H_{\parallel d} = 2H_{om}\left[\cos(kz \sin\psi) + i\frac{z}{a}\sin(kz \sin\psi)\right]\sin\psi\cos\psi\left\{1 + 3\left[\frac{i}{kr} - \frac{1}{(kr)^2}\right]\right\}\frac{e^{ikr}}{r} \qquad (146)$$

$$E_{\perp} = -i2E_{om} \sin(kz \sin\psi) \cos\psi\left[1 + \frac{i}{kr}\right]\frac{e^{ikr}}{r} \qquad (147)$$

where $r >> z$

From the above equations we see that the amplitude of $E_{\parallel z}$ may be determined over a perfect earth by measuring $H_{\perp}$ and using the following relation:

$$\left|E_{\parallel z}\right| = \left|H_{\perp} \cos\psi\left\{1 + (1 - 2\tan^2\psi)\left[\frac{i}{kr} - \frac{1}{(kr)^2}\right]\right\} \Big/ \left[1 + \frac{i}{kr}\right]\right| \qquad (148)$$

where $r >> z$

and, similarly, the amplitude of $E_{\perp}$ may be determined over a perfect earth by measuring $H_{\parallel z}$ and using the following relation:

$$\left|E_{\perp}\right| = \left|H_{\parallel z}\left[1 + \frac{i}{kr}\right] \Big/ \cos\psi\left\{1 + (1 - 2\tan^2\psi)\left[\frac{i}{kr} - \frac{1}{(kr)^2}\right]\right\}\right| \qquad (149)$$

where $r >> z$

It will be noted that the factor in (149) is just the reciprocal of the factor in (148); this factor is shown graphically in Figure 23 with $\psi = 0°$, $15°$, $30°$, $35°\ 15'\ 51''$, and $45°$, as a function of the distance r expressed in fractions of the wavelength. It should also be noted that, when z is less than a quarter wavelength, $E_{\parallel z} > E_{\parallel d}$* while $H_{\parallel d} > H_{\parallel z}$.

The modifications in the above equations due to the finite conductivity of the ground are considerable, especially at the higher frequencies where x may

*The $E_{\parallel d}$ and $H_{\parallel d}$ of this part of the report refer to the components in the direction of the unit vector $\underline{d}$ and have no reference to the values of the downcoming ionospheric wave of the preceding sections.

not be very large. As has been shown in recent papers by the author this effect may be represented by introducing the plane wave reflection coefficients, $R_{\parallel}$ and $R_{\perp}$, as factors in the expressions for the ground-reflected waves and by adding a surface wave;[18] thus, at a distance $d > \lambda$ we may write:

$$\underline{E}_{\parallel} = iE_{oe}\left\{\cos\psi_1 \frac{e^{ikr_1}}{r_1}\underline{\psi}_1 + \cos\psi_2 R_{\parallel}\frac{e^{ikr_2}}{r_2}\underline{\psi}_2 + \cos\psi_2(1-R_{\parallel})f(P_e,B_e)\left[\cos\psi_2\,\underline{k} + \frac{\sqrt{n^2-\cos^2\psi_2}}{n^2}\,\underline{d}\right]\frac{e^{i(\phi+kr_2)}}{r_2}\right\} \quad (150)$$

$$\underline{H}_{\perp} = -iH_{oe}\,\underline{\theta}\left\{\cos\psi_1\frac{e^{ikr_1}}{r_1} + \cos\psi_2 R_{\parallel}\frac{e^{ikr_2}}{r_2} + \cos\psi_2(1-R_{\parallel})f(P_e,B_e)\frac{e^{i(\phi+kr_2)}}{r_2}\right\} \quad (151)$$

$$\underline{E}_{\perp} = E_{om}\,\underline{\theta}\left\{\cos\psi_1\frac{e^{ikr_1}}{r_1} + \cos\psi_2 R_{\perp}\frac{e^{ikr_2}}{r_2} + \cos\psi_2(1-R_{\perp})f(P_m,B_m)\frac{e^{i(\phi+kr_2)}}{r_2}\right\} \quad (152)$$

$$\underline{H}_{\parallel} = H_{om}\left\{\cos\psi_1\frac{e^{ikr_1}}{r_1}\underline{\psi}_1 + \cos\psi_2 R_{\perp}\frac{e^{ikr_2}}{r_2}\underline{\psi}_2 + \cos\psi_2(1-R_{\perp})f(P_m,B_m)\left[\cos\psi_2\,\underline{k} + \sqrt{n^2-\cos^2\psi_2}\,\underline{d}\right]\frac{e^{i(\phi+kr_2)}}{r_2}\right\} \quad (153)$$

It is understood in the above equations that the time factor $e^{-i\omega t}$ is to be introduced and that the fields are represented by the real parts of the resulting equations. $R_{\parallel}$ and $R_{\perp}$ are the plane wave reflection coefficients as defined in (100) and (103) but with ψ replaced by ψ_2; the third term in each equation represents the surface wave and $f(P,B)e^{i\phi}$ is the surface wave attenuation function which is given graphically as a function of P and B in figures 24 and 25.

$$f(P,B)\,e^{i\phi} = 1 + i\sqrt{\pi P_1}\,e^{-P_1}\,\mathrm{erfc}\,(-i\sqrt{P_1}) \quad (154)$$

$$P_1 = P\,e^{iB} \quad (155)$$

---

[18] K. A. Norton "Physical Reality of Space and Surface Waves in the Radiation Field of Radio Antennas", Proc. I.R.E., Vol. 25, Sept. 1937, pp. 1192-1202; "The Propagation of Radio Waves Over the Surface of the Earth and in the Upper Atmosphere", Part II, Proc. I.R.E., Vol. 25, Sept. 1937, pp. 1203-1236; "The Calculation of Ground-Wave Field Intensity Over a Finitely Conducting Spherical Earth", Proc. I.R.E., Vol. 29, Dec. 1941, pp. 623-639. The equations given here differ slightly from those in the earlier papers due to a correction obtained by retaining an additional term in the series expansion for R' in equation (34) of the second reference above and rearranging some of the other terms. This results in a factor $\cos^2\psi_2$ multiplying $f(P,B)$ in $E_{\parallel z}$ and $H_{\parallel z}$ and a factor $1/\cos^2\psi_2$ in the expressions for P_e and P_m. These changes have the effect of decreasing the intensity of the surface wave much more rapidly as the angle ψ_2 is increased from zero. Exact expressions for the electric and vertical magnetic fields at any distance from a vertical magnetic dipole over a finitely conducting earth are given in an appendix for the case when the transmitting and receiving antennas are on the surface.

$$P_e\, e^{iB_e} = \frac{i\,k\,r_2}{2\cos^2\psi_2}\left[\sin\psi_2 + \frac{\sqrt{n^2 - \cos^2\psi_2}}{n^2}\right]^2 \qquad (156)$$

$$P_m\, e^{iB_m} = \frac{i\,k\,r_2}{2\cos^2\psi_2}\left[\sin\psi_2 + \sqrt{n^2 - \cos^2\psi_2}\right]^2 \qquad (157)$$

P_e and P_m are called "numerical distances"; both increase with increasing values of ψ_2 but P_e decreases while P_m increases with increasing values of x and of ε. The angle B_e lies between 0 and 90° while the angle B_m lies between 90° and 180°. Since $P_m \equiv n^4 P_e$ when $\psi_2 < \psi_m$, the surface wave from the vertical magnetic dipole is very much more rapidly attenuated with distance than the surface wave from the vertical electric dipole. In fact, when $d > \lambda$ and $|n^2| > 10$, P_m will be sufficiently large so that $f(P_m, B_m)$ may be accurately represented by the first term in its asymptotic expansion:

$$f(P, B)\, e^{i\phi} = -\frac{e^{-iB}}{2P} - \frac{1\cdot 3\cdot e^{-i2B}}{(2P)^2} - \frac{1\cdot 3\cdot 5\cdot e^{-i3B}}{(2P)^3} \cdots\cdots \qquad (158)$$

Notice also that the attenuation of the surface wave from the vertical magnetic dipole increases with decreasing frequency. On the other hand, the surface wave from the vertical electric dipole is much less rapidly attenuated at all frequencies, the attenuation increasing with increasing frequency.

A comparison of the above equations with the corresponding equations for plane downcoming waves as given in Part III indicates that, due to the presence of the surface wave, the field from a local transmitter is not the same as that from the ionosphere; however, if we let the distance r increase without limit, keeping ψ fixed, then the surface wave is attenuated more rapidly than the sum of the direct and ground-reflected waves and thus becomes a negligible component of the resultant field, ψ_1 and ψ_2 approach ψ, r_1 approaches $r - z\sin\psi$, r_2 approaches $r + z\sin\psi$ and we obtain from (150):

$$\underline{E}_{\parallel} = \frac{iE_{oe}\cos\psi e^{ik(r - z\sin\psi)}}{r}\left\{\cos\psi(1 + R_{\parallel} e^{i2kz\sin\psi})\,\underline{k} + \sin\psi(1 - R_{\parallel} e^{i2kz\sin\psi})\,\underline{d}\right\} \qquad (159)$$

(where r approaches ∞)

We see that the above equation becomes identical to (112) for downcoming ionospheric waves when we write:

$$\frac{i\,E_{oe}\cos\psi e^{ik(r - z\sin\psi)}}{r} = E_{\parallel d} \qquad (160)$$

In a similar manner it can be shown that (151), (152) and (153) become identical to (121), (113) and (124) respectively when r is allowed to increase without limit. Thus we see from the above that, in order to simulate downcoming ionospheric waves by means of a local transmitter, it is necessary to transmit from such a distance that the surface wave is a

negligible component of the resulting field; this distance decreases as the angle ψ_2 increases since the surface wave decreases while the space wave (vector sum of the direct and ground-reflected waves) increases with increasing values of ψ_2. Thus, keeping r_2 fixed, we may write approximately for the relation between the intensity of the vertical component of the surface wave with $\psi_2 = 0$ and its value at ψ_2:

$$E_{\parallel zSU}(\psi_2) = \frac{E_{\parallel zSU}(0)\,(\cos\psi_2)^{m+1}}{\left(1+\dfrac{n^2\sin\psi_2}{\sqrt{n^2-\cos^2\psi_2}}\right)^m} \tag{161}$$

where $m = 1$ at short numerical distances ($P_e < 0.1$) and $m = 3$ at large numerical distances ($P_e > 20$); the corresponding expression for the surface wave field from the vertical magnetic dipole is:

$$E_{\perp SU}(\psi_2) = \frac{E_{\perp SU}(0)\,\cos^4\psi_2}{\left(1+\dfrac{\sin\psi_2}{\sqrt{n^2-\cos^2\psi_2}}\right)^3} \tag{162}$$

where $P_m > 20$

From the above equations we see that the surface wave from the vertical electric dipole decreases much more rapidly with ψ_2 than the surface wave from the vertical magnetic dipole. The above equations show that (with r_2 fixed) the surface wave decreases monotonically with increasing values of ψ_2 and thus with increasing values of either a or z.

In order to obtain a clearer picture of the relative importance of the space and surface waves we will consider the expressions for the received wave at the surface of the ground ($z = 0$); in this case, $r_1 = r_2 = r$ and $\psi_1 = \psi_2 = \psi$ and we obtain:

$$\underline{E}_{\parallel} = iE_{oe}\cos\psi\left[(1+R_{\parallel})+(1-R_{\parallel})f(P_e,B_e)e^{i\phi}\right]\left(\cos\psi\,\underline{k}+\frac{\sqrt{n^2-\cos^2\psi}}{n^2}\,\underline{d}\right)\frac{e^{ikr}}{r} \tag{163}$$

$$\underline{H}_{\perp} = -iH_{oe}\cos\psi\,\underline{\theta}\left[(1+R_{\parallel})+(1-R_{\parallel})f(P_e,B_e)e^{i\phi}\right]\frac{e^{ikr}}{r} \tag{164}$$

$$\underline{E}_{\perp} = E_{om}\cos\psi\,\underline{\theta}\left[(1+R_{\perp})+(1-R_{\perp})f(P_m,B_m)e^{i\phi}\right]\frac{e^{ikr}}{r} \tag{165}$$

$$\underline{H}_{\parallel} = H_{om}\cos\psi\left[(1+R_{\perp})+(1-R_{\perp})f(P_m,B_m)e^{i\phi}\right]\left(\cos\psi\,\underline{k}+\sqrt{n^2-\cos^2\psi}\,\underline{d}\right)\frac{e^{ikr}}{r} \tag{166}$$

where $z = 0$ and $d > \lambda$

The first terms in the square brackets in the above equations represent the space waves while the second terms in the square brackets represent the surface waves. In the case of transmission from the vertical electric dipole we may write for the ratio of the intensities of the surface wave to the space wave:

$$\left|\frac{E_{\parallel SU}}{E_{\parallel SP}}\right| = \left|\frac{H_{\perp SU}}{H_{\perp SP}}\right| \simeq \left|\frac{\sqrt{n^2 - \cos^2\psi}}{n^2 \sin\psi}\right| \cdot f(P_e, B_e) \qquad (167)$$

where $z = 0$ $\quad d > \lambda$

Since $\left|\sqrt{n^2 - \cos^2\psi}/n^2\right| = \sin\psi_B$, we see by (167) that the space wave will be stronger than the surface wave at all distances whenever ψ is greater than the Brewster angle ψ_B; at the larger numerical distances the surface wave is comparable in intensity to the space wave only for very small angles. Figure 26 shows the relative importance of the space and surface waves at the surface of the ground for several different frequencies and angles of elevation over average ground as a function of the distance expressed in wavelengths. It is evident from this figure that the importance of the surface wave relative to the space wave decreases rapidly with increasing elevation angle, ψ. If we assume that the surface wave is negligible when it has an intensity less than 1% of the space wave, we see by Figure 26 that transmissions designed to simulate ionospheric wave transmission must be made from a distance of the order of 2 wavelengths when $\psi = 45^\circ$, 50 wavelengths when $\psi = 15^\circ$ and 500 wavelengths when $\psi = 5^\circ$. The curves on this figure are also applicable for other values of the ground conductivity if the frequency is simultaneously changed in the same proportion; for example, the 0.5 mc curves are also applicable to 2 mc over ground with a dielectric constant of 15 but with a conductivity equal to 2×10^{-13} e.m.u.

Over sea water the surface wave from the vertical electric dipole is smaller relative to the space wave than over land. Table No. II gives the ratio of the surface to space wave intensity at the surface of the ground for a vertical electric dipole at a distance of one wavelength over sea water.

Table II

The Ratio $\left|E_{\parallel SU} / E_{\parallel SP}\right|$ Over Sea Water at a Distance r/λ Equal to One Wavelength From a Vertical Electric Dipole

($z = 0$; $\sin\psi = a/r$; $\varepsilon = 80$; $\sigma = 5 \times 10^{-11}$ e.m.u.)

f_{mc}	$\psi = 5^\circ$	$\psi = 10^\circ$	$\psi = 15^\circ$	$\psi = 30^\circ$	$\psi = 45^\circ$
0.5	0.02219	0.009237	0.005058	0.001382	0.0004603
1	0.03138	0.01306	0.007153	0.001955	0.0006510
2	0.04439	0.01847	0.01012	0.002764	0.0009207
5	0.07018	0.02921	0.01600	0.004371	0.001456
10	0.09925	0.04131	0.02262	0.006182	0.002059
20	0.1404	0.05841	0.03199	0.008741	0.002911

The surface wave from the vertical magnetic dipole is, relatively, of less importance than that from the vertical electric dipole; thus, at the surface of the ground, we obtain from (165) and (166):

$$\left|\frac{E_{\perp SU}}{E_{\perp SP}}\right| = \left|\frac{H_{\parallel SU}}{H_{\parallel SP}}\right| = \left|\frac{\sqrt{n^2 - \cos^2\psi}}{\sin\psi}\right| \cdot f(P_m, B_m) \qquad (168)$$

where $z = 0$ $\quad d > \lambda$

When we subsitute in (168) the first term in the asymptotic expansion for $f(P_m, B_m)$ we obtain

$$\left|\frac{E_{\perp SU}}{E_{\perp SP}}\right| = \left|\frac{H_{\parallel SU}}{H_{\parallel SP}}\right| = \frac{\cos^2\psi}{2\pi(r/\lambda)\sin\psi\left|\sqrt{n^2 - \cos^2\psi} + 2\sin\psi + \sin^2\psi/\sqrt{n^2 - \cos^2\psi}\right|} \qquad (169)$$

where $z = 0$ $\quad d > \lambda$ $\quad |n^2| > 10$

Table III gives the ratio of the surface to the space wave intensity at the surface of the ground for a vertical magnetic dipole at a distance of one wavelength over average ground.

Table III

The Ratio $\left|E_{\perp SU} / E_{\perp SP}\right|$ Over Average Land at a Distance r/λ Equal to One Wavelength From a Vertical Magnetic Dipole

($z = 0$; $\sin\psi = a/r$; $\varepsilon = 15$; $\sigma = 5 \times 10^{-14}$ e.m.u.)

f_{mc}	$\psi = 5^\circ$	$\psi = 15^\circ$	$\psi = 45^\circ$
0.5	0.1338	0.04154	0.007763
1	0.1874	0.05774	0.01057
2	0.2588	0.07875	0.01399
5	0.3672	0.1093	0.01851
10	0.4261	0.1251	0.02062
20	0.4513	0.1317	0.02146

At larger distances the ratio may be obtained simply by dividing the ratios given in Table III by the distance expressed in wavelengths. As in the case of the vertical electric dipole the values of the ratio at a given distance in wavelengths are the same for other ground conductivities if the frequency is changed in the same proportion, i.e. x is kept constant.

The Measurement of the Dielectric Constant and Conductivity of the Ground

Equation (163) provides the basis for the wave tilt method of measuring the ground constants. We see by (163) that both the space and surface wave

components of the ground wave have the same polarization at the surface of the ground. This forward tilt and polarization of the electric vector are discussed and illustrated graphically in a recent paper by the author;[19] see also Figure 16 in this report. The ground constants are determined by measuring the forward tilt and the ratio of the minor to the major axes of the polarization ellipse of the electric vector. However, since measurements of the electric field intensity must be made, electric dipole receiving antennas must be used and measurements with such antennas are difficult to make accurately because of disturbances to the electric field due to the presence of the field intensity meter and the operator. However, we see by (166) that the magnetic vector from a vertical magnetic dipole is also elliptically polarized in the plane of incidence and thus may be used in an alternate and in general preferable method for determining the ground constants. (166) may be written:

$$\underline{H}_{\parallel} = H_{\parallel d} \left[\underline{d} + \frac{\cos \psi}{\sqrt{n^2 - \cos^2 \psi}} \underline{k} \right] e^{-i\omega t} \qquad (170)$$

$$z = 0; \quad d > \lambda$$

If we write

$$\alpha e^{-iB} = \frac{\cos \psi}{\sqrt{n^2 - \cos^2 \psi}} = \frac{1}{\sqrt{\varepsilon' - 1 + i x'}} \qquad (171)$$

$$\text{where } \varepsilon' = \frac{\varepsilon}{\cos^2 \psi} \qquad (172)$$

$$x' = \frac{x}{\cos^2 \psi} \qquad (173)$$

then (170) becomes

$$\underline{H}_{\parallel} = H_{\parallel d} \left[\underline{d} \cos \omega t + \underline{k} \alpha \cos (\omega t + \beta) \right] \qquad (174)$$

$$z = 0; \quad d > \lambda$$

The above equation shows that the vector magnetic field from a vertical magnetic dipole rotates in an ellipse in the plane of incidence with its major axis tilted a few degrees above the horizontal. The magnetic vector reaches its maximum extension when $\omega t = -\delta$ and its minimum extension when $\omega t = \pi/2 - \delta$ where

$$\tan \delta = \frac{1}{2T} \left[\sqrt{1 + 4T^2} - 1 \right] \qquad (175)$$

---

[19] See the second reference in footnote 18.

$$\tau = \frac{\alpha^2 \sin 2\beta}{2\left[1+\alpha^2 \cos 2\beta\right]} \tag{176}$$

The measurable properties of the ellipse are Θ, the tilt of the major axis above the horizontal and K, the ratio of the minor to the major axes.

$$\tan \Theta = \alpha \left[\cos\beta + \sin\beta \tan\delta\right] \tag{177}$$

$$K = \tan\delta \cot\Theta \tag{178}$$

Figure 27 shows Θ and K as a function of x' for $\varepsilon' = 5$, 10, 20 and 80.

The procedure for determining the ground constants from the above results is as follows. A small transmitter is used with a loop antenna[20] which is set up with its axis in the plane of incidence (see Figure 27) at a distance greater than one wavelength from the point at which the ground constants are to be determined and at a height such that an easily measurable field intensity is obtained at the receiving point. Using a field intensity meter with a loop antenna set up in such a manner that it can be rotated about an axis perpendicular to the plane of incidence but with the loop axis always lying in the plane of incidence, measurements are made of Θ and K; the loop on the field intensity meter is to be placed as near the ground as possible but in no case at a height greater than a small fraction of a wavelength or a small fraction of the height a above the ground. Having measured Θ and K, a corresponding set of values of ε' and x' may be determined by means of the graphs of Figure 27. Finally ε and σ are determined by means of the following equations:

$$\varepsilon = \varepsilon' \cos^2\psi \tag{179}$$

$$\sigma = x' \cos^2\psi \, f_{mc} \cdot 5.56387 \cdot 10^{-16} \text{ e.m.u.} \tag{180}$$

At very high frequencies, x' will be small and we may write

$$\varepsilon' = \frac{1}{\sin^2\Theta} \tag{181}$$

$$x' = \frac{2K}{\sin^2\Theta \tan\Theta} \tag{182}$$

where $x' << (\varepsilon' - 1)$

---

[20] A horizontal electric dipole may be used instead of the loop antenna at the transmitter (see Appendix I); in this case the axis of the receiving loop should lie in the equatorial plane of the horizontal electric dipole which should be placed as nearly horizontal as possible in order to avoid stray vertical electric fields; however, these stray fields will not cause as much difficulty in connection with ground constant determinations as they would in testing a direction finder.

We see by the above equations that the dielectric constant, ε, may be determined at the very high frequencies simply by measuring θ whereas a determination of the conductivity, σ, requires a measurement of both θ and K. At very low frequencies, on the other hand, x' will be large and we may write

$$x' = \frac{1}{2 \tan^2 \theta} = \frac{1}{2 K^2} \qquad (183)$$

where $x' >> (\varepsilon' - 1)$

We see by the above equations that the conductivity, σ, may be determined at very low frequencies by measuring either θ or K but that the dielectric constant, ε, may not be measured at all; this is no particular defect of the method since the dielectric constant has no appreciable effect on the propagation at these low frequencies. Accurate measurements of K may be made only provided the loop on the field intensity meter is well shielded or balanced so that its minimum reading on a linearly polarized magnetic field (such as is generated by a vertical electric antenna) is much less than K times its maximum reading on the same field.

The Calculation of Electric Field Intensities From Measurements of Magnetic Field Intensities

Since most field intensity meters use loop antennas as wave collectors they measure the magnetic rather than the electric field intensity. The appropriate correction factors to be used at any distance from vertical electric or magnetic dipoles over a perfect earth have been given in (148) and (149) and shown graphically in Figure 23. We will here consider the corresponding expressions for distances greater than a wavelength and for an earth of finite conductivity. When the distance $r >> z$, (150) to (153) may be written

$$E_{\parallel z} = i E_{oe} \cos^2 \psi \left[1 + R_{\parallel} e^{i2kz \sin \psi} + (1 - R_{\parallel}) f(P_e, B_e) e^{i(\phi + 2kz \sin \psi)} \right] \frac{e^{ik(r - z \sin \psi)}}{r} \qquad (184)$$

$$E_{\parallel d} = i E_{oe} \cos \psi \left[\sin \psi \left(1 - \frac{z}{a}\right) - \sin \psi \left(1 + \frac{z}{a}\right) R_{\parallel} e^{i2kz \sin \psi} + \frac{\sqrt{n^2 - \cos^2 \psi}}{n^2} (1 - R_{\parallel}) f(P_e, B_e) e^{i(\phi + 2kz \sin \psi)} \right] \frac{e^{ik(r - z \sin \psi)}}{r} \qquad (185)$$

$$H_{\perp} = \frac{- H_{oe} E_{\parallel z}}{E_{oe} \cos \psi} \qquad (186)$$

$$E_{\perp} = E_{om} \cos \psi \left[1 + R_{\perp} e^{i2kz \sin \psi} + (1 - R_{\perp}) f(P_m, B_m) e^{i(\phi + 2kz \sin \psi)} \right] \frac{e^{ik(r - z \sin \psi)}}{r} \qquad (187)$$

$$H_{\parallel z} = \frac{H_{om} E_{\perp} \cos \psi}{E_{om}} \tag{188}$$

$$H_{\parallel d} = H_{om} \cos \psi \left[\sin \psi \left(1 - \frac{z}{a}\right) - \sin \psi \left(1 + \frac{z}{a}\right) R_{\perp} e^{i2kz \sin \psi} \right.$$

$$\left. + \sqrt{n^2 - \cos^2 \psi} \, (1 - R_{\perp}) f(P_m, B_m) \, e^{i(\phi + 2kz \sin \psi)} \right] \frac{e^{ik(r - z \sin \psi)}}{r} \tag{189}$$

where $r >> z$ and $r > \lambda$

The above equations show that, when $r >> z$ and E and H are expressed in units such that they are equal in free space (see footnote 17), $E_{\parallel z}$ may be determined by multiplying $H_{\perp}$ by $\cos \psi$ while $E_{\perp}$ may be determined by dividing $H_{\parallel z}$ by $\cos \psi$; this latter result is of particular importance since $H_{\parallel z}$ is usually much smaller than $H_{\parallel d}$ near the surface of the earth so that measurements of the magnitude of $H_{\parallel}$ rather than $H_{\parallel z}$ would provide much too large a value for $E_{\perp}$. In fact, at the surface of the earth, since $\sin \psi \, (1 - R_{\parallel}) = \frac{\sqrt{n^2 - \cos^2 \psi}}{n^2} (1 + R_{\parallel})$ and $\sin \psi \, (1 - R_{\perp}) = \sqrt{n^2 - \cos^2 \psi}(1 + R_{\perp})$, (185) and (189) may be written

$$E_{\parallel d} = - \frac{E_{oe} \sqrt{n^2 - \cos^2 \psi} \, H_{\perp}}{H_{oe} \, n^2} \tag{190}$$

$$E_{\perp} = \frac{E_{om} \, H_{\parallel d}}{H_{om} \sqrt{n^2 - \cos^2 \psi}} \tag{191}$$

where $z = 0$ $\quad r > \lambda$

and we see that $E_{\perp}$ is very much smaller than the value which would be obtained by measuring $H_{\parallel d}$ and using no correction factor.

The Ground Wave Field Intensity at a Depth Δ Below the Surface

The electric and magnetic field intensities at a depth Δ below the surface of the ground and at a distance d from a vertical electric or vertical magnetic dipole at a height a (see Figure 22) may be expressed

$$\underline{E}_{\parallel t} = \frac{i \, E_{oe} \cos \psi}{n^2} \left[(1 + R_{\parallel}) \right.$$

$$\left. + (1 - R_{\parallel}) f(P_e, B_e) \, e^{i\phi} \right] \left(\cos \psi \, \underline{k} + \sqrt{n^2 - \cos^2 \psi} \, \underline{d} \right) \frac{e^{ik(r + \Delta \sqrt{n^2 - \cos^2 \psi})}}{r} \tag{192}$$

$$\underline{H}_{\perp t} = -\,i\,H_{oe}\cos\psi\,\underline{\theta}\left[(1+R_{\parallel})+(1-R_{\parallel})f(P_e,B_e)\;e^{i\phi}\right]\frac{e^{ik(r+\Delta\sqrt{n^2-\cos^2\psi})}}{r} \quad (193)$$

$$\underline{E}_{\perp t} = E_{om}\cos\psi\,\underline{\theta}\left[(1+R_{\perp})+(1-R_{\perp})f(P_m,B_m)\;e^{i\phi}\right]\frac{e^{ik(r+\Delta\sqrt{n^2-\cos^2\psi})}}{r} \quad (194)$$

$$\underline{H}_{\parallel t} = H_{om}\cos\psi\left[(1+R_{\perp})\right.$$

$$\left.+(1-R_{\perp})f(P_m,B_m)\;e^{i\phi}\right]\left(\cos\psi\,\underline{k}+\sqrt{n^2-\cos^2\psi}\,\underline{d}\right)\frac{e^{ik(r+\Delta\sqrt{n^2-\cos^2\psi})}}{r} \quad (195)$$

A comparison of the above equations with equations (163) to (166) for the field intensity just above the surface indicates that they give the same value of field intensity with $\Delta = 0$ for all of the components except $E_{\parallel z}$ which is n^2 times as strong just above the surface as it is just below the surface. The ratios of the surface to space wave components given in (167), (168), and (169) and in Figure 26 and Tables II and III are also applicable to the transmitted wave under the surface of the ground.

Part V. Conclusions.

The principal purpose of this report has been to provide a picture of the nature of the polarization of downcoming ionospheric radio waves with emphasis on those characteristics which have an effect on the operation of a direction finder. It was found convenient to separate this study into two parts (a) a study of the polarization of the downcoming waves before they reach the surface of the earth and (b) the modification in the polarization caused by the fact that the wave collectors of the direction finder are placed near the ground so that the resulting wave at the direction finder consists of both a direct wave and a wave reflected from the ground.

For a study of direction finding the polarization of a downcoming wave is adequately described when we can specify the ratio of the intensities of the components of the electric and magnetic fields polarized parallel and perpendicular to the plane of incidence and the relative phase between these components. It was found that, at very high frequencies, the ratio $(E_{\perp d}/E_{\parallel d})$ in the downcoming wave varies from a value much less than one to a value much greater than one, the median value of the ratio being one; for one per cent of the time it is greater than 10 and for one per cent of the time it is less than 0.1. At very low frequencies $(E_{\perp d}/E_{\parallel d})$ is distributed over a narrower range of values and the median value will be much less than one when the transmitted wave is polarized parallel to the plane of incidence at the ionosphere and will be much greater than one when the transmitted wave is polarized perpendicular to the plane of incidence at the ionosphere (see equations (96) and (97)). Near the magneto-ionic frequency, f_h, (for definition of f_h see equation (62)) the extraordinary wave is absorbed in the ionosphere and the ratio $(E_{\perp d}/E_{\parallel d})$ becomes equal to the constant value R_d (for definition of R_d see equations (66) and (26)). Just below the maximum usable frequency, only the extraordinary wave returns to the earth and the ratio $(E_{\perp d}/E_{\parallel d})$

becomes equal to the constant value $1/R_d$. At very high frequencies the relative phase between $E_{\perp d}$ and $E_{\parallel d}$ is random whereas, at very low frequencies, values of the relative phase near B (for definition of B see equation (66)) are more probable when the transmitted wave is polarized parallel to the plane of incidence while values near $(B - 180^\circ)$ are more probable when the transmitted wave is polarized perpendicular to the plane of incidence. Near the magneto-ionic frequency, f_h, the relative phase becomes equal to the constant value B and just below the maximum usable frequency the relative phase becomes equal to the constant value $(B - 180^\circ)$.

For wave collectors near the ground, the effect of the ground is to suppress the perpendicular component in favor of the parallel component of the resulting wave under most circumstances (see Figures 18, 19 and 20). When the elements of the direction finder responsive to the undesired perpendicular components of the resulting wave are buried underground as in the shielded U direction finder, this suppression will be very large indeed (see equations (138) and (112)) so that such a direction finder should be comparatively free from polarization error. On the other hand, when a direction finder is to be operated primarily at the shorter distances so that the elevation angles of the downcoming ionospheric waves are large, the parallel components of the downcoming waves will be suppressed in favor of the horizontal components for wave collectors above the ground and a direction finder designed to operate on these latter components, such as one with spaced vertical magnetic dipole wave collectors, would be expected to have some advantages. When, as in most direction finders, the vertical component of the electric field (or the perpendicular component of the magnetic field) is the desired component while the perpendicular component of the electric field is the undesired component, there will be less polarization error when the direction finder is located over soil with the largest possible value of the index of refraction, n, i.e. over soil with the highest possible dielectric constant and conductivity. In Part IV a simple method for measuring these ground constants is described.

The problems arising when testing a direction finder by means of fields transmitted from a source at a comparatively short distance away are discussed in Part IV. Due to the great complexity of the fields at distances less than one wavelength from a transmitting antenna and the lack of any reasonably simple, yet accurate, equations for the field at these short distances, it is considered desirable to keep the source for testing the direction finder at a distance greater than one wavelength. It is shown that, due to the presence of a surface wave from the nearby transmitter which is absent in the case of the downcoming ionospheric waves, tests for determining the magnitude of the polarization error of a direction finder can only be made for high elevation angles unless the source is removed to a very great distance or unless appropriate correction is made for the effect of the surface wave. In general it would appear that the National Bureau of Standards method of testing a direction finder for polarization error is to be preferred; in this method the polarization of the test wave is measured at the direction finder and the direction finder performance is then calculated using the equations in Part III of this report.

The method of calculating the electric field corresponding to the magnetic field as measured by a loop antenna is also given in Part IV. In particular, it is shown that $E_{\perp}$ may be determined from $H_{\parallel z}$ by dividing by cos ψ when the distance $r \gg z$ and $r \gg \lambda$.

A direction finder site should be on very level land with uniform ground conductivity. Although it has not been tried, it seems likely that information of value concerning a proposed site could be obtained very easily and rapidly by transmitting from a vertical magnetic dipole and measuring the ground constants at various points on the site using the method described in Part IV.

Acknowledgment.

I wish to acknowledge the assistance in preparing this report of Mr. E. W. Allen who made many of the calculations, of Mr. Robert E. Carter who prepared most of the figures and of Mrs. Ruth H. Driscoll who typed the report.

I am also indebted to my colleagues at the National Bureau of Standards, Mr. Harry Diamond, Mr. L. M. Poast, Dr. H. Lifschutz and Dr. Newbern Smith for a helpful discussion of many of the points considered in the report.

The author is also indebted for permission to make this study to Dr. L. P. Wheeler, Chief of the Technical Information Division, Engineering Department, and to Mr. E. K. Jett, Chief Engineer of the Federal Communications Commission.

The author would very much appreciate receiving comments regarding the report and, in particular, would like to be informed in case errors are discovered in it. Communications of this kind should be addressed to Mr. Kenneth A. Norton, now in the Office of the Chief Signal Officer, War Department, Washington, D.C. Additional copies of this report may be obtained by writing to Dr. J. H. Dellinger, Radio Section, National Bureau of Standards, Washington, D.C.

Appendix I

The Electric and Magnetic Fields from Horizontal Electric and Magnetic Dipoles.

At a distance $d > \lambda$ the electric and magnetic field intensities from a horizontal electric dipole at a height a and pointing in the positive $\underline{i}$ direction may be expressed:

$$\underline{E}_{\perp} = i\, E_{oe} \sin\theta\, \underline{\theta} \left\{ \frac{e^{ikr_1}}{r_1} + R_{\perp} \frac{e^{ikr_2}}{r_2} + (1 - R_{\perp}) f(P_m, B_m) \frac{e^{i(\phi + k r_2)}}{r_2} \right\} \quad (196)$$

$$\underline{E}_{\parallel} = i\, E_{oe} \cos\theta \left\{ \sin\psi_1 \frac{e^{ikr_1}}{r_1} \underline{\psi}_1 + \sin\psi_2\, R_{\parallel} \frac{e^{ikr_2}}{r_2} \underline{\psi}_2 \right.$$

$$\left. + \frac{\sqrt{n^2 - \cos^2\psi_2}}{n^2} (1 - R_{\parallel}) f(P_e, B_e) \left[\cos\psi_2\, \underline{k} + \frac{\sqrt{n^2 - \cos^2\psi_2}}{n^2} \underline{d} \right] \frac{e^{i(\phi + k r_2)}}{r_2} \right\} \quad (197)$$

$$\underline{H}_{\parallel} = i\, H_{oe} \sin\theta \left\{ \frac{e^{ikr_1}}{r_1} \underline{\psi}_1 + R_{\perp} \frac{e^{ikr_2}}{r_2} \underline{\psi}_2 \right.$$

$$\left. + (1 - R_{\perp}) f(P_m, B_m) \left[\cos\psi_2\, \underline{k} + \sqrt{n^2 - \cos^2\psi_2}\, \underline{d} \right] \frac{e^{i(\phi + k r_2)}}{r_2} \right\} \quad (198)$$

$$\underline{H}_{\perp} = -i\, H_{oe} \cos\theta\, \underline{\theta} \left\{ \sin\psi_1 \frac{e^{ikr_1}}{r_1} + \sin\psi_2\, R_{\parallel} \frac{e^{ikr_2}}{r_2} \right.$$

$$\left. + \frac{\sqrt{n^2 - \cos^2\psi_2}}{n^2} (1 - R_{\parallel}) f(P_e, B_e) \frac{e^{i(\phi + k r_2)}}{r_2} \right\} \quad (199)$$

where $d > \lambda$.

The angle θ together with the other geometrical parameters in the above equation are adequately defined in Figure 28 and in Figure 22 which illustrates the geometry in the plane of incidence. The unit vectors $\underline{\theta}$ and $\underline{d}$ may be defined $\underline{\theta} = \cos\theta\, \underline{j} - \sin\theta\, \underline{i}$ and $\underline{d} = \cos\theta\, \underline{i} + \sin\theta\, \underline{j}$

When the receiving point lies in the equatorial plane of the horizontal electric dipole, $\theta = 90^{\circ}$, $\underline{E}_{\parallel} = \underline{H}_{\perp} = 0$ and (196) and (198) become very similar to the expressions (152) and (153) for the vertical magnetic dipole except for the factors $\cos\psi_1$ and $\cos\psi_2$. On the other hand, when the receiving point lies in the $\underline{i} - \underline{k}$ plane, i.e. for transmission off the end of the horizontal electric dipole, $\theta = 0$, $\underline{E}_{\perp} = \underline{H}_{\parallel} = 0$ and the electric field will lie entirely in the plane of incidence; the surface

wave is weaker in this case in proportion to the factor $\sqrt{n^2 - \cos^2 \psi_2}/n^2 \cos \psi_2$ than the surface wave from the vertical electric dipole

Consider the case of transmission along the equatorial plane of the horizontal electric dipole for the purpose of testing a direction finder; when the center of the direction finder lies in the equatorial plane, then $\underline{E}_{\parallel}$ at one of the wave collectors will be equal to $-\underline{E}_{\parallel}$ for the other wave collector since θ will be slightly greater than 90° for one of the wave collectors and will be slightly less than 90° for the other wave collector.

At a distance $d > \lambda$ the electric and magnetic field intensities from a horizontal magnetic dipole at a height a and with its axis pointing in the positive $\underline{i}$ direction may be expressed:

$$\underline{E}_{\parallel} = E_{om} \sin \theta \left\{ \frac{e^{ikr_1}}{r_1} \underline{\psi}_1 + R_{\parallel} \frac{e^{ikr_2}}{r_2} \underline{\psi}_2 + (1 - R_{\parallel}) f(P_e, B_e) \left[\cos \psi_2 \underline{k} + \frac{\sqrt{n^2 - \cos^2 \psi_2}}{n^2} \underline{d} \right] \frac{e^{i(\phi + k r_2)}}{r_2} \right\} \quad (200)$$

$$\underline{E}_{\perp} = E_{om} \cos \theta \, \underline{\theta} \left\{ \sin \psi_1 \frac{e^{ikr_1}}{r_1} + \sin \psi_2 R_{\perp} \frac{e^{ikr_2}}{r_2} + \sqrt{n^2 - \cos^2 \psi_2} (1 - R_{\perp}) f(P_m, B_m) \frac{e^{i(\phi + k r_2)}}{r_2} \right\} \quad (201)$$

$$\underline{H}_{\perp} = - H_{om} \sin \theta \, \underline{\theta} \left\{ \frac{e^{ikr_1}}{r_1} + R_{\parallel} \frac{e^{ikr_2}}{r_2} + (1 - R_{\parallel}) f(P_e, B_e) \frac{e^{i(\phi + k r_2)}}{r_2} \right\} \quad (202)$$

$$\underline{H}_{\parallel} = H_{om} \cos \theta \left\{ \sin \psi_1 \frac{e^{ikr_1}}{r_1} \underline{\psi}_1 + \sin \psi_2 R_{\perp} \frac{e^{ikr_2}}{r_2} \underline{\psi}_2 + \sqrt{n^2 - \cos^2 \psi_2} (1 - R_{\perp}) f(P_m, B_m) \left[\cos \psi_2 \underline{k} + \sqrt{n^2 - \cos^2 \psi_2} \underline{d} \right] \frac{e^{i(\phi + k r_2)}}{r_2} \right\} \quad (203)$$

When the receiving point lies in the equatorial plane of the horizontal magnetic dipole, $\theta = 90°$, $\underline{E}_{\perp} = \underline{H}_{\parallel} = 0$ and (200) and (202) become very similar to the expressions (150) and (151) for the vertical electric dipole except for the factors $\cos \psi_1$ and $\cos \psi_2$. On the other hand, when the receiving point lies in the $\underline{i} - \underline{k}$ plane, $\theta = 0$, $\underline{E}_{\parallel} = \underline{H}_{\perp} = 0$ and the magnetic field will lie entirely in the plane of incidence. The surface wave is stronger in this latter case in proportion to the factor $\sqrt{n^2 - \cos^2 \psi_2}/\cos \psi_2$ than the surface wave from the vertical magnetic dipole; this suggests that the trans-

missions from a loop antenna with its axis parallel to the plane of incidence for the purpose of measuring the ground constants will be strongest when the loop axis is parallel to the ground.

Appendix II

Exact Equations for the Field at the Surface Radiated from a Vertical Magnetic Dipole on the Surface

Equations (150) to (153) are applicable only at distances greater than one wavelength and then only when $n^2 >> 1$. Wise[21] has given exact series expansions for the vertical electric dipole and these have been evaluated by Burrows[22] at distances less than one wavelength for several different values of the dielectric constant, with $x = 0$ and with $(a + z) = 0$, i.e. with the transmitting and receiving antennas on the ground.

Exact expressions are given below for the vertical magnetic and the horizontal electric fields at the surface of the earth radiated from a vertical magnetic dipole at the surface of the earth:

$$E_{\perp} = \frac{-2\,E_{om}}{ikd(n^2-1)}\left[\left(1 - n^2\, e^{ik(n-1)d}\right) + \frac{3i}{kd}\left(1 - n\, e^{ik(n-1)d}\right) - \frac{3}{(kd)^2}\left(1 - e^{ik(n-1)d}\right)\right]\frac{e^{i(kd-\omega t)}}{d} \quad (204)$$

$$H_{//z} = \frac{-2\,H_{om}}{ikd(n^2-1)}\left[\left(1 - n^3\, e^{ik(n-1)d}\right) + \frac{4i}{kd}\left(1 - n^2\, e^{ik(n-1)d}\right) - \frac{9}{(kd)^2}\left(1 - n\, e^{ik(n-1)d}\right) - \frac{9i}{(kd)^3}\left(1 - e^{ik(n-1)d}\right)\right]\frac{e^{i(kd-\omega t)}}{d} \quad (205)$$

The above exact equations were derived from the exact expression for the wave

---

[21] See footnote 14; also W. Howard Wise, "The Grounded Condenser Antenna Radiation Formula", Proc. I.R.E., Vol. 19, pp. 1684-1689, Sept. 1931, and "Note on Dipole Radiation Theory", Physica, Vol. 4, pp. 354-358, Oct. 1933.

[22] Charles R. Burrows, "Radio Propagation Over Plane Earth - Field Strength Curves", Bell System Technical Journal, Vol. 16, pp. 45-75, Jan. 1937, and an addendum to the above paper in Bell System Technical Journal, Vol. 16, pp. 574-577, Oct. 1937.

function obtained by van der Pol[23] for a vertical magnetic dipole on the surface; an equation for $H_{\phi d}$ could not be obtained since it involves differentiation with respect to z which does not appear in the wave function for the case $(a+z) = 0$. At very short distances, we see by the above equations that the field will oscillate with distance due to the terms containing the exponential $e^{ik(n-1)d}$. At large distances, since $ik(n-1)d$ will have a large negative real part, the exponential will approach zero, the quantities in the square brackets in (204) and (205) approach one, and (204) and (205) become identical to the first terms in the asymptotic expansions of equations (152) and (153) with $(a+z) = 0$.

Since the above equations are confined to the case $(a+z) = 0$ and since the field from the vertical magnetic dipole increases very rapidly as $(a+z)$ is increased, they are of little interest except from the academic point of view. Unfortunately, equally simple exact equations for the field with $(a+z)$ different from zero cannot be obtained; the infinite series expansions obtained by Wise for this case (given in the second reference in footnote 21) may be useful in some applications but, at distances less than one wavelength where (150) to (153) are not sufficiently accurate, so many terms must be retained in these series expansions that they are very difficult to use.

---

[23] Balth van der Pol, "Uber die Ausbreitung Elektromagnetischer Wellen", Jahrbuch der Drahtlosen Telegraphie und Telephonie, Zeitschrift fur Hochfrequenztechnik, Band 37, Heft 4, pp. 152-156, April 1931.

THE POLARIZATION OF A DOWNCOMING RADIO WAVE

(AS VIEWED BY AN OBSERVER LOOKING BACK ALONG THE WAVE NORMAL IN THE NEGATIVE $\underline{i}$ DIRECTION)

$f = 1$ MC $\quad f_h = 1.53$ MC
$\theta = 90^\circ$ (WEST – EAST) $\quad \phi = 45^\circ$
$I = 68^\circ\ 30'$ $\quad Z = 0.306$

$$\underline{E}_{od} = \underline{K}\cos\omega t + \underline{j}\,0.7187\cos(\omega t + 255^\circ\ 42'\ 30'')$$
$$\underline{E}_{xd} = \underline{K}\,0.7187\cos\omega t - \underline{j}\cos(\omega t + 255^\circ\ 42'\ 30'')$$

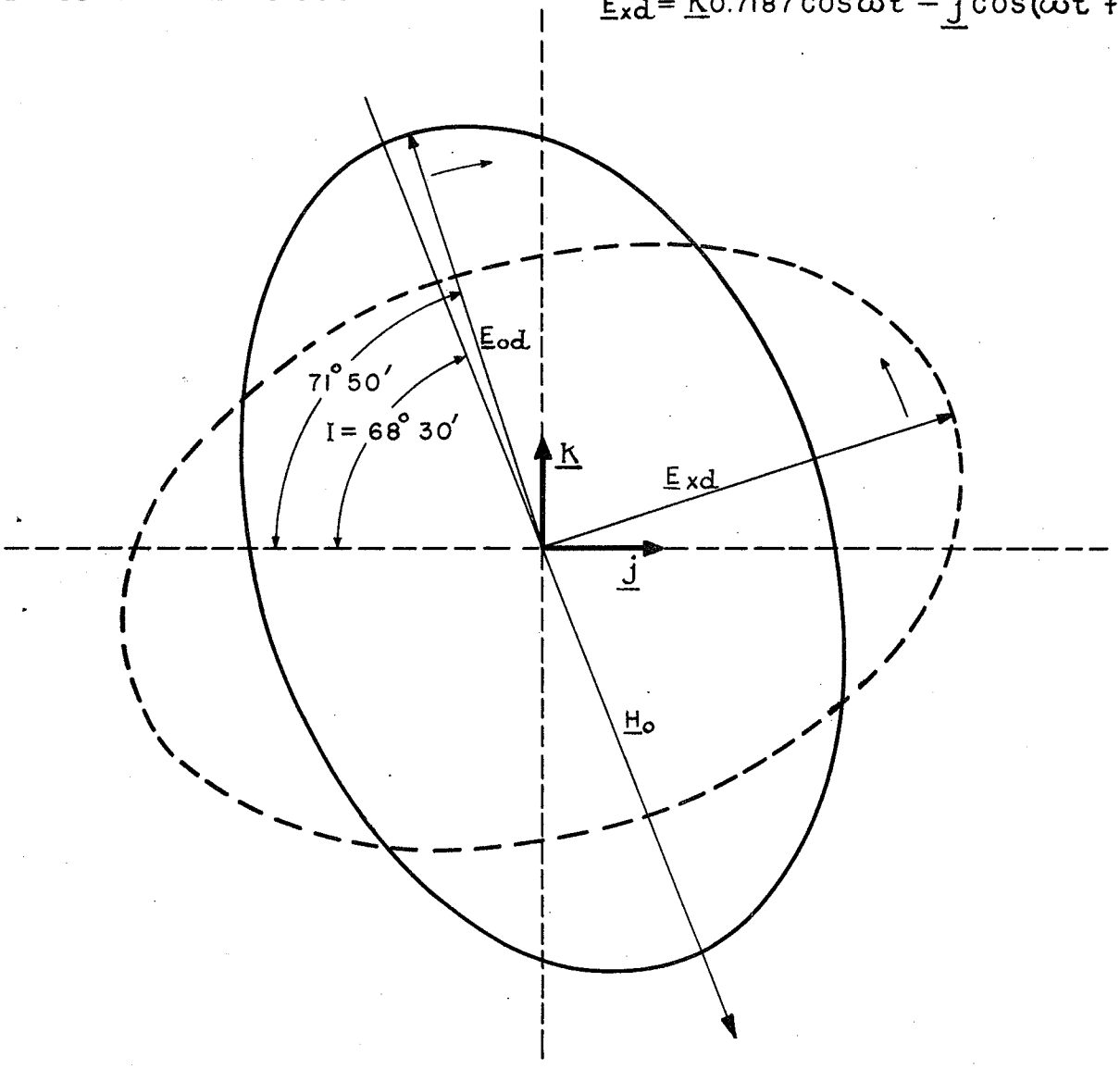

NOTE: THIS FIGURE SHOWS ONLY THE SHAPES OF THE POLARIZATION ELLIPSES; ON THIS FREQUENCY THE EXTRAORDINARY WAVE ELLIPSE WILL BE MUCH SMALLER THAN THE ORDINARY WAVE ELLIPSE DUE TO THE GREATER ATTENUATION OF THE EXTRAORDINARY WAVE. $\underline{E}_{od}$ AND $\underline{E}_{xd}$ ARE SHOWN AT MAXIMUM EXTENSION.

Fig. 1

THE POLARIZATION OF A DOWNCOMING RADIO WAVE

(AS VIEWED BY AN OBSERVER LOOKING BACK ALONG THE WAVE NORMAL IN THE NEGATIVE $\underline{i}$ DIRECTION)

$f = 1\ MC \quad f_h = 1.53\ MC$
$\Theta = 270^\circ$ (EAST–WEST) $\phi = 45^\circ$
$I = 68^\circ 30' \quad z = 0.306$

$$\underline{E}_{od} = \underline{k}\cos\omega t + \underline{j}\,0.7715\cos(\omega t + 310^\circ 55')$$
$$\underline{E}_{xd} = \underline{k}\,0.7715\cos\omega t - \underline{j}\cos(\omega t + 310^\circ 55')$$

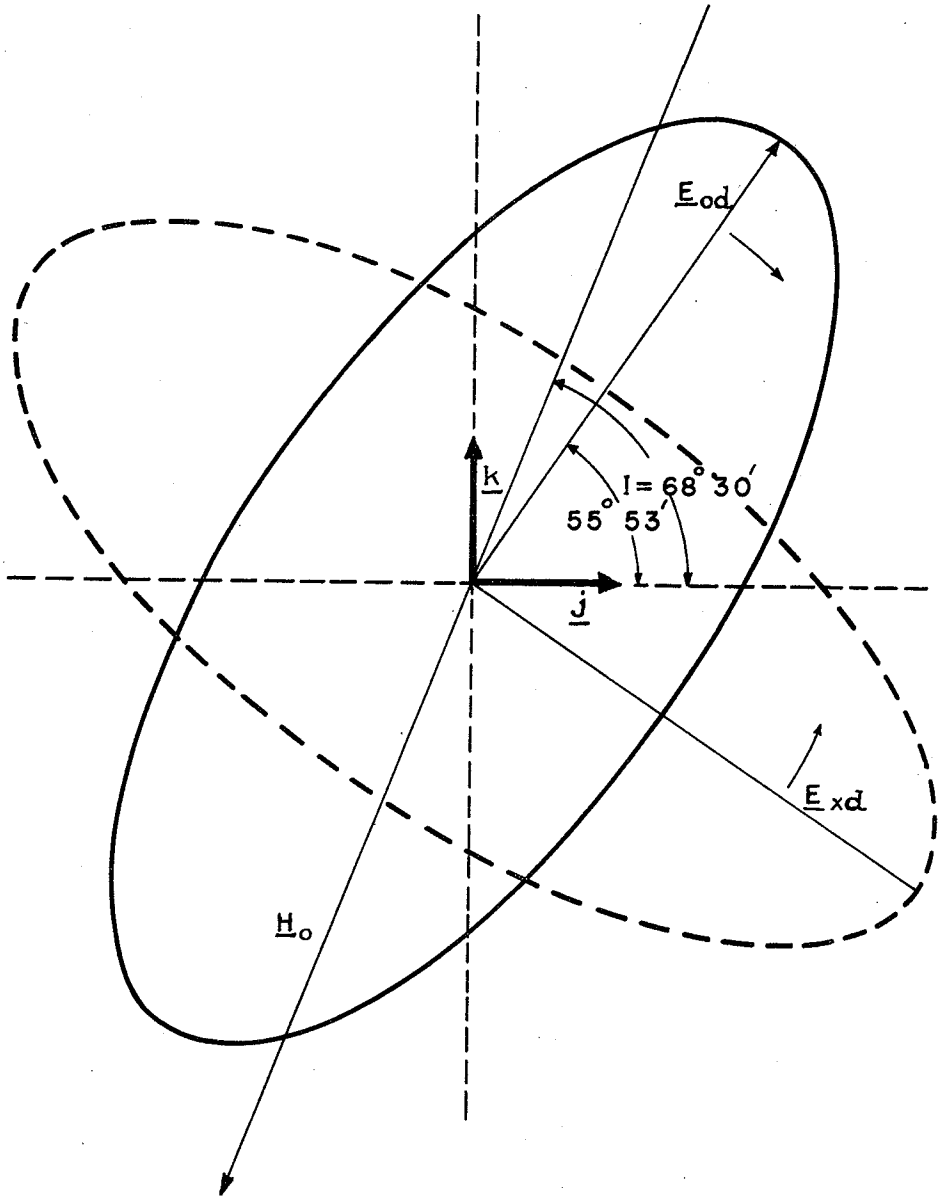

NOTE: THIS FIGURE SHOWS ONLY THE SHAPES OF THE POLARIZATION ELLIPSES; ON THIS FREQUENCY THE EXTRAORDINARY WAVE ELLIPSE WILL BE MUCH SMALLER THAN THE ORDINARY WAVE ELLIPSE DUE TO THE GREATER ATTENUATION OF THE EXTRAORDINARY WAVE. $\underline{E}_{od}$ AND $\underline{E}_{xd}$ ARE SHOWN AT MAXIMUM EXTENSION.

Fig. 2

THE POLARIZATION OF A DOWNCOMING RADIO WAVE

(AS VIEWED BY AN OBSERVER LOOKING BACK ALONG THE WAVE NORMAL IN THE NEGATIVE $\underline{i}$ DIRECTION)

$f = 1\ MC \quad f_h = 1.53\ MC$

$\Theta = 180^\circ$ (NORTH – SOUTH) $\phi = 45^\circ$

$I = 68^\circ\ 30' \quad z = 0.306$

$\underline{E}_{od} = \underline{k}\cos\omega t + \underline{j}0.2957\cos(\omega t + 287^\circ 1')$

$\underline{E}_{xd} = \underline{k}\,0.2957\cos\omega t - \underline{j}\cos(\omega t + 287^\circ 1')$

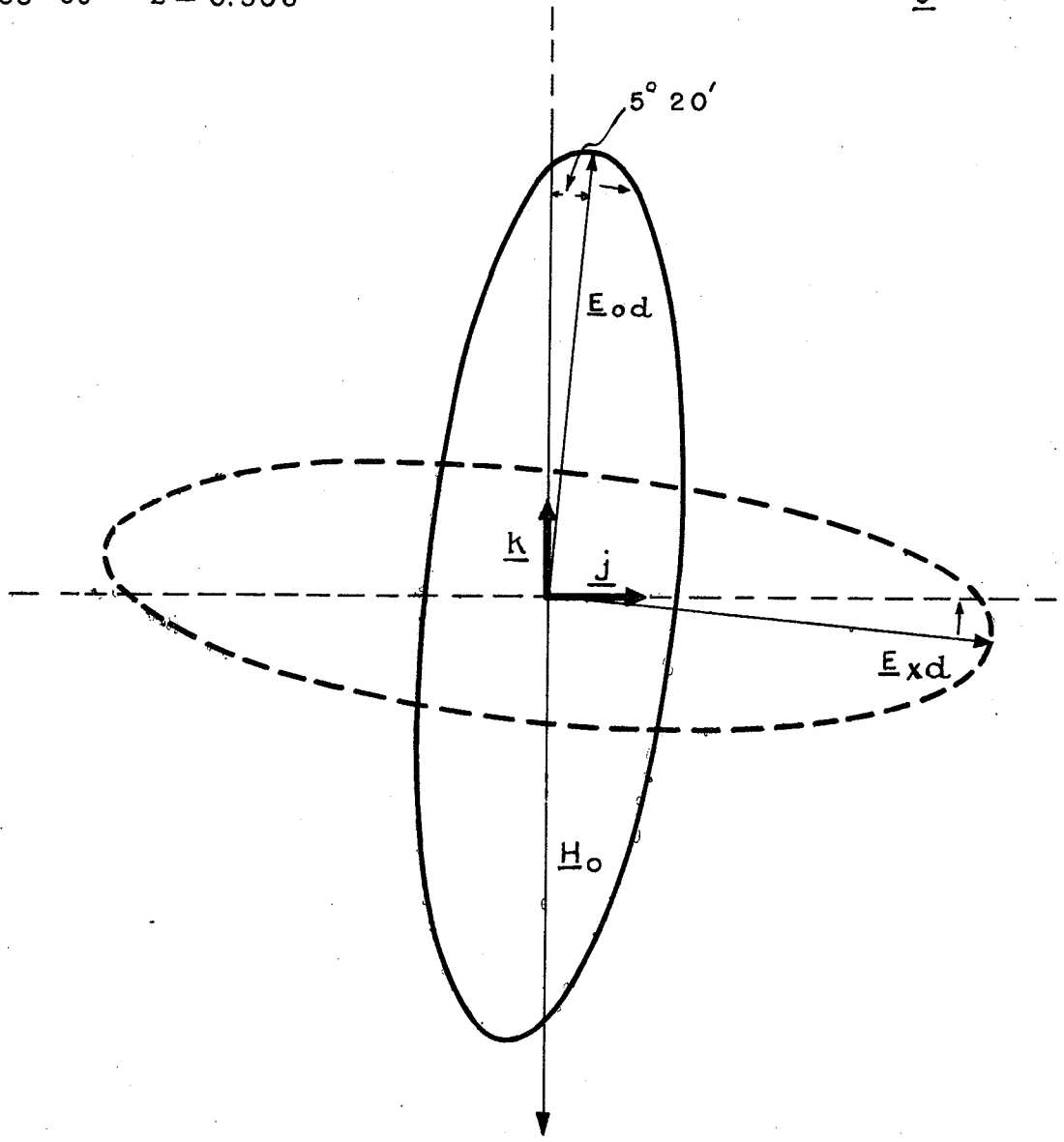

NOTE: THIS FIGURE SHOWS ONLY THE SHAPES OF THE POLARIZATION ELLIPSES; ON THIS FREQUENCY THE EXTRAORDINARY WAVE ELLIPSE WILL BE MUCH SMALLER THAN THE ORDINARY WAVE ELLIPSE DUE TO THE GREATER ATTENUATION OF THE EXTRAORDINARY WAVE. $\underline{E}_{od}$ AND $\underline{E}_{xd}$ ARE SHOWN AT MAXIMUM EXTENSION.

Fig. 3

THE POLARIZATION OF A DOWNCOMING RADIO WAVE

(AS VIEWED BY AN OBSERVER LOOKING BACK ALONG THE WAVE NORMAL IN THE NEGATIVE $\underline{i}$ DIRECTION)

$f = 1$ MC $\quad f_h = 1.53$ MC $\quad \theta = 0°$ (SOUTH-NORTH) $\quad I = 68° 30'$ $\quad z = 0.306$

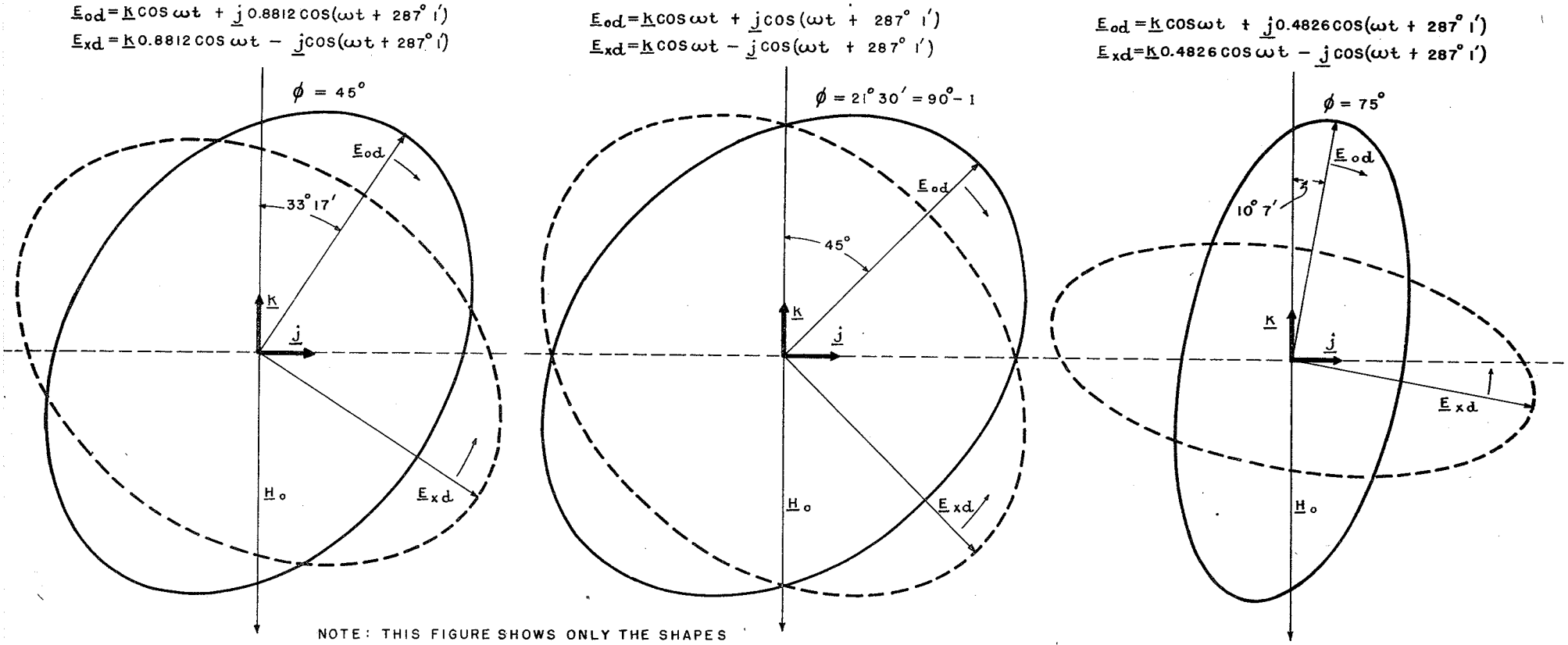

NOTE: THIS FIGURE SHOWS ONLY THE SHAPES OF THE POLARIZATION ELLIPSES; ON THIS FREQUENCY THE EXTRAORDINARY WAVE ELLIPSE WILL BE MUCH SMALLER THAN THE ORDINARY WAVE ELLIPSE DUE TO THE GREATER ATTENUATION OF THE EXTRAORDINARY WAVE. $\underline{E}_{od}$ AND $\underline{E}_{xd}$ ARE SHOWN AT MAXIMUM EXTENSION.

FIGURE 4

THE POLARIZATION OF A DOWNCOMING RADIO WAVE

(AS VIEWED BY AN OBSERVER LOOKING BACK ALONG THE WAVE NORMAL IN THE NEGATIVE $\underline{i}$ DIRECTION)

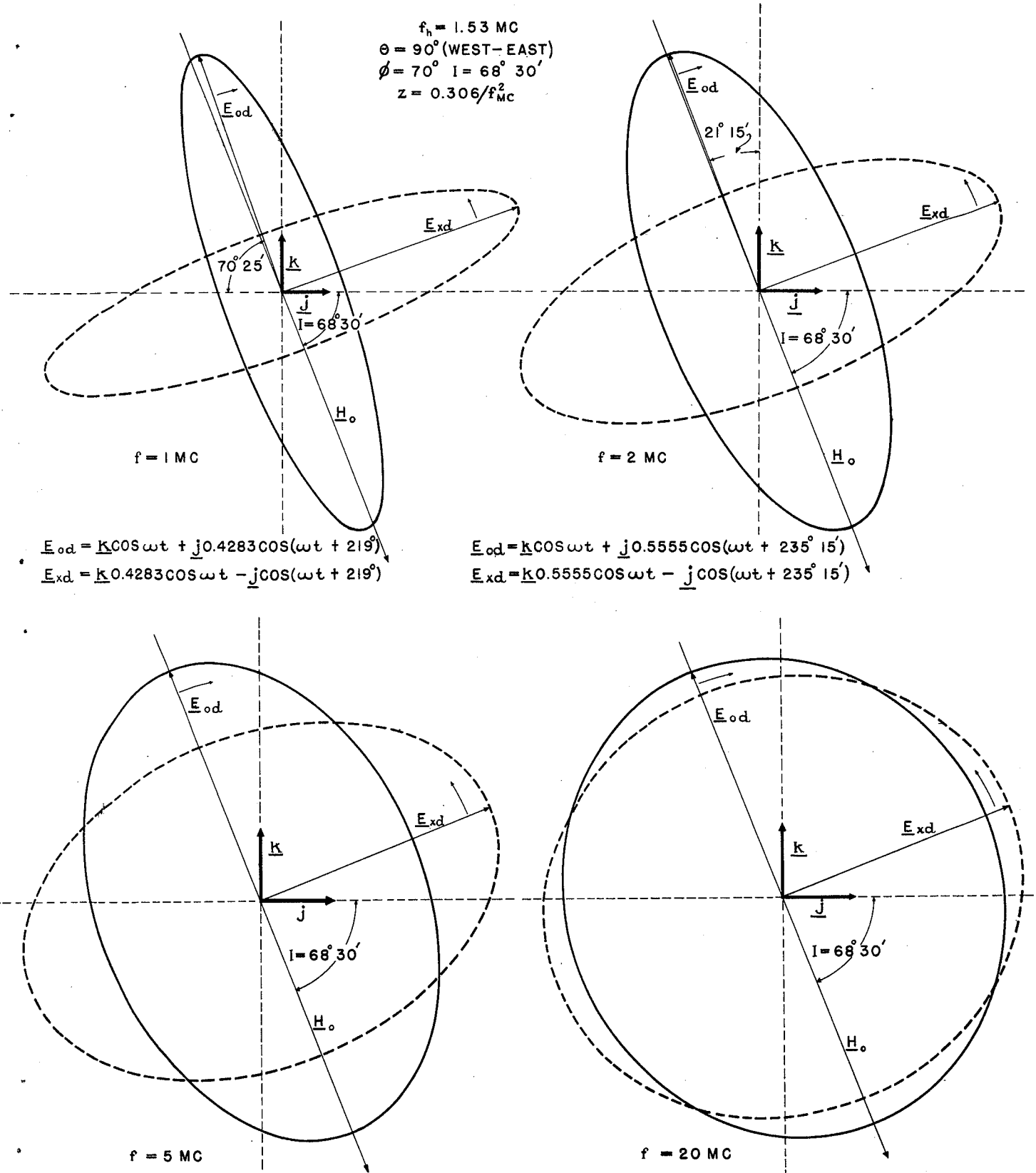

$\underline{E}_{od} = \underline{K}\cos\omega t + \underline{j}0.4283\cos(\omega t + 219°)$

$\underline{E}_{xd} = \underline{K}0.4283\cos\omega t - \underline{j}\cos(\omega t + 219°)$

$\underline{E}_{od} = \underline{K}\cos\omega t + \underline{j}0.5555\cos(\omega t + 235° 15')$

$\underline{E}_{xd} = \underline{K}0.5555\cos\omega t - \underline{j}\cos(\omega t + 235° 15')$

$\underline{E}_{od} = \underline{K}\cos\omega t + \underline{j}0.7508\cos(\omega t + 253° 31')$

$\underline{E}_{xd} = \underline{K}0.7508\cos\omega t - \underline{j}\cos(\omega t + 253° 31')$

$\underline{E}_{od} = \underline{K}\cos\omega t + \underline{j}0.9273\cos(\omega t + 265° 38')$

$\underline{E}_{xd} = \underline{K}0.9273\cos\omega t - \underline{j}\cos(\omega t + 265° 38')$

Fig. 6

THE DISTRIBUTION OF THE AMPLITUDE OF THE VECTOR SUM OF A LARGE NUMBER OF SCATTERED WAVES WITH RANDOM RELATIVE PHASES FOR THE CASE WHERE THE EQUIVALENT UNSCATTERED AMPLITUDE IS UNITY

$$P = 100 e^{-F^2}$$

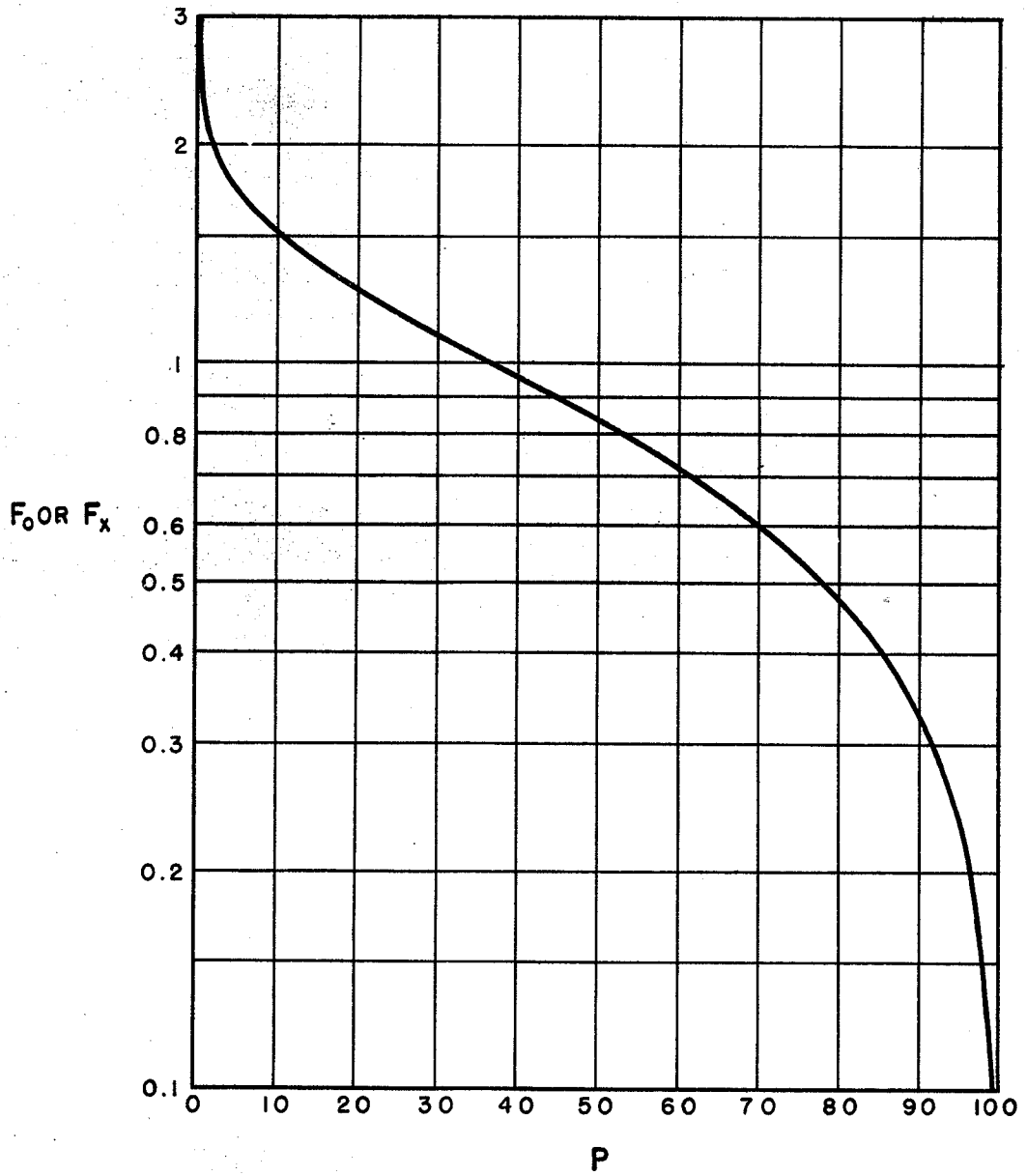

PERCENTAGE OF THE TIME THAT F_0 OR F_x EXCEEDS THE ORDINATE VALUES

FIGURE 6

THE DISTRIBUTION OF THE RATIO OF THE AMPLITUDE OF TWO VECTORS EACH VARYING INDEPENDENTLY IN TIME IN ACCORDANCE WITH THE RAYLEIGH DISTRIBUTION

$$P = \frac{100}{1 + q^2}$$

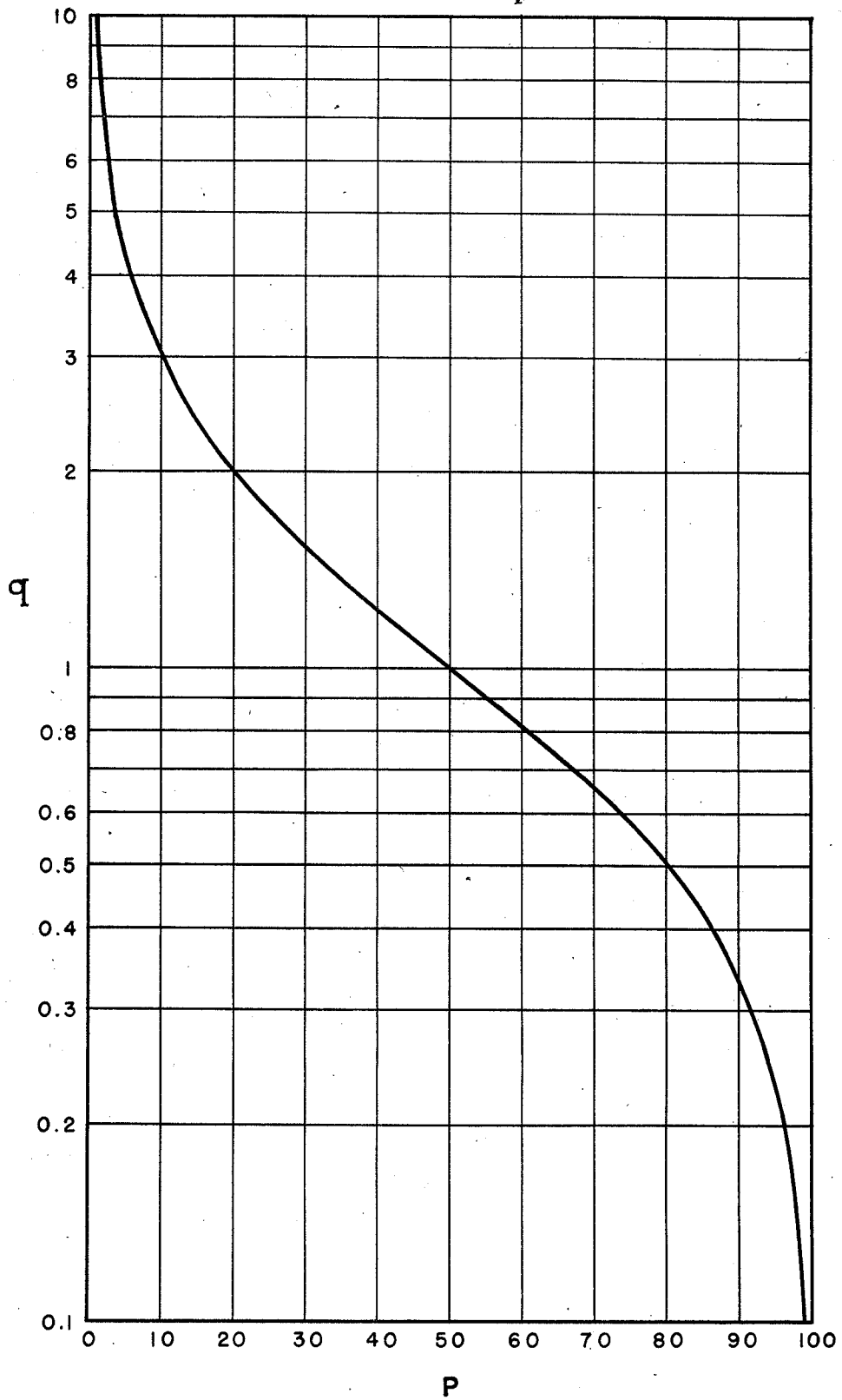

PERCENTAGE OF THE TIME THAT q EXCEEDS THE ORDINATE VALUES

FIGURE 7

THE DISTRIBUTION OF THE RATIO $\left|E_{\perp d}/E_{\parallel d}\right|$ FOR 10 FIXED VALUES OF q

$f = 5$ MC $\quad R_i = 0.7523 \quad R_d = 0.7508 \quad (A_x/A_0) = 1 \quad \underline{E_i} = E_{\perp i}\underline{j}$

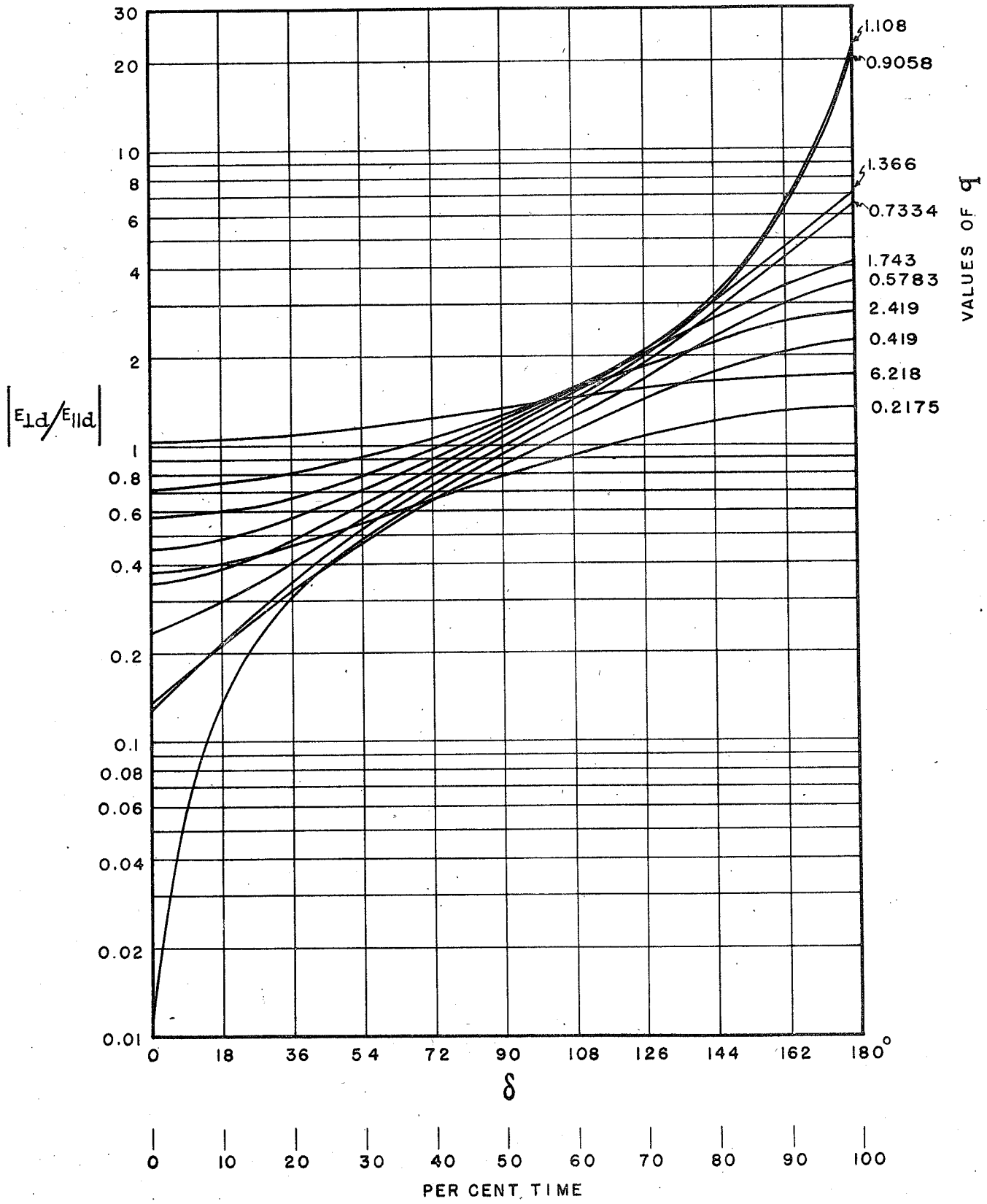

FIGURE 8

THE DISTRIBUTION OF THE RELATIVE PHASE BETWEEN $E_{\perp d}$ AND $E_{\parallel d}$ FOR 10 FIXED VALUES OF q

$f = 5$ MC $\quad R_i = 0.7523 \quad R_d = 0.7508 \quad (A_x/A_o) = 1 \quad \underline{E_i} = E_{\perp ij}$

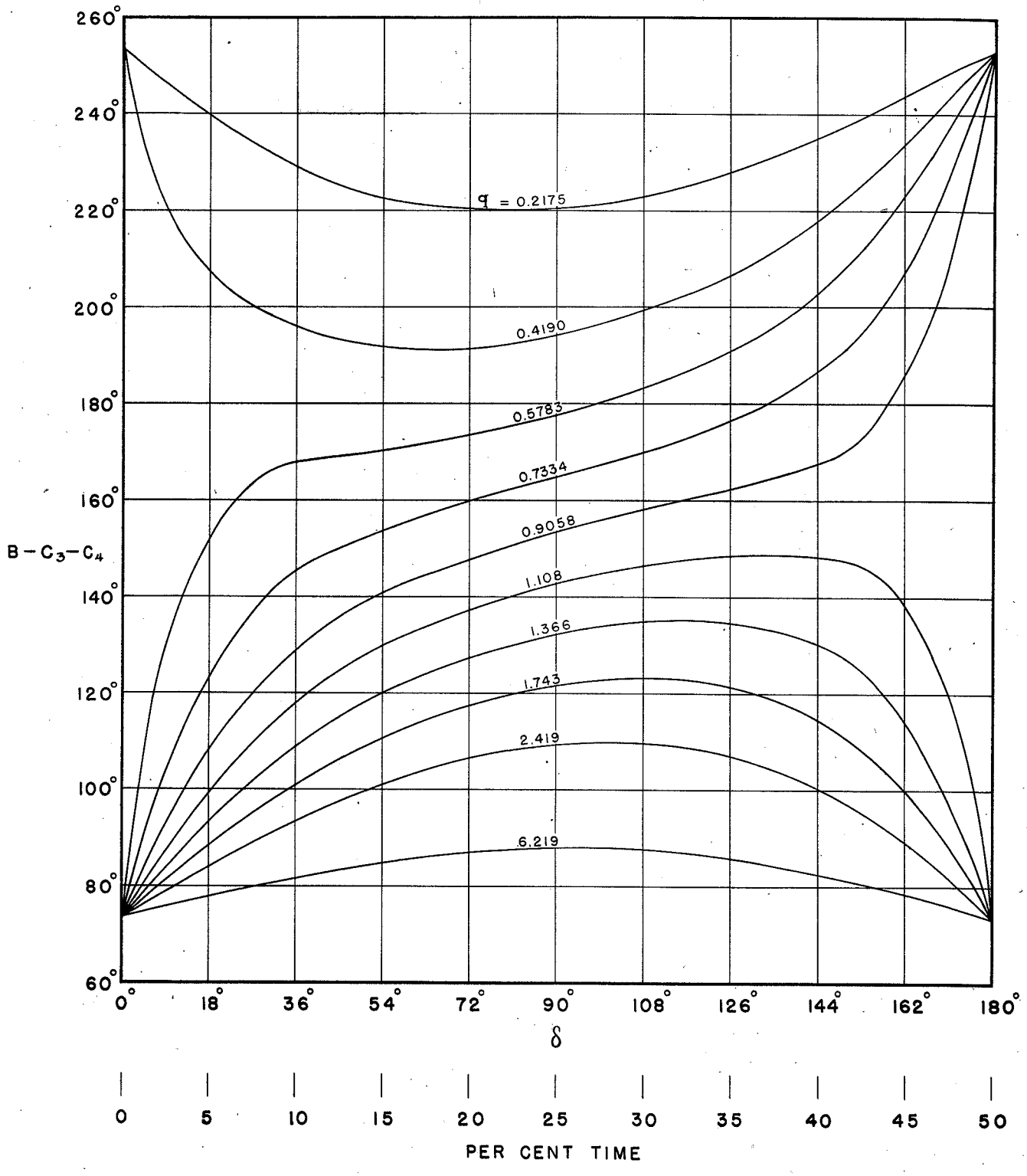

FIGURE 9

DISTRIBUTION OF $\left|E_{\perp d}/E_{\parallel d}\right|$

$\theta = 90^\circ$ (WEST TO EAST) $\quad \phi = 70^\circ$

(a) $\underline{E}_i = E_{\parallel i}\underline{k}$ } $f = 1$ MC $\quad Z = 0.306 \quad B = 219^\circ$
(b) $\underline{E}_i = E_{\perp i}\underline{j}$ } $R_i = 0.5117 \quad R_d = 0.4283 (A_x/A_o) = 0.1$

(c) $\underline{E}_i = E_{\parallel i}\underline{k}$ } $f = 5$ MC $\quad Z = 0.01224 \quad B = 253^\circ 31'$
(d) $\underline{E}_i = E_{\perp i}\underline{j}$ } $R_i = 0.7523 \quad R_d = 0.7508 (A_x/A_o) = 1$

--- CURVE FOR $R_i R_d (A_x/A_o) = 1$

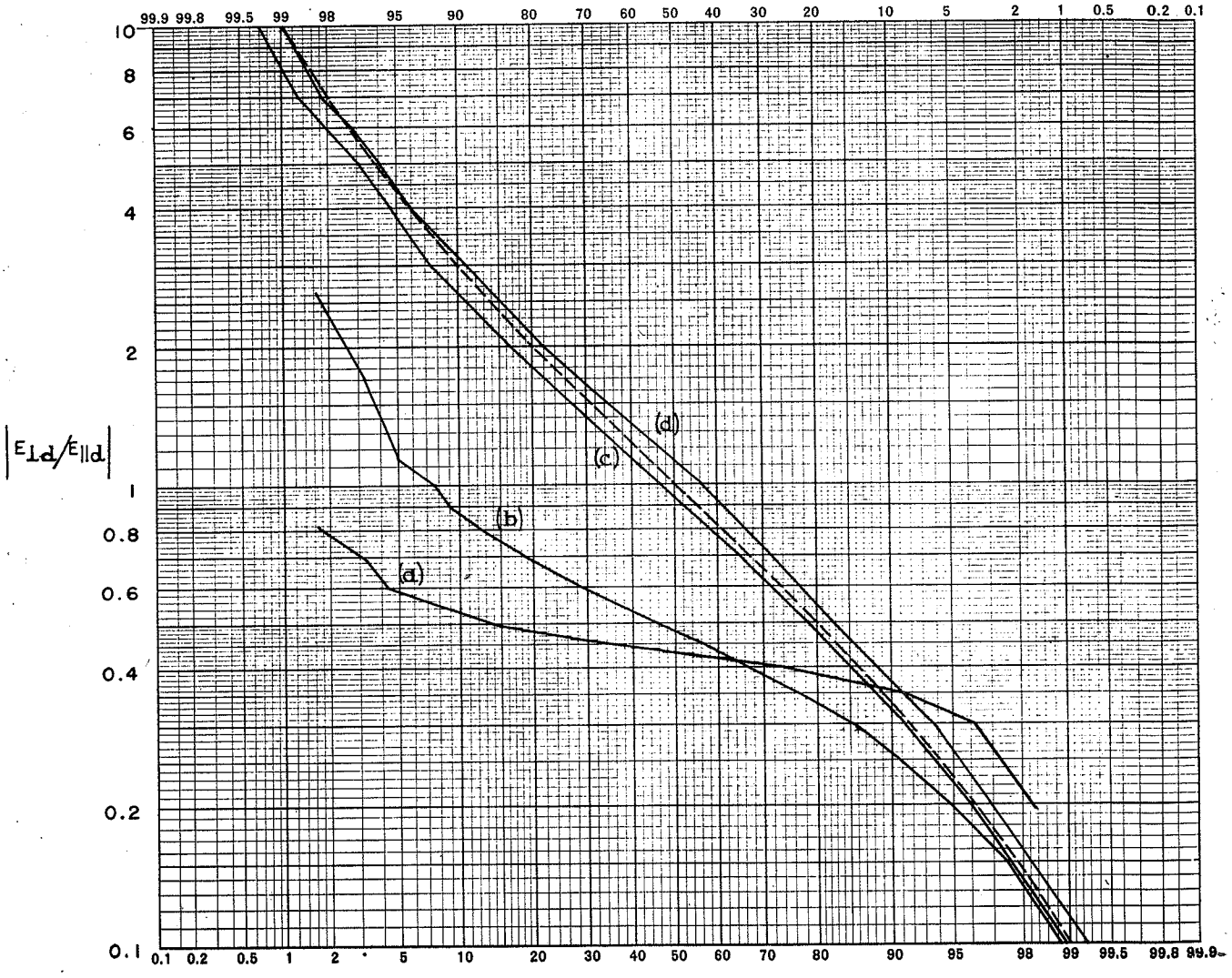

PER CENT TIME

FIGURE 10

DISTRIBUTION OF THE RELATIVE PHASE BETWEEN $E_{\perp d}$ AND $E_{\parallel d}$

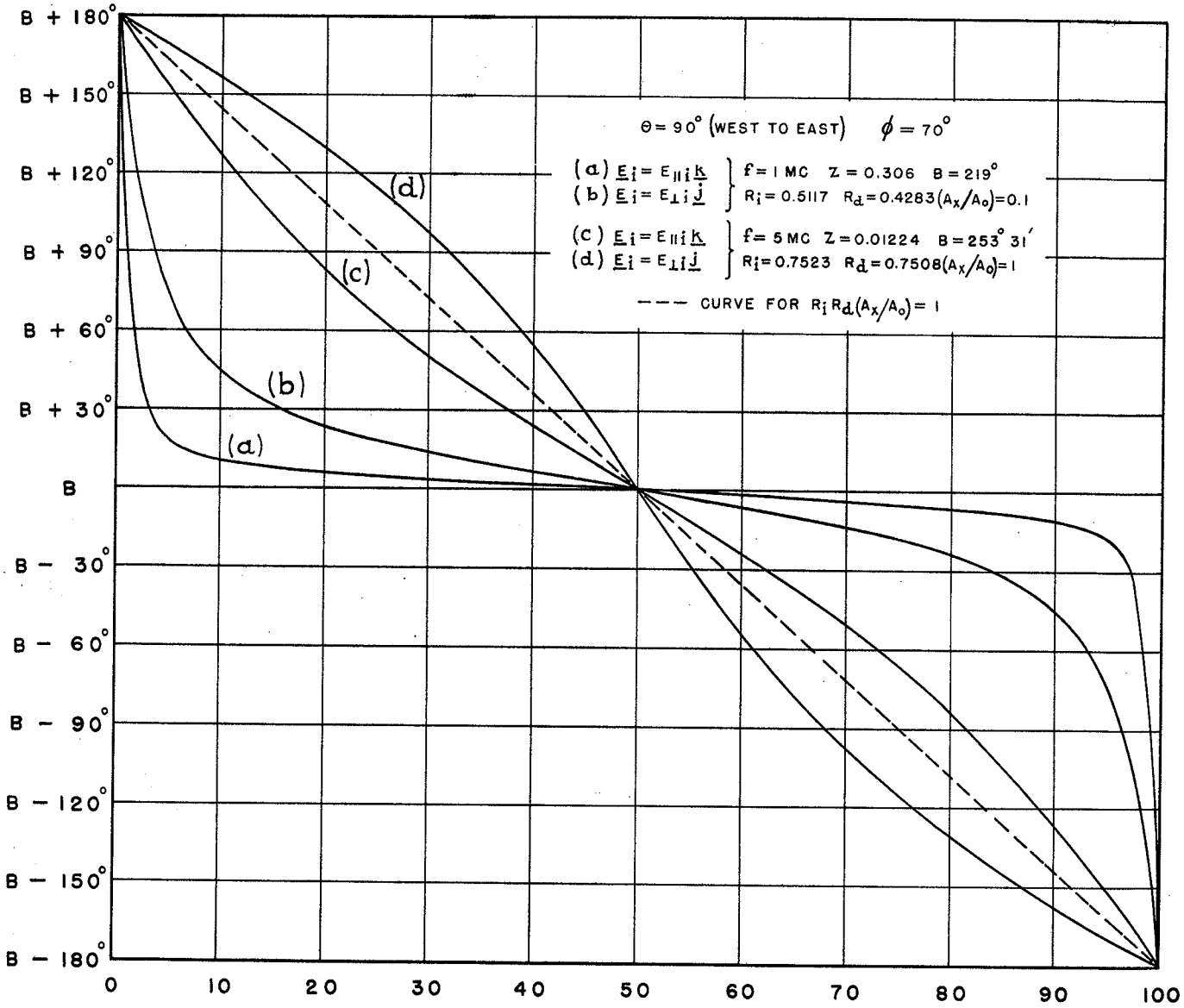

FIGURE 11

PROBABILITY THAT THE RELATIVE PHASE BETWEEN $E_{\perp d}$ AND $E_{\parallel d}$ HAS A VALUE EQUAL TO THE ABSCISSAE ± 10°

$\Theta = 90°$ (WEST TO EAST) $\quad \phi = 70°$

(a) $\underline{E}_i = E_{\parallel i}\underline{k}$ } $f = 1$ MC $\quad Z = 0.306 \quad B = 219°$
(b) $\underline{E}_i = E_{\perp i}\underline{j}$ } $R_i = 0.5117 \quad R_d = 0.4283(A_x/A_o) = 0.1$

(c) $\underline{E}_i = E_{\parallel i}\underline{k}$ } $f = 5$ MC $\quad Z = 0.01224 \quad B = 253° 31'$
(d) $\underline{E}_i = E_{\perp i}\underline{j}$ } $R_i = 0.7523 \quad R_d = 0.7508(A_x/A_o) = 1$

— — — CURVE FOR $R_i R_d (A_x/A_o) = 1$

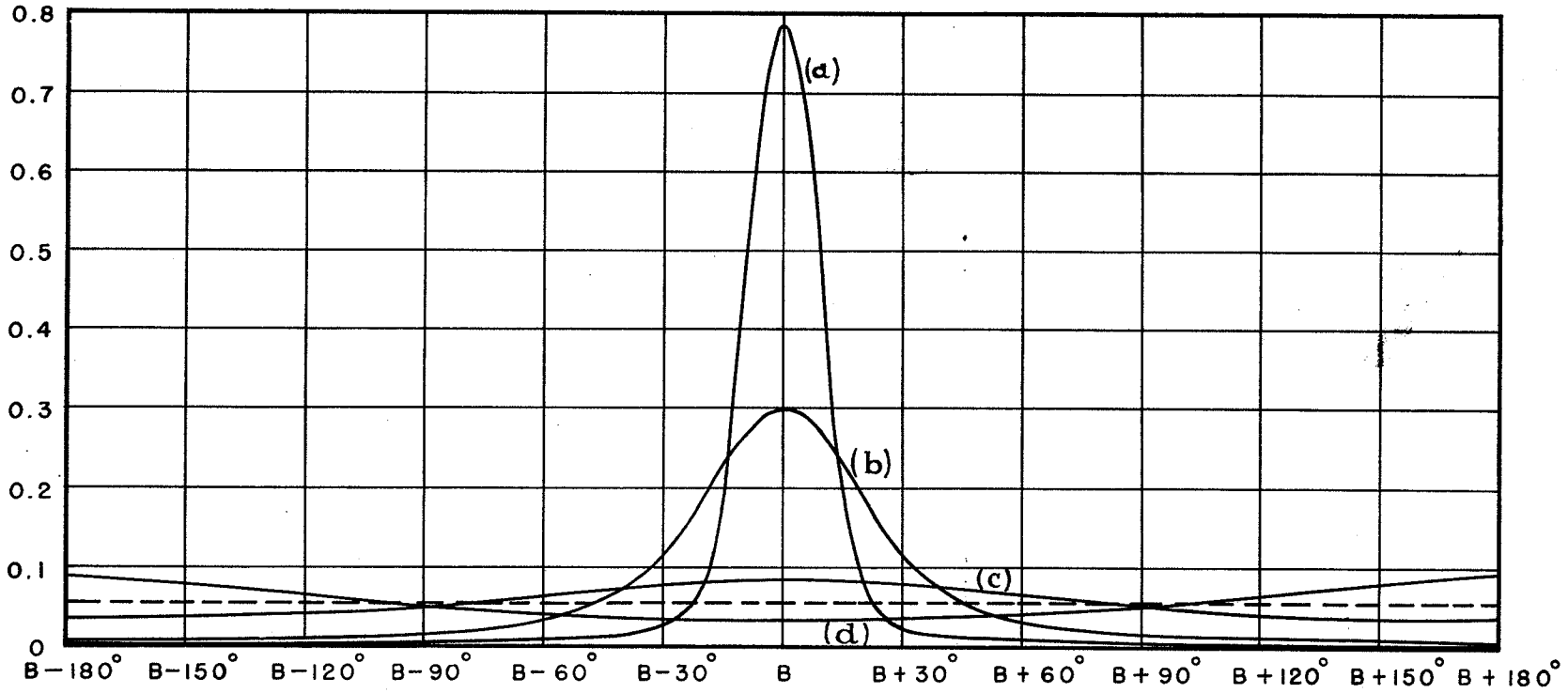

FIGURE 12

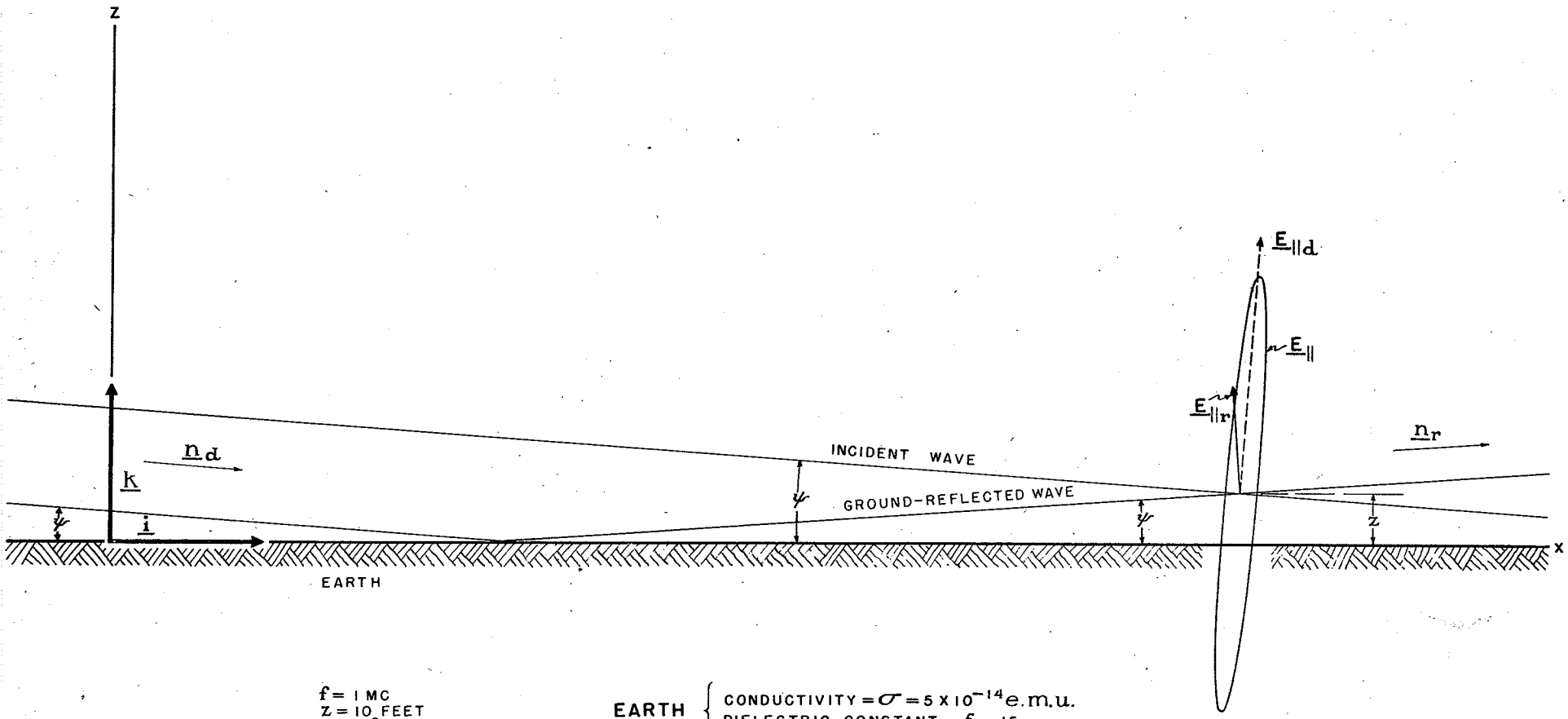

f = 1 MC
z = 10 FEET
ψ = 4°

EARTH { CONDUCTIVITY = $\sigma = 5 \times 10^{-14}$ e.m.u.
DIELECTRIC CONSTANT = $\epsilon = 15$

FIGURE 13

VECTOR REPRESENTATION OF GROUND REFLECTED WAVE

|| ELECTRIC VECTOR PARALLEL TO PLANE OF INCIDENCE
⊥ ELECTRIC VECTOR NORMAL TO PLANE OF INCIDENCE
----- INCIDENT PLANE WAVE, ——— GROUND REFLECTED WAVE
ψ_m = BREWSTER'S ANGLE

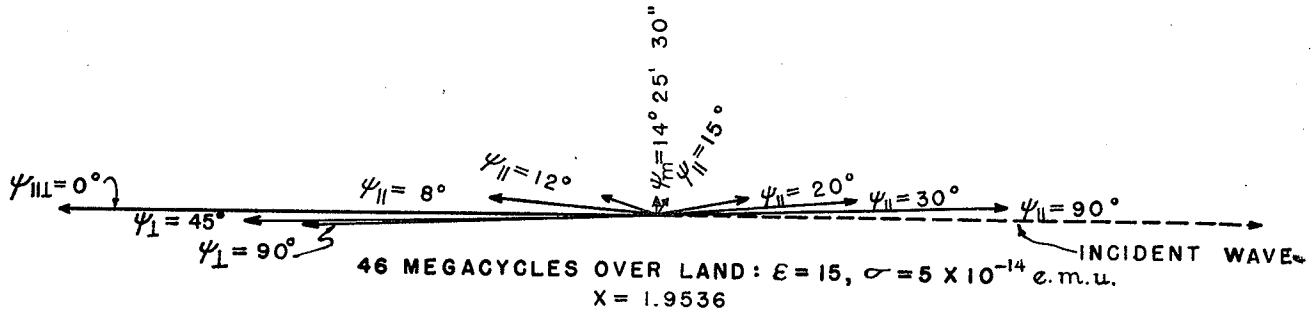

46 MEGACYCLES OVER LAND: $\varepsilon = 15$, $\sigma = 5 \times 10^{-14}$ e.m.u.
X = 1.9536

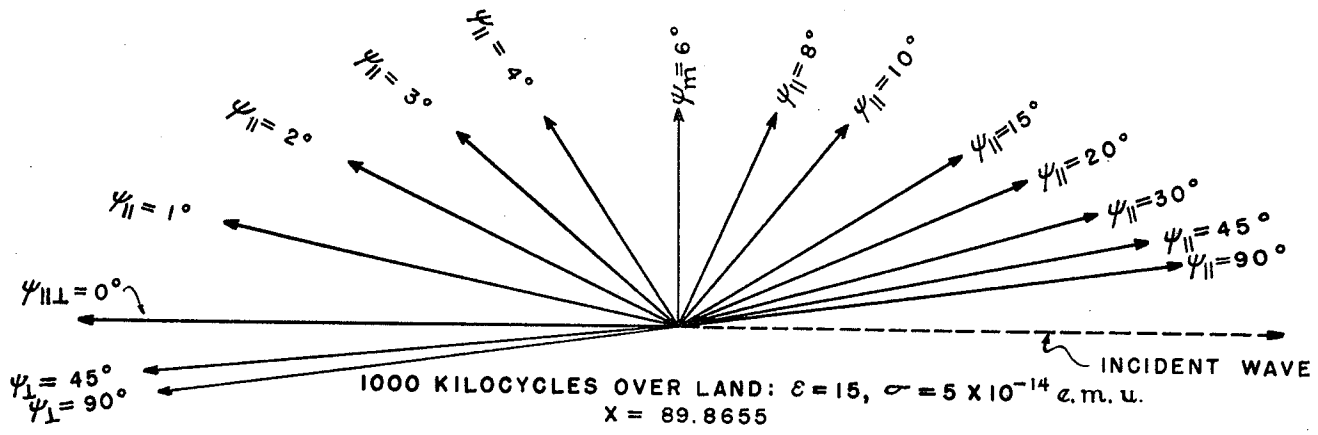

1000 KILOCYCLES OVER LAND: $\varepsilon = 15$, $\sigma = 5 \times 10^{-14}$ e.m.u.
X = 89.8655

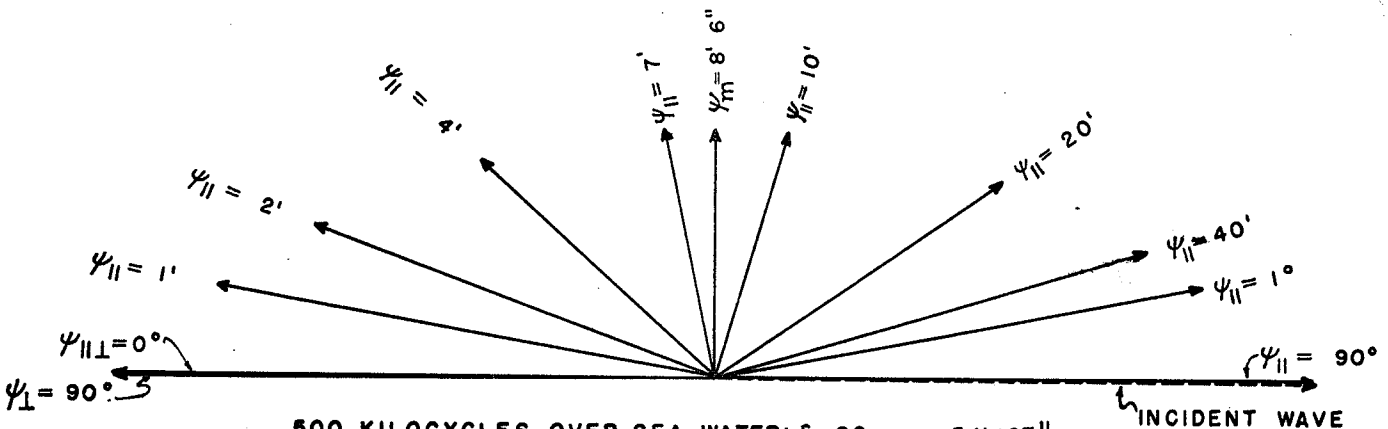

500 KILOCYCLES OVER SEA WATER: $\varepsilon = 80$, $\sigma = 5 \times 10^{-11}$ e.m.u.
X = 179,731

FIGURE 14

CURVES RELATING THE BREWSTER ANGLE, ψ_m, AND THE CORRESPONDING MINIMUM VALUE OF PLANE WAVE REFLECTION COEFFICIENT, $|R_{\parallel}|_m$, WITH ϵ AND X

$$X = \frac{1.79731 \cdot 10^{15} \sigma_{e.m.u.}}{f_{mc}}$$

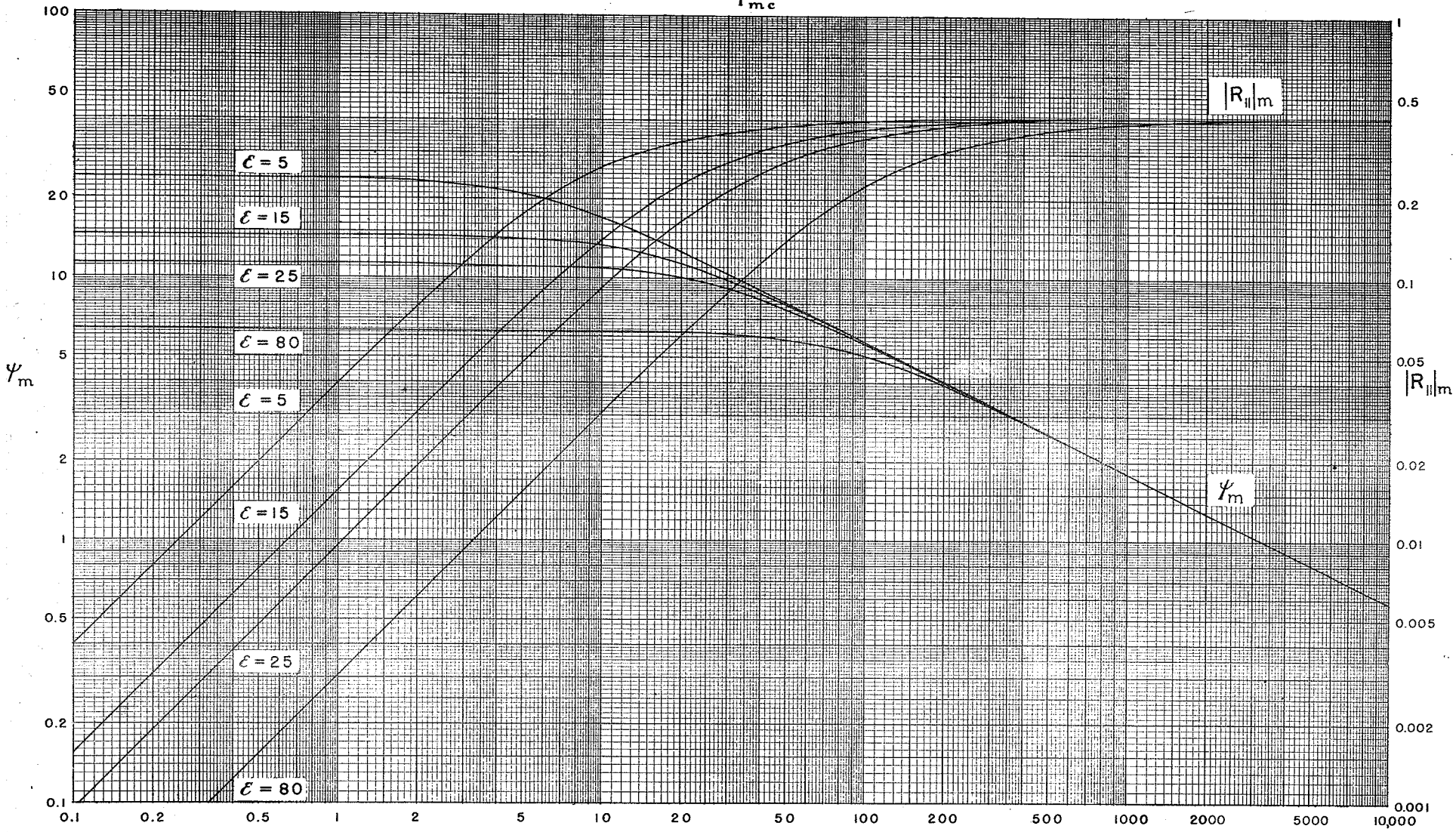

FIGURE 15

THE POLARIZATION OF THE ELECTRIC VECTOR NEAR THE EARTH'S SURFACE WHEN A WAVE WITH ITS ELECTRIC VECTOR PARALLEL TO THE PLANE OF INCIDENCE IS INCIDENT AT AN ANGLE $\Psi << \Psi_m$

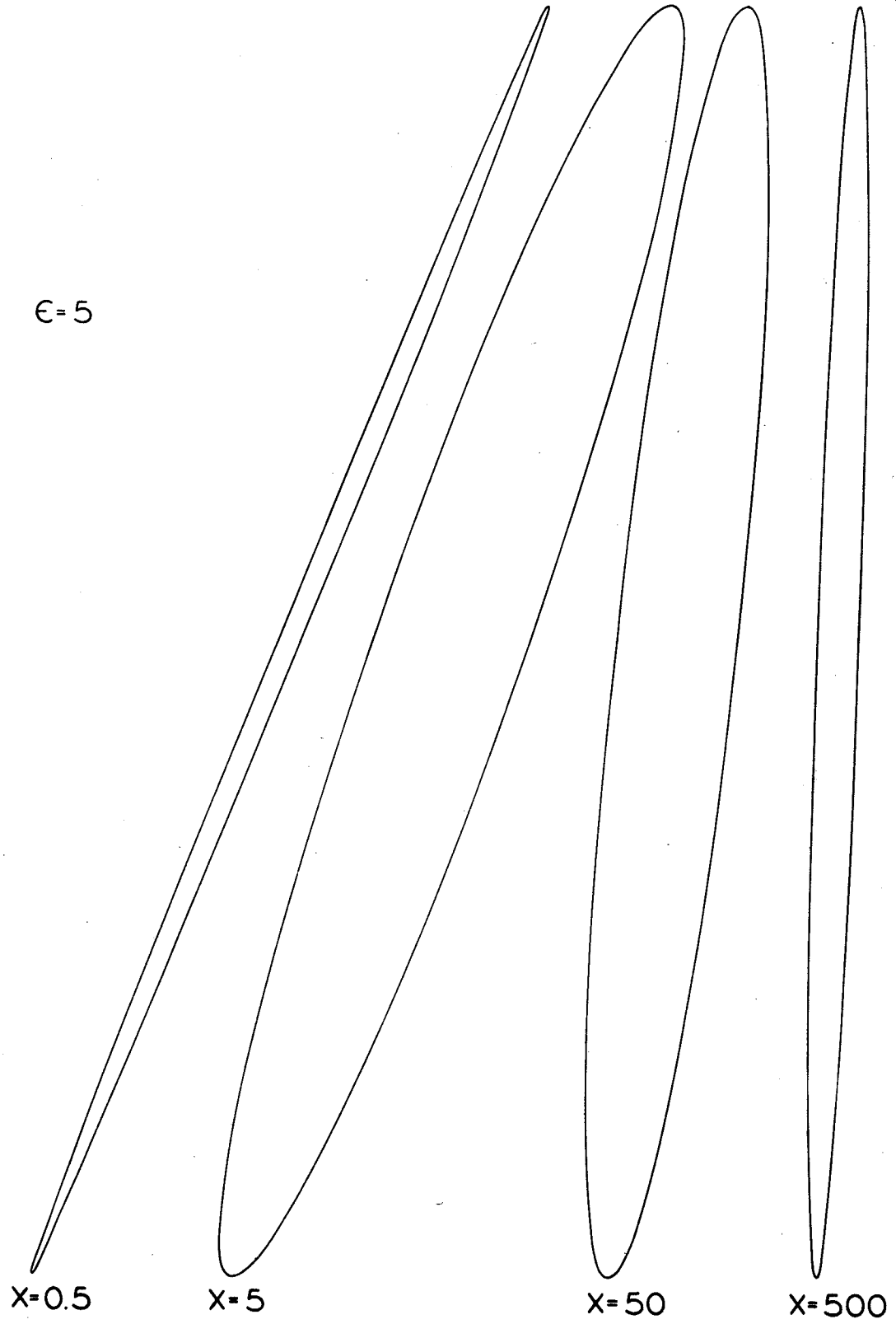

FIGURE 16

THE VERTICAL AND HORIZONTAL COMPONENTS OF THE TOTAL FIELD NEAR THE EARTH'S SURFACE WHEN A PLANE WAVE OF UNIT INTENSITY IS INCIDENT AT THE ANGLE ψ

(A) $X = 179,731$; $\varepsilon = 80$
(B) $X = 89.8655$; $\varepsilon = 15$
(C) $X = 1.95360$; $\varepsilon = 15$

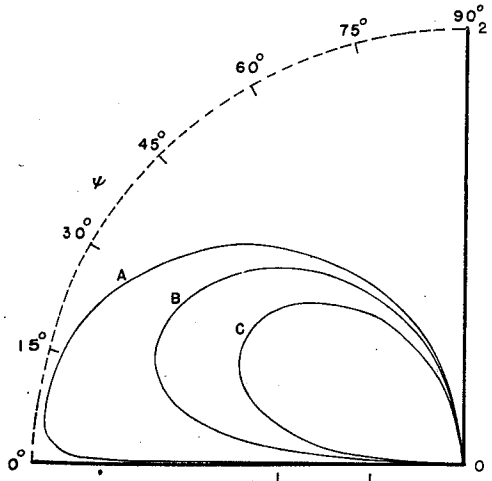

$E_{\parallel z} = \cos.\psi \left| 1 + R_{\parallel} \right|$

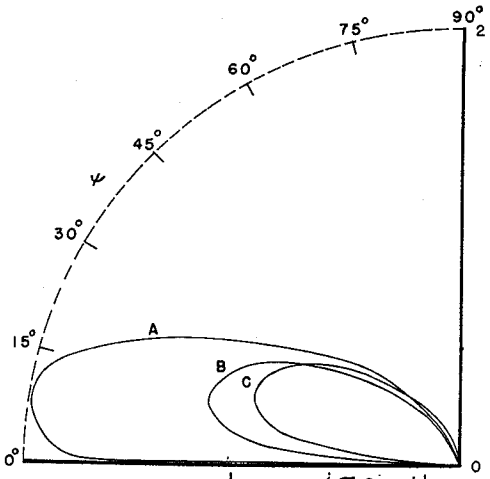

$E_{\parallel z} = \cos.\psi \left| 1 + R_{\parallel} e^{i\pi \sin.\psi} \right|$

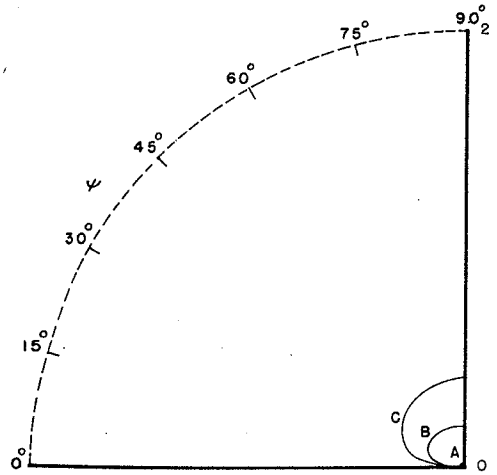

$E_{\parallel x} = \sin.\psi \left| 1 - R_{\parallel} \right|$

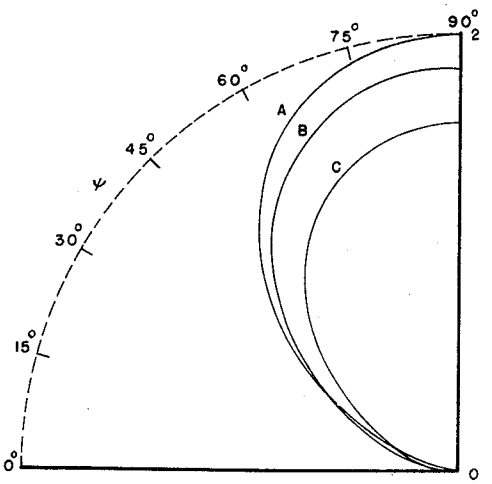

$E_{\parallel x} = \sin.\psi \left| 1 - R_{\parallel} e^{i\pi \sin\psi} \right|$

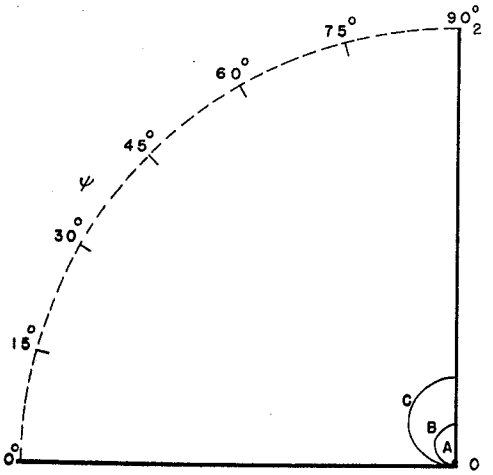

$E_{\perp} = \left| 1 + R_{\perp} \right|$

FIELD AT THE SURFACE

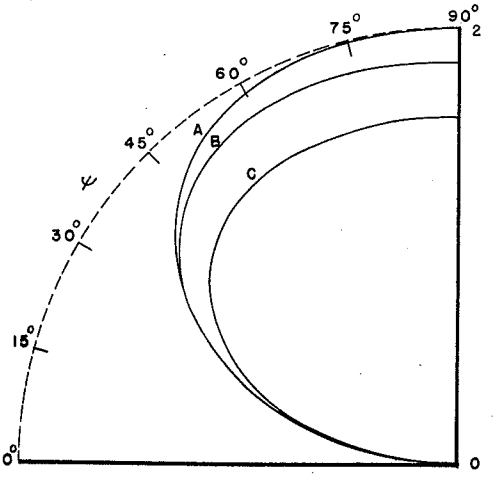

$E_{\perp} = \left| 1 + R_{\perp} e^{i\pi \sin\psi} \right|$

FIELD $\frac{1}{4}\lambda$ ABOVE THE SURFACE

FIGURE 17

THE RATIO OF THE RESULTANT HORIZONTAL TO VERTICAL ELECTRIC FIELD COMPONENTS WHEN A PLANE WAVE WITH EQUAL ∥ AND ⊥ COMPONENTS IS INCIDENT ON THE GROUND AT AN ANGLE OF ELEVATION ψ

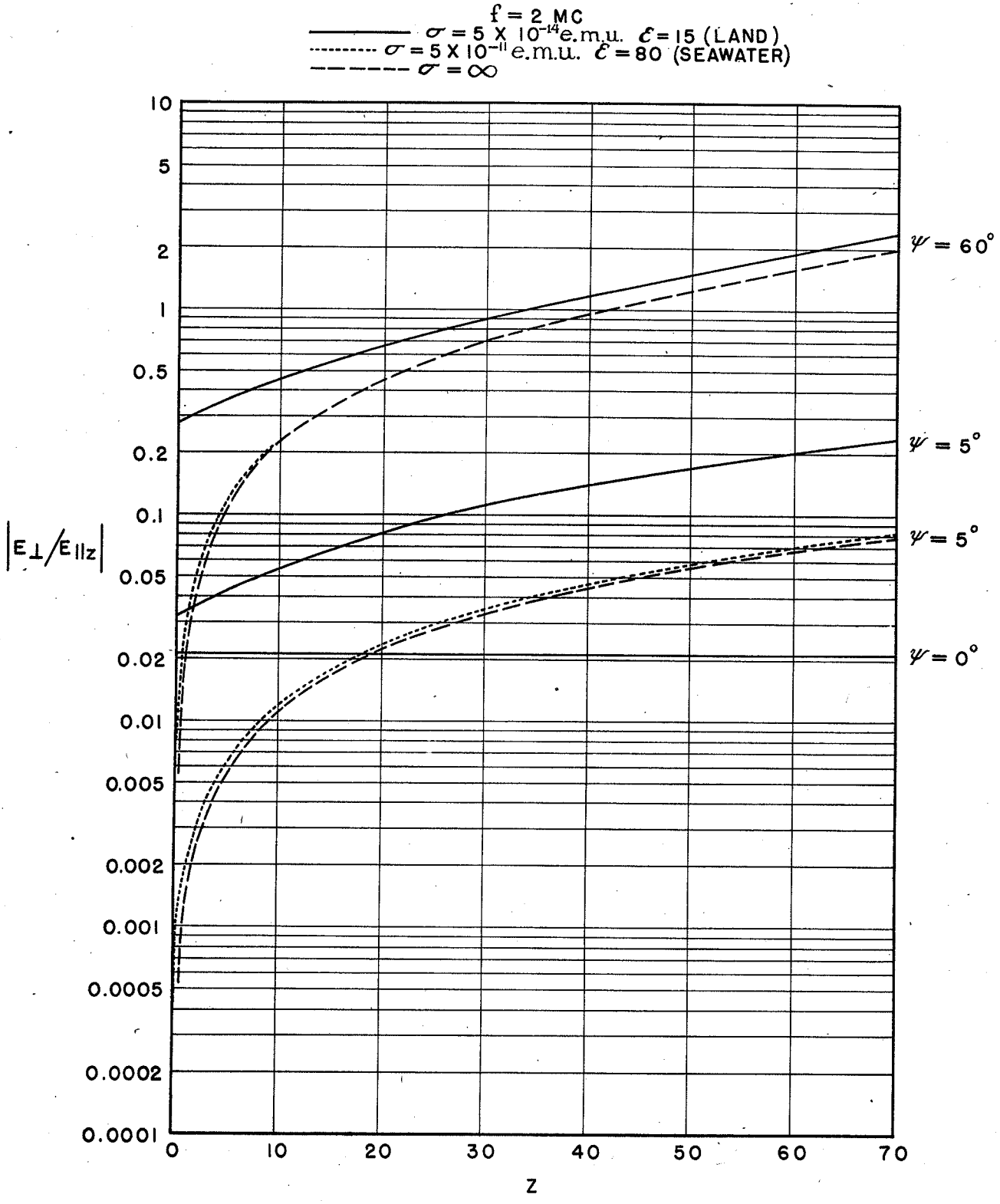

FIGURE 18

THE RATIO OF THE RESULTANT HORIZONTAL TO VERTICAL ELECTRIC FIELD COMPONENTS WHEN A PLANE WAVE WITH EQUAL II AND ⊥ COMPONENTS IS INCIDENT ON THE GROUND AT AN ANGLE OF ELEVATION ψ

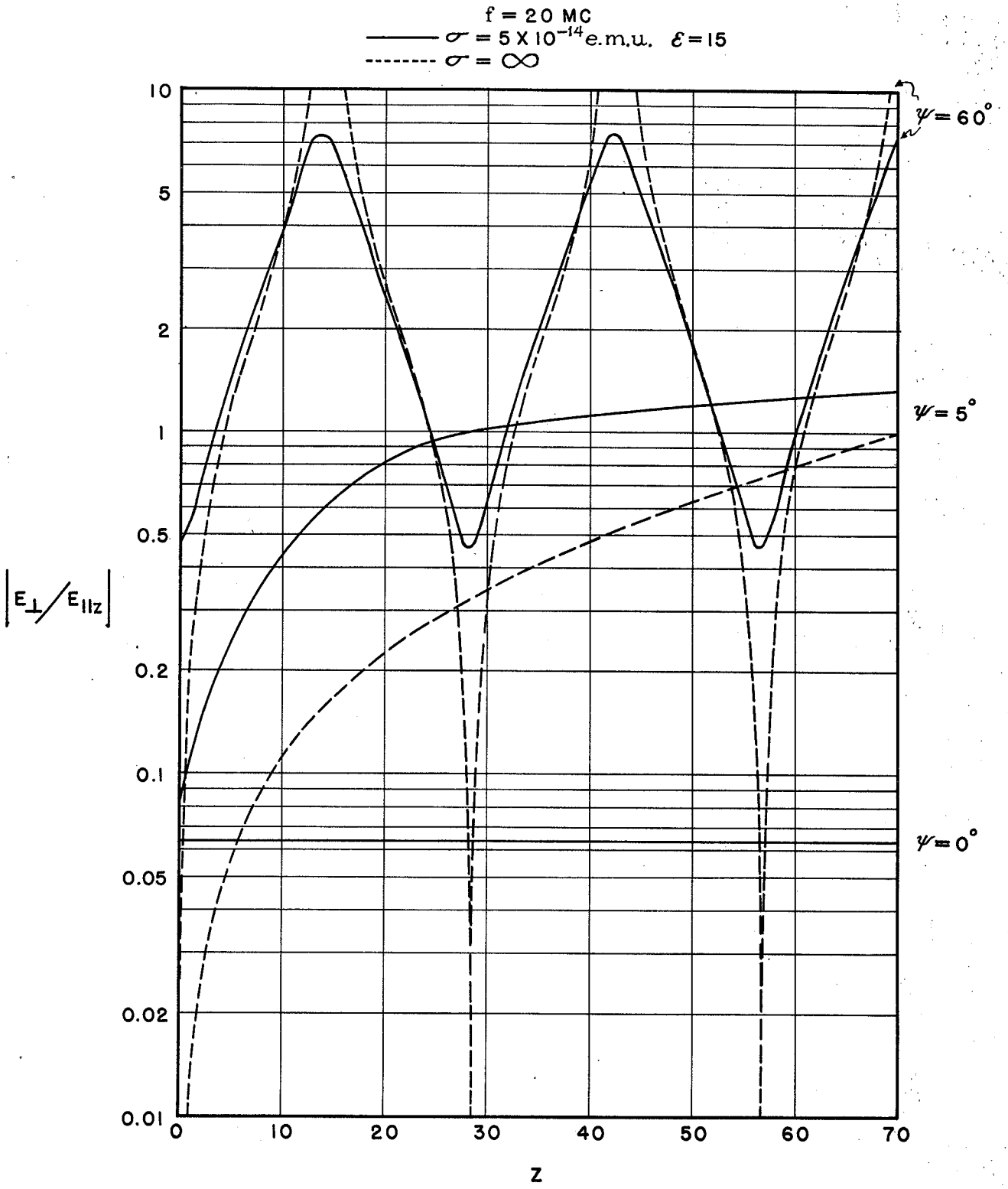

HEIGHT IN FEET ABOVE THE GROUND

FIGURE 19

THE LOWEST HEIGHT ABOVE PERFECT GROUND AT WHICH $\left|E_{\perp}/E_{\parallel z}\right| = \left|E_{\perp d}/E_{\parallel d}\right|$

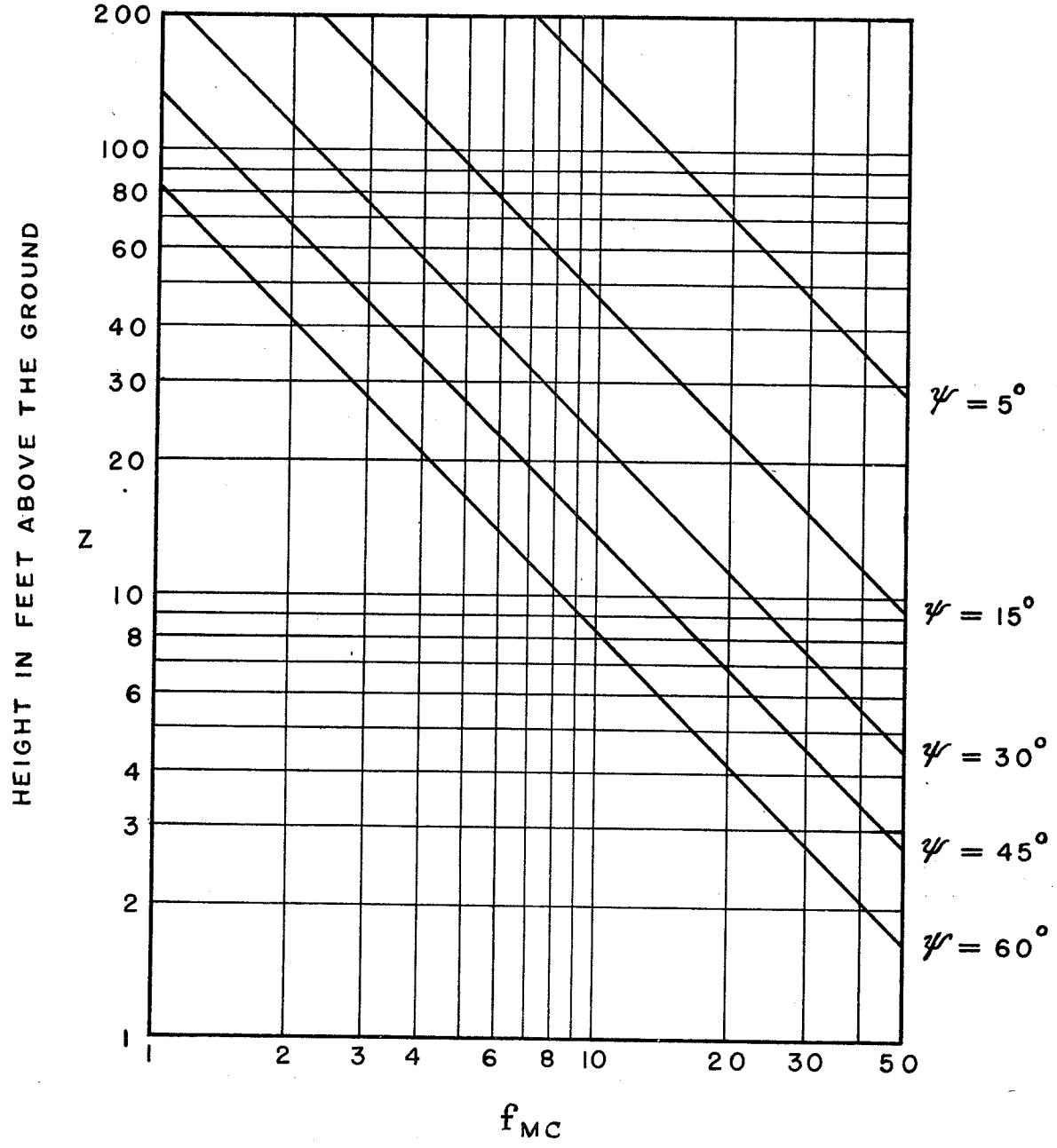

FREQUENCY IN MEGACYCLES PER SECOND

FIGURE 20

ABSORPTION OF PLANE RADIO WAVES IN THE EARTH

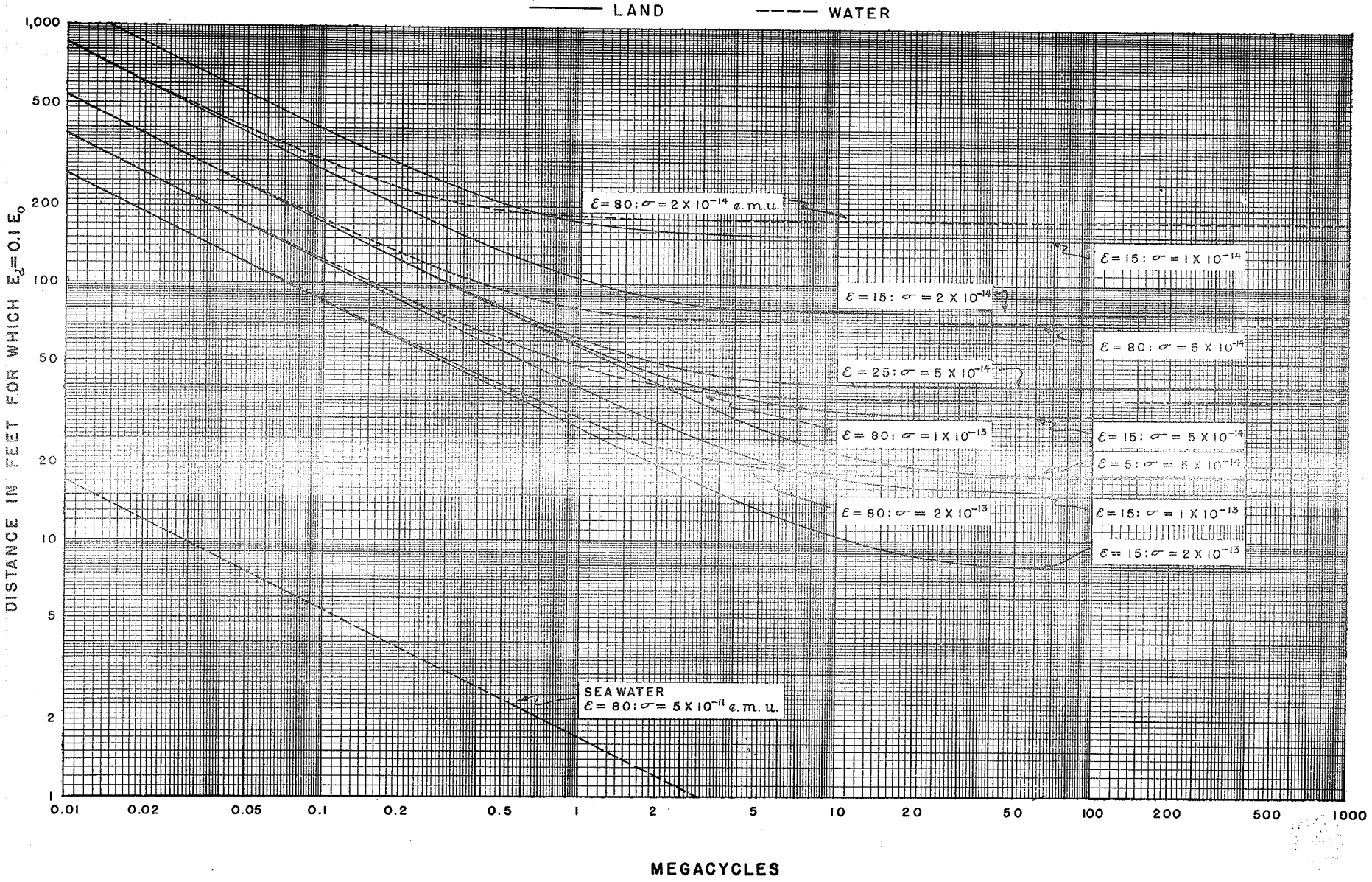

FIGURE 21

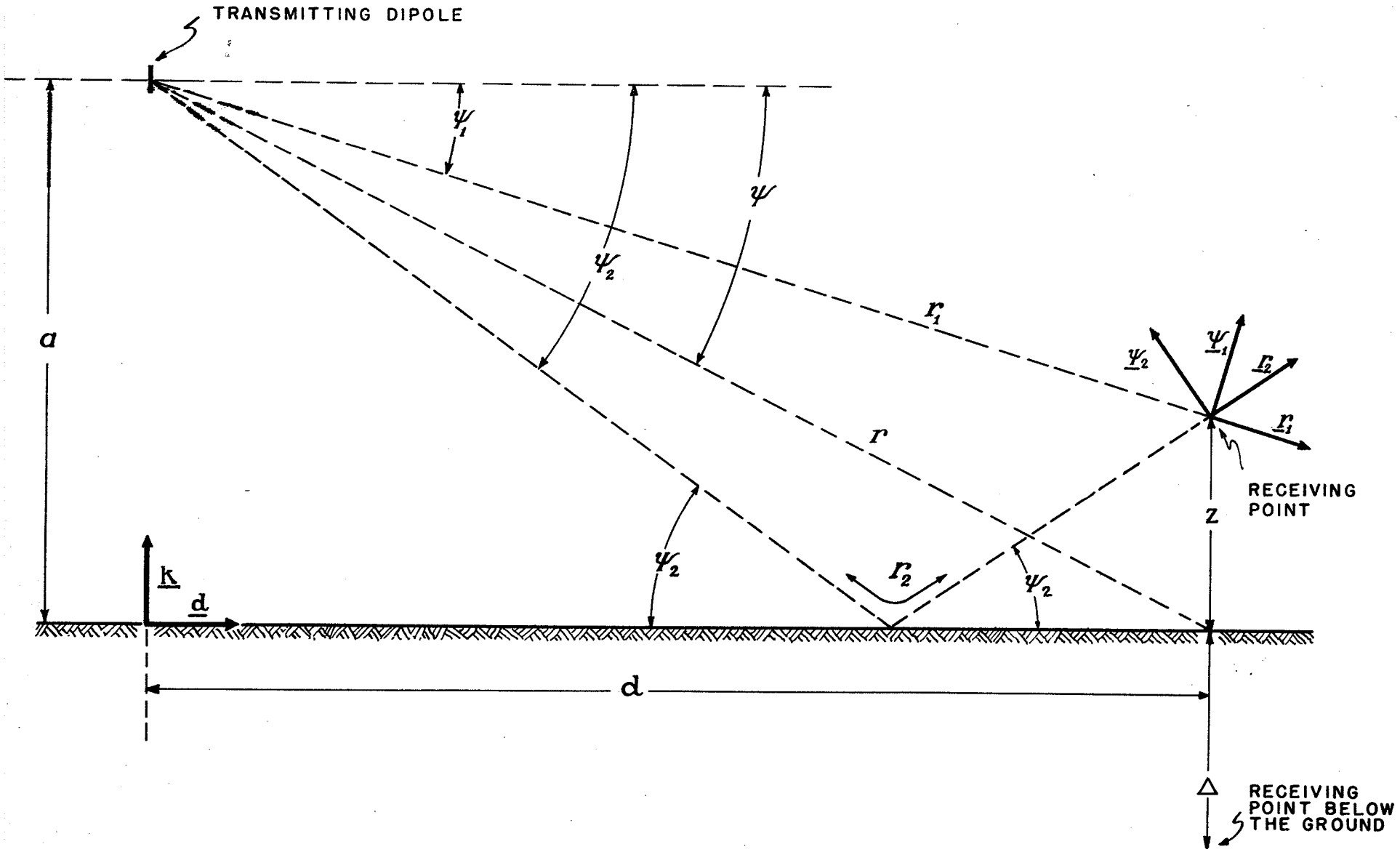
TRANSMITTING DIPOLE
ψ_1
ψ
ψ_2
r_1
a
ψ_2
ψ_1
r_2
r_1
r
RECEIVING POINT
z
k
d
ψ_2
r_2
ψ_2
d
RECEIVING POINT BELOW THE GROUND

FIGURE 22

CORRECTION FACTOR FOR DETERMINING THE VERTICAL COMPONENT OF THE ELECTRIC FIELD INTENSITY FROM A VERTICAL ELECTRIC DIPOLE BY MEANS OF MEASUREMENTS OF THE HORIZONTAL MAGNETIC FIELD INTENSITY

(ALSO APPLICABLE TO DETERMINATION OF $E_\perp$ FROM VERTICAL MAGNETIC DIPOLE BY MEANS OF MEASUREMENTS OF $H_{\parallel z}$)

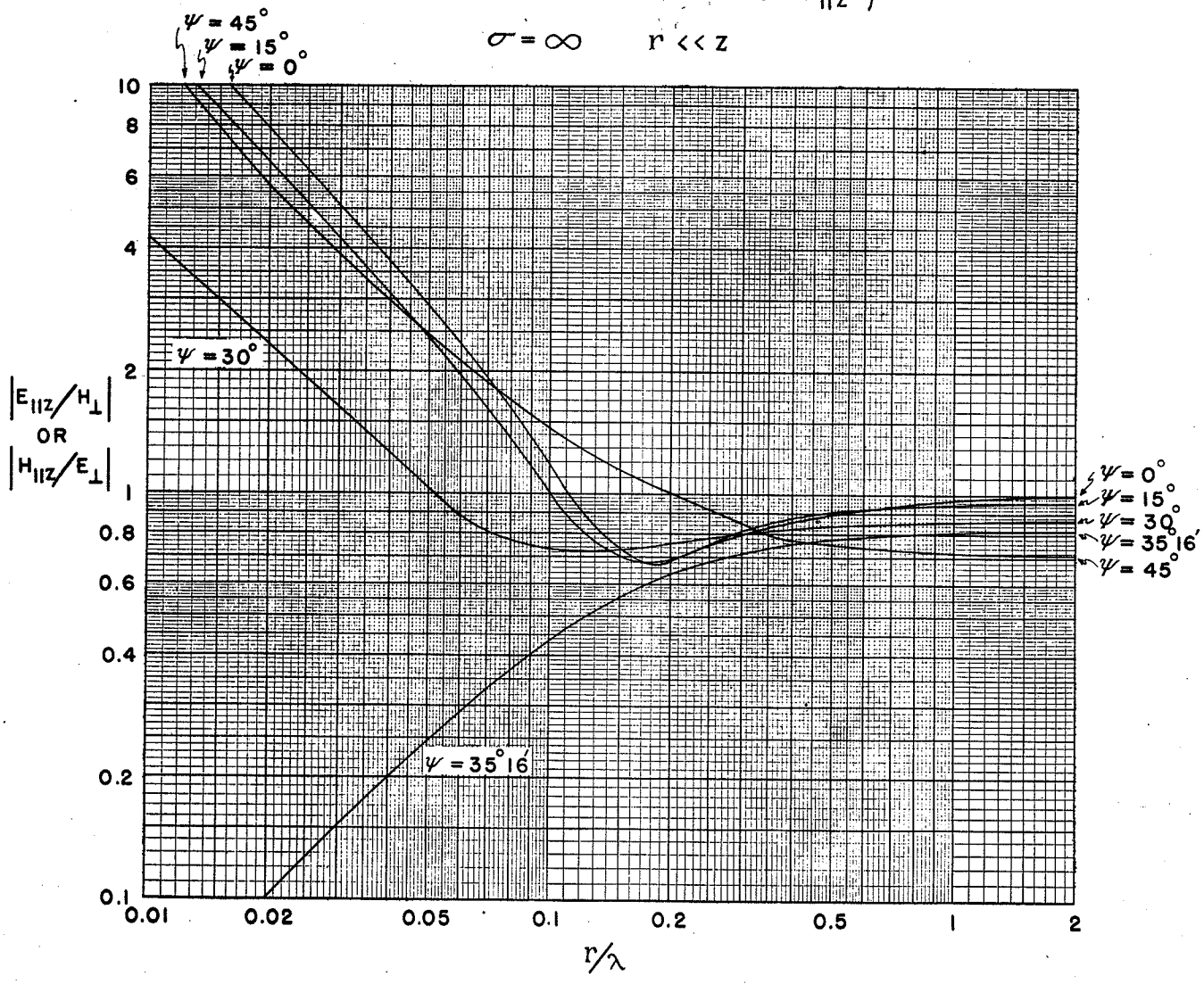

FIGURE 23

THE SURFACE WAVE ATTENUATION FUNCTION

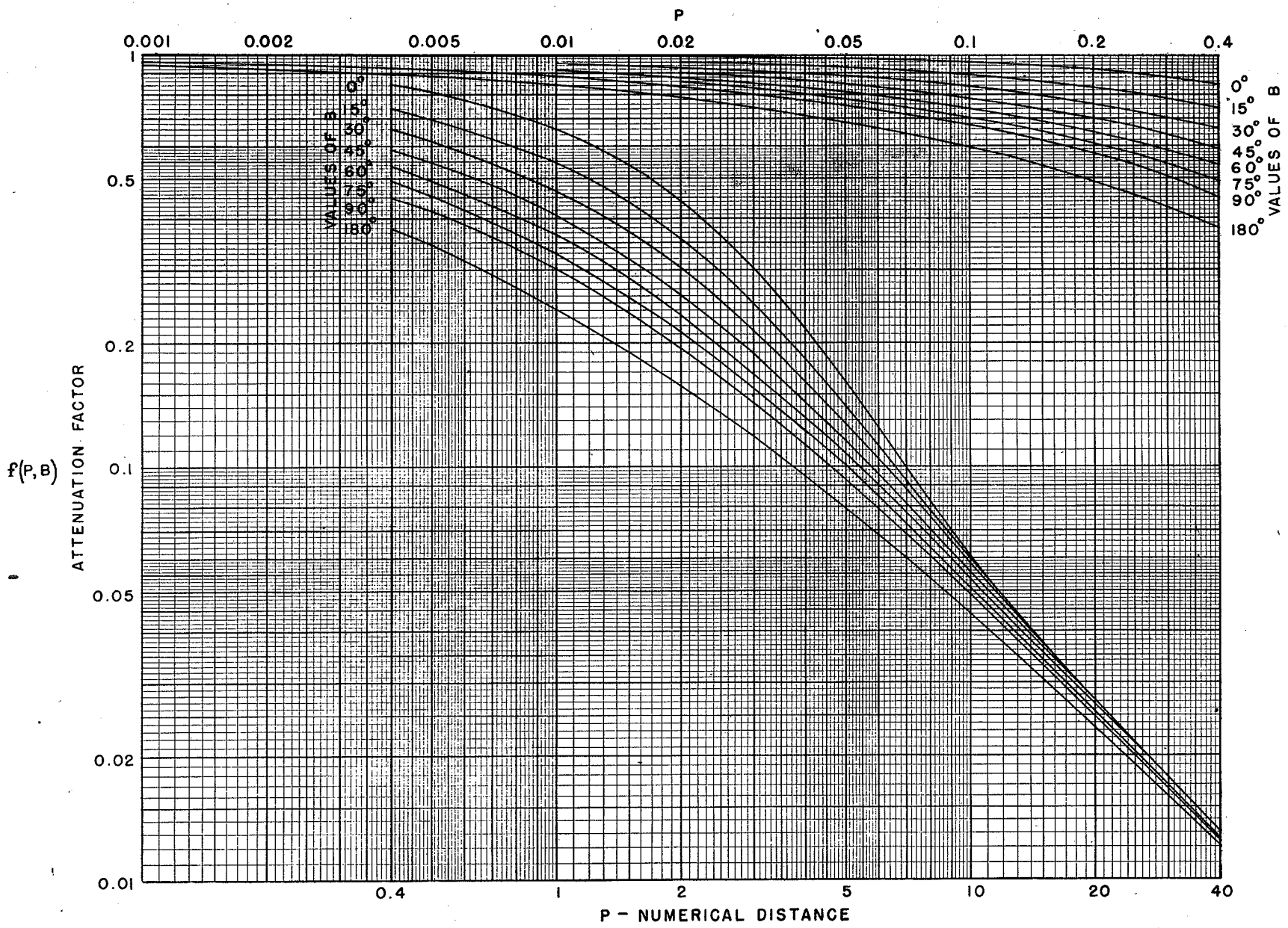

FIGURE 24

PHASE OF THE SURFACE WAVE ATTENUATION FUNCTION

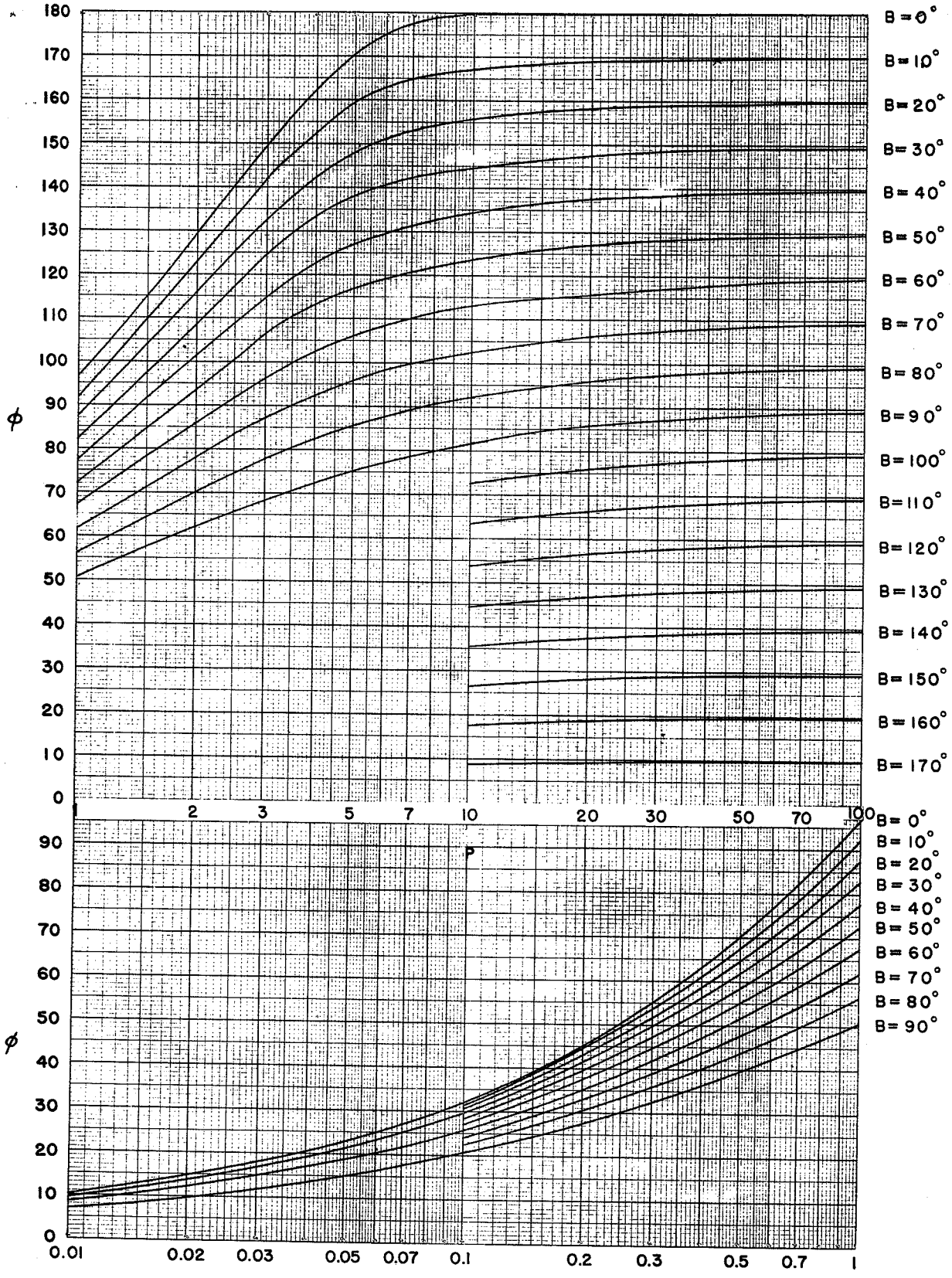

FIGURE 25

RATIO OF SURFACE TO SPACE WAVE INTENSITIES AT THE SURFACE OF THE EARTH RADIATED FROM A VERTICAL ELECTRIC DIPOLE AT A HEIGHT d

(FOR THE FREQUENCIES EXPRESSED IN MEGACYCLES FOR WHICH THE CURVES ARE LABELLED)

$z = 0$; $\epsilon = 15$; $\sigma = 5 \times 10^{-14}$ e.m.u.; $\sin\psi = d/r$

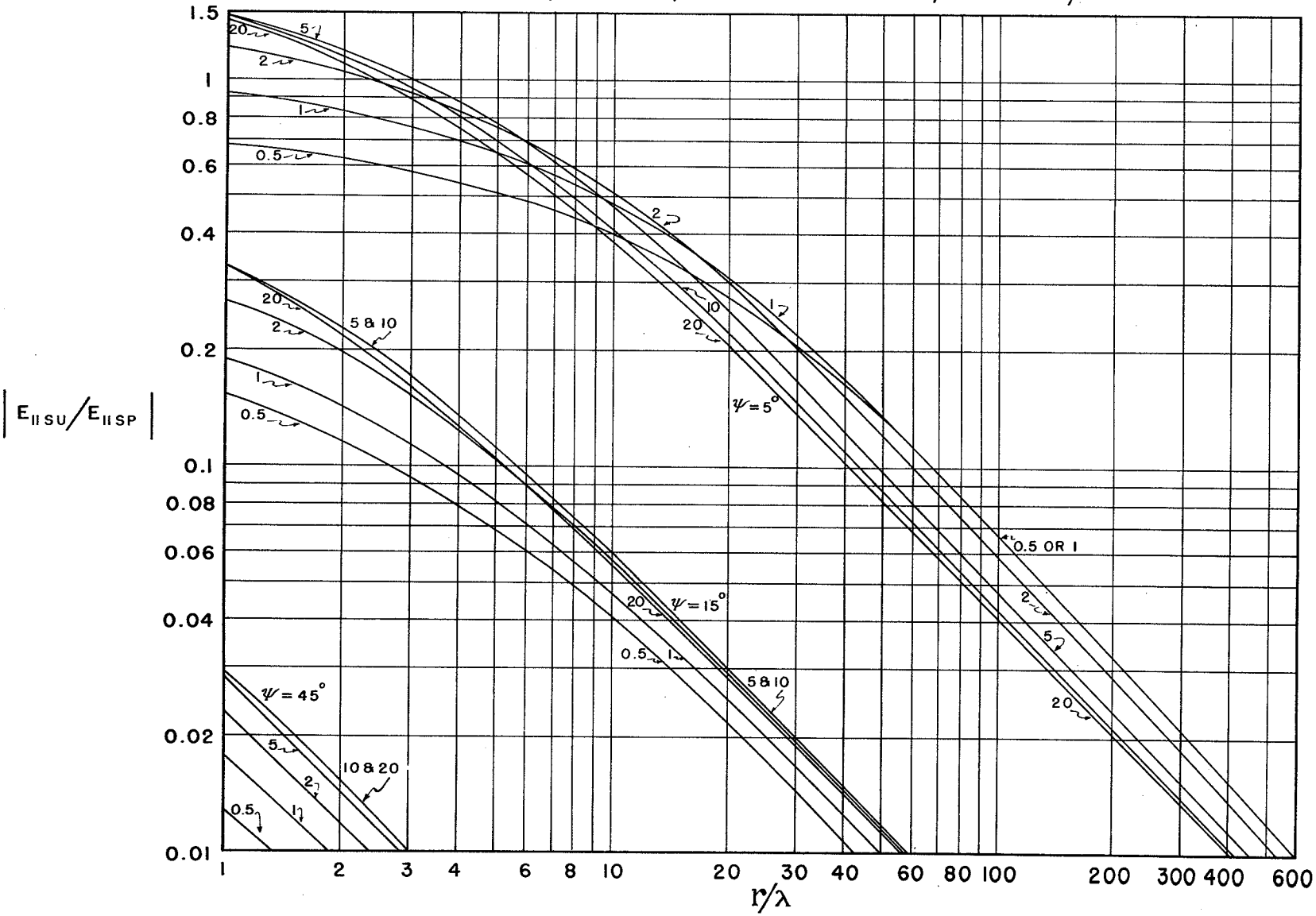

FIGURE 26

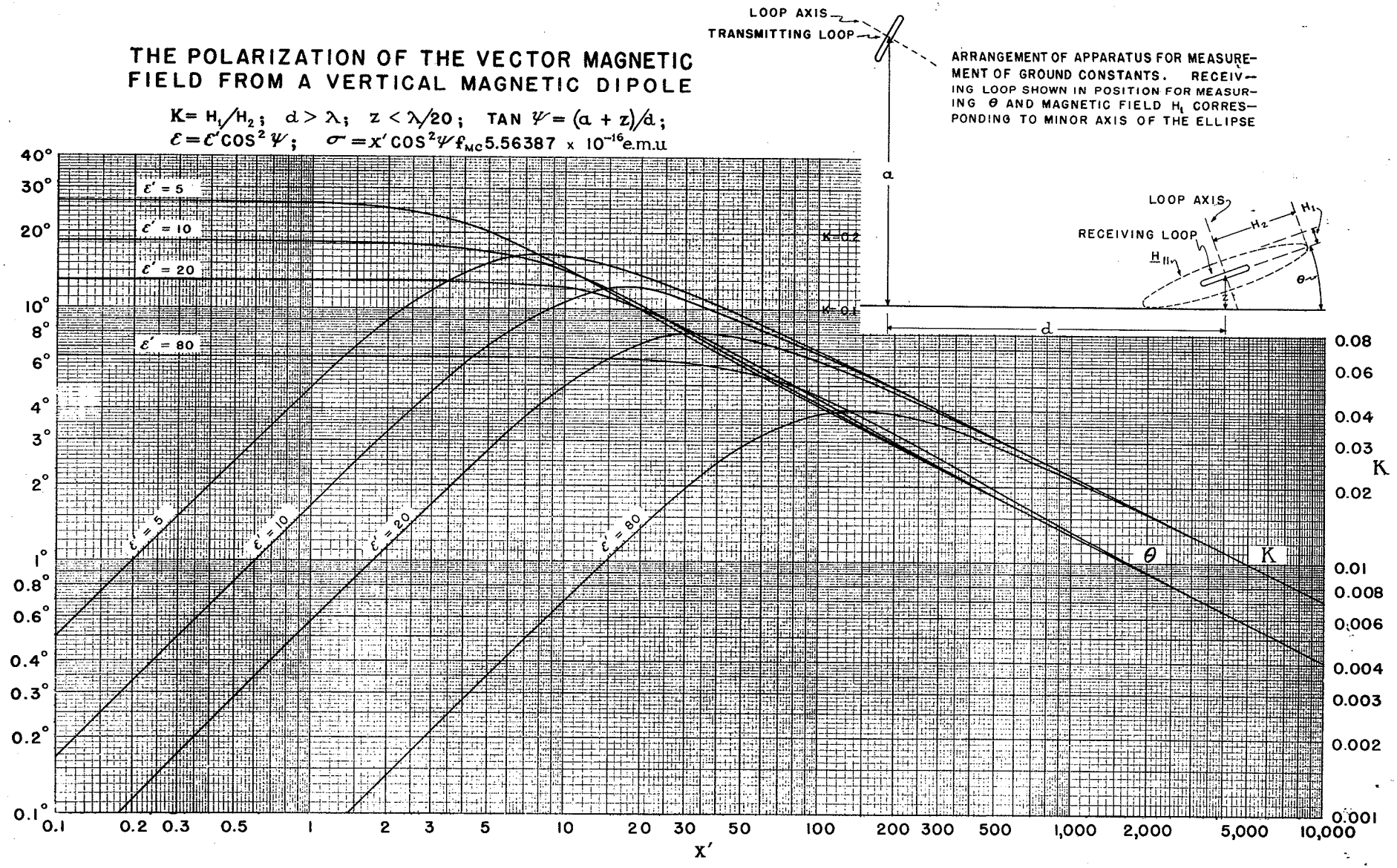
THE POLARIZATION OF THE VECTOR MAGNETIC FIELD FROM A VERTICAL MAGNETIC DIPOLE
K= H1/H2; d > λ; z < λ/20; TAN Ψ = (a + z)/d;
ε = ε' COS² Ψ; σ = x' COS² Ψ fMC 5.56387 x 10⁻¹⁶ e.m.u
LOOP AXIS
TRANSMITTING LOOP
ARRANGEMENT OF APPARATUS FOR MEASUREMENT OF GROUND CONSTANTS. RECEIVING LOOP SHOWN IN POSITION FOR MEASURING θ AND MAGNETIC FIELD H1 CORRESPONDING TO MINOR AXIS OF THE ELLIPSE
a
d
LOOP AXIS
RECEIVING LOOP
H1
H2
H II
θ
z
K=0.2
K=0.1
ε' = 5
ε' = 10
ε' = 20
ε' = 80
θ
K
40°
30°
20°
10°
8°
6°
4°
3°
2°
1°
0.8°
0.6°
0.4°
0.3°
0.2°
0.1°
0.08
0.06
0.04
0.03
0.02
0.01
0.008
0.006
0.004
0.003
0.002
0.001
K
0.1
0.2
0.3
0.5
1
2
3
5
10
20
30
50
100
200
300
500
1,000
2,000
5,000
10,000
X'

FIGURE 27

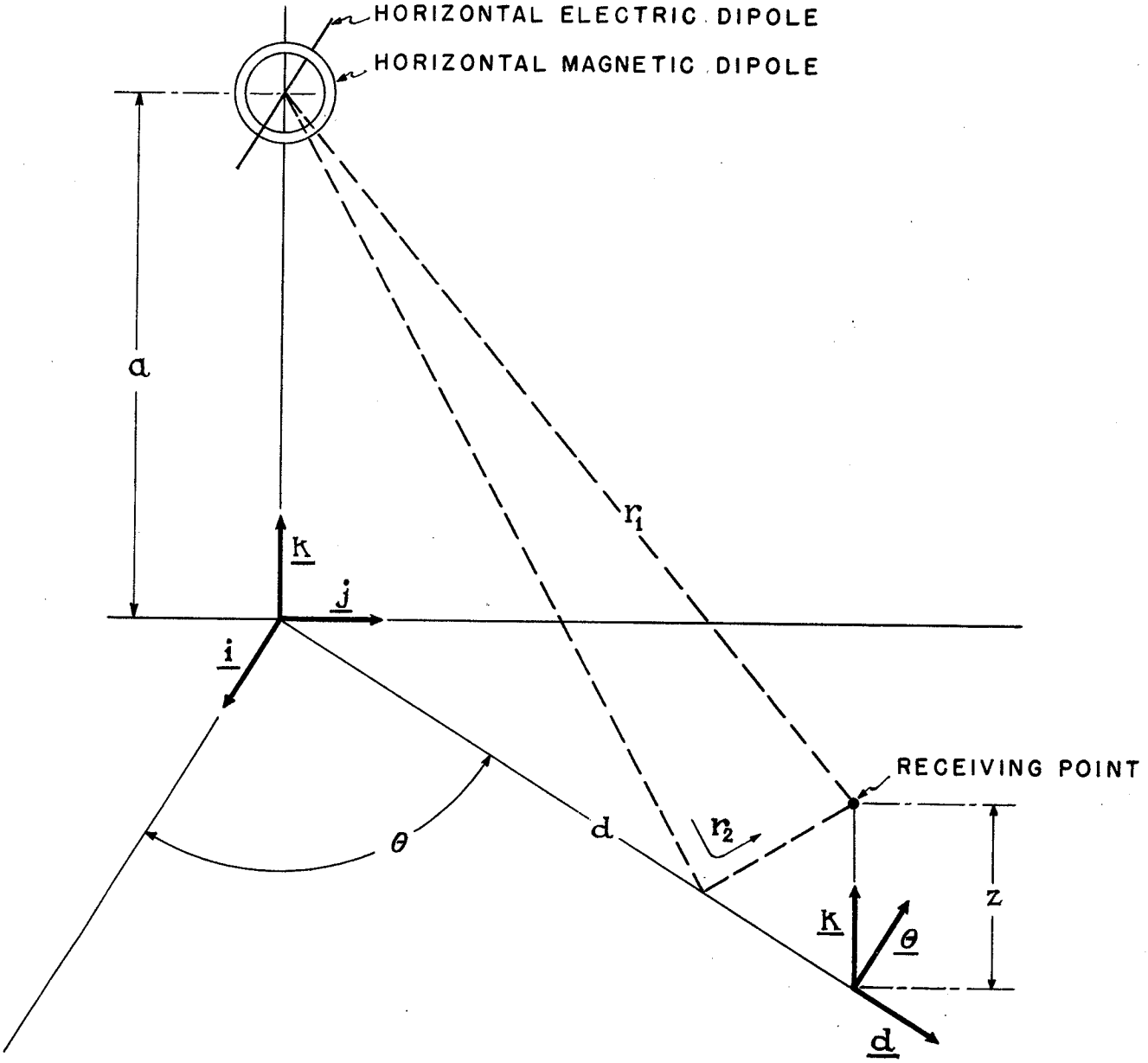
HORIZONTAL ELECTRIC DIPOLE
HORIZONTAL MAGNETIC DIPOLE
a
r1
k
j
i
RECEIVING POINT
θ
d
r2
z
k
θ
d

FIGURE 28